

INFORMATION TO USERS

This manuscript has been reproduced from the microfilm master. UMI films the text directly from the original or copy submitted. Thus, some thesis and dissertation copies are in typewriter face, while others may be from any type of computer printer.

The quality of this reproduction is dependent upon the quality of the copy submitted. Broken or indistinct print, colored or poor quality illustrations and photographs, print bleedthrough, substandard margins, and improper alignment can adversely affect reproduction.

In the unlikely event that the author did not send UMI a complete manuscript and there are missing pages, these will be noted. Also, if unauthorized copyright material had to be removed, a note will indicate the deletion.

Oversize materials (e.g., maps, drawings, charts) are reproduced by sectioning the original, beginning at the upper left-hand corner and continuing from left to right in equal sections with small overlaps.

Photographs included in the original manuscript have been reproduced xerographically in this copy. Higher quality 6" x 9" black and white photographic prints are available for any photographs or illustrations appearing in this copy for an additional charge. Contact UMI directly to order.

ProQuest Information and Learning
300 North Zeeb Road, Ann Arbor, MI 48106-1346 USA
800-521-0600

UMI[®]

***Nramp* genes: roles in resistance to infection and in iron metabolism**

Samantha Gruenheid

Department of Biochemistry
McGill University
Montréal, Québec, Canada

August 1999

A thesis submitted to the Faculty of Graduate Studies and Research
in partial fulfillment of the requirements of the degree of Doctor of Philosophy

© Samantha Gruenheid, August 1999



**National Library
of Canada**

**Acquisitions and
Bibliographic Services**

**395 Wellington Street
Ottawa ON K1A 0N4
Canada**

**Bibliothèque nationale
du Canada**

**Acquisitions et
services bibliographiques**

**395, rue Wellington
Ottawa ON K1A 0N4
Canada**

Your file Votre référence

Our file Notre référence

The author has granted a non-exclusive licence allowing the National Library of Canada to reproduce, loan, distribute or sell copies of this thesis in microform, paper or electronic formats.

The author retains ownership of the copyright in this thesis. Neither the thesis nor substantial extracts from it may be printed or otherwise reproduced without the author's permission.

L'auteur a accordé une licence non exclusive permettant à la Bibliothèque nationale du Canada de reproduire, prêter, distribuer ou vendre des copies de cette thèse sous la forme de microfiche/film, de reproduction sur papier ou sur format électronique.

L'auteur conserve la propriété du droit d'auteur qui protège cette thèse. Ni la thèse ni des extraits substantiels de celle-ci ne doivent être imprimés ou autrement reproduits sans son autorisation.

0-612-64565-7

Canada

Abstract

The *Nramp1* locus controls the innate resistance or susceptibility of mice to infection with a group of unrelated intracellular parasites which includes *Salmonella*, *Leishmania*, and *Mycobacterium*. *Nramp1* is expressed exclusively in professional phagocytes and encodes an integral membrane protein that shares structural characteristics with ion channels and transporters. Its mechanism of action is not known. The intracellular localization of the Nramp1 protein was analyzed in control 129/sv and mutant *Nramp1*^{-/-} macrophages. Nramp1 was localized to the late endosomal/lysosomal compartments. Immunofluorescence studies and direct purification of latex bead-containing phagosomes demonstrated that upon phagocytosis, Nramp1 is recruited to the membrane of the phagosome. cDNA clones corresponding to a second mouse *Nramp* gene, *Nramp2*, were isolated. Nucleotide and predicted amino acid sequence analyses of full length cDNA clones for *Nramp2* indicate that this novel protein is closely related to Nramp1, and that the two genes form part of a small family. The two Nramp proteins share 63% identical residues and are predicted to have very similar secondary structures, including identical hydropathy profiles and predicted membrane organization. Analysis of the distribution of *Nramp2* mRNA transcripts in normal mouse tissues by Northern blotting revealed that in contrast to the previously described macrophage-specific *Nramp1* gene, *Nramp2* mRNAs are expressed ubiquitously. Specific antiserum was generated and used to detect Nramp2 in a number of cell types. Nramp2 is expressed as a 90-100 kDa integral membrane protein that is extensively modified by glycosylation. Subcellular localization studies indicate distinct and non-overlapping localizations for Nramp1 and Nramp2. Nramp2 is expressed primarily in recycling endosomes and also to a lower extent at the plasma membrane, colocalizing with transferrin. Together with the concurrent reports that mutations in *Nramp2* result in iron deficiency, these results support the hypothesis that Nramp2 plays a key role in the metabolism of transferrin-bound iron, transporting free Fe²⁺ across the endosomal membrane and into the cytoplasm. The identification of a divalent cation transport function for the Nramp family, together with the localization of Nramp1 to the phagosomal membrane suggests that Nramp1 may act by sequestering iron and other divalent cations away from microbes during infection.

Résumé

La résistance ou susceptibilité innée des souris à un groupe de parasites intracellulaires non-parents incluant les genres *Salmonella*, *Leishmania* et *Mycobacterium* est contrôlée par le locus *Nramp1*. Le gène *Nramp1* est exclusivement exprimé chez les phagocytes professionnels et code pour une protéine membranaire dont les caractéristiques structurales rappellent celles des canaux ioniques et des transporteurs membranaires. Le mode d'action antiparasitaire de cette protéine reste inconnu. Nous avons étudié la localisation intracellulaire de la protéine *Nramp1* dans les lignées de macrophages contrôles 129/sv et *Nramp1*^{-/-}, permettant de la situer aux compartiments endocytiques tardifs. Des études d'immunofluorescence et la purification de phagosomes contenant des billes de latex ont démontré qu'après la phagocytose, *Nramp1* est recrutée à la membrane du phagosome. Nous avons isolé des clones de cDNA correspondants à un second gène *Nramp* murin, *Nramp2*. La séquence nucléotidique de clones de cDNA complets et la séquence peptidique résultante indiquent que *Nramp2* et *Nramp1* sont des gènes parents faisant partie d'une même famille. Avec 63% de résidus identiques et des profils d'hydropathie identiques, ces deux protéines partagent des prédictions de structures secondaires et d'organisation membranaire très similaires. L'analyse par "Northern blotting" de la distribution des transcripts d'ARNm de *Nramp2* dans les tissus de souris normales révèlent que, contrairement à la spécificité d'expression de *Nramp1* pour les macrophages, les ARNm de *Nramp2* sont exprimés de façon ubiquitaire. *Nramp2* est une glycoprotéine membranaire intégrale d'un poids moléculaire apparent de 90-100 kDa. Des études de localisation subcellulaire indiquent que *Nramp1* et *Nramp2* sont localisées à des sites distincts et non-chevauchants. *Nramp2* est principalement retrouvée dans les endosomes de recyclage et, de façon moindre, à la membrane plasmique, colocalisant avec la transferrine. En concordance avec des rapports démontrant que des mutations dans *Nramp2* résultent en une carence en fer, ces résultats soutiennent l'hypothèse que *Nramp2* joue un rôle important dans le métabolisme du fer lié à la transferrine, transportant le Fe²⁺ libre au travers de la membrane endosomale vers le cytoplasme. La confirmation du rôle de transporteur de cations pour la famille de protéines *Nramp* ainsi que la localisation de *Nramp1* à la membrane du phagosome suggèrent que le mode d'action de *Nramp1* consiste à sequestrer le fer et autres métaux divalents hors de portée des pathogènes lors d'une infection.

Preface

The work described in Chapters 2, 3, and 4 of this thesis have been published as follows:

Chapter 2: Gruenheid S, Pinner E, Desjardins M, Gros P: Natural resistance to infection with intracellular pathogens: the *Nramp1* protein is recruited to the membrane of the phagosome. *J Exp Med* **185**:717-730, 1997.

Chapter 3: Gruenheid S, Cellier M, Vidal S, Gros P: Identification and characterization of a second mouse *Nramp* gene. *Genomics* **25**:514-525, 1995.

Chapter 4: Gruenheid S, Canonne-Hergaux F, Gauthier S, Hackam DJ, Grinstein S, Gros P: The iron transport protein NRAMP2 is an integral membrane glycoprotein that colocalizes with transferrin in recycling endosomes. *J Exp Med* **189**:831-841, 1999.

Contributions of co-authors

Chapter 2: The work described is essentially my own. I optimized the conditions for immunofluorescence and performed all experiments shown in all figures. I took all photomicrograph images from the immunofluorescence microscope. Diane Gingras assisted me in obtaining the laser confocal images shown in figure 4. Elhanan Pinner provided the *Nramp1*-transfected cell line, used in figure 5. I performed the fractionation experiment from figure 5, using a protocol developed by Michel Desjardins. I performed the kinetic experiment of figure 6, including the observation and enumeration. Michel Desjardins provided advice concerning all experiments.

Chapter 3: The work described is entirely my own. This includes plating and screening of cDNA libraries, Southern blotting and sequence analysis of the isolated clones shown in figure 1 and 2. I performed the computer analyses shown in figure 3 and table I, with advice from Tony Kwan. For figure 5, I dissected mice, prepared mRNA from their organs and performed the northern blot analyses. The PCRs and data analysis for the chromosomal mapping were all done by me as well. Mathieu Cellier originally

isolated the *Nramp2*-specific probe, and many of the studies performed were based on previous experiments on *Nramp1* by Silvia Vidal, who also supervised me during the cDNA library screening.

Chapter 4: The work is my own, but with the collaboration of the co-authors as follows: I designed and constructed the vectors for expression of the fusion proteins, and purified the fusion proteins for rabbit immunizations. The injection and bleeding of rabbits was done by technicians at the McIntyre Animal Resources Center. I tested the immune sera for immunoreactivity, devised the strategy for affinity purification, and affinity purified the anti-*Nramp2* antiserum. Using an adaptation of my protocols, Francois Canonne-Hergaux performed the purification of the anti-*Nramp1* antiserum. The constructs and transfections for the *Nramp2*-transfected cell lines were done by me. The *Nramp1*-transfected cell lines had previously been made by Elhanan Pinner. The membrane preparations and anti-*Nramp2* and c-myc Western blots in figure 1A were performed by me. Francois Canonne-Hergaux performed the anti-*Nramp1* Western blot. Susan Gauthier performed the immunoprecipitations in figure 1B. I purified RNA and performed the Northern blots shown in figure 2A, as well as the glycosylation studies in figure 3C. Susan Gauthier made the membrane preparations and Francois Canonne-Hergaux performed the Western in figure 2B. Figure 3 and 4 are entirely my own. I performed the immunofluorescence in figure 5, and it was analyzed by confocal microscopy by David Hackam. Figure 6 and 7 are entirely my own. I conceived and designed figure 8 with input from Philippe Gros.

Philippe Gros provided expert supervision and advice throughout the course of all three studies.

Table of Contents

	Page
Abstract	i
Resume	ii
Preface/Contributions of co-authors	iii
Table of Contents	v
List of Figures	viii
List of Tables	x
Acknowledgements	xi
Objectives of the Presented Work	xii
Chapter 1 Introduction and Literature Review	1
1.1 The genetic approach to the study of host defense	2
1.2 The <i>Bcg/Ity/Lsh</i> locus and the <i>Nramp1</i> gene	3
1.3 <i>NRAMP1</i> and its role in human disease	6
1.4 <i>Nramp1</i> expression in professional phagocytes	10
1.5 Characterization of the Nramp1 protein	11
1.6 Functional studies	12
1.6.1 Historical perspective	12
1.6.2. Transfection studies	13
1.6.3. Studies in <i>Nramp1</i> ^{-/-} mice	14
1.6.4 <i>Nramp1</i> and <i>Mycobacterium tuberculosis</i>	15
1.6.5 <i>Nramp1</i> and Phagosomal Acidification	16
1.7 Pathogenesis of <i>Nramp1</i> -controlled diseases in mice and humans	19
1.7.1 <i>Mycobacterium</i> species	20
1.7.2 <i>Leishmania</i>	22
1.7.3 <i>Salmonella</i>	24

1.8	Modifiers of <i>Nramp1</i>	26
1.9	The <i>Nramp</i> gene family and divalent cation transport	28
1.9.1	<i>Nramp2</i>	29
1.9.2	<i>Nramp</i> homologues from other species	36
Chapter 2	The Nramp1 protein is recruited to the membrane of the phagosome	41
	Abstract	42
	Introduction	43
	Materials and Methods	47
	Results	54
	Discussion	75
Chapter 3	Identification and Characterization of a Second Mouse <i>Nramp</i> Gene	86
	Abstract	87
	Introduction	88
	Materials and Methods	91
	Results	96
	Discussion	115
Chapter 4	The iron transport protein Nramp2 is an integral membrane glycoprotein that colocalizes with transferrin in recycling endosomes	125
	Abstract	126
	Introduction	127
	Materials and Methods	130
	Results	137

Discussion	159
Chapter 5 Summary and Perspectives	165
5.1 Future perspectives: <i>Nramp1</i>	166
5.1.1 <i>Nramp1</i> and intracellular infections	166
5.1.2 <i>Nramp1</i> and iron recycling	174
5.2 Future perspectives: <i>Nramp2</i>	175
5.2.1 The recurring <i>Nramp2</i> mutation	176
5.2.2 <i>NRAMP2</i> involvement in human disease	177
5.2.3 Tissue-specific roles of <i>Nramp2</i>	178
<i>Intestine</i>	178
<i>Red Blood Cells</i>	181
<i>Brain</i>	182
5.3 Final Conclusions	185
References	186
Original Contributions to Knowledge	228

List of Figures

		Page
Chapter 1		
Figure 1	Splice forms of <i>Nramp2</i> mRNA	31
Chapter 2		
Figure 1	Subcellular localization of the Nramp1 protein in macrophages	56
Figure 2	Colocalization of Nramp1 and Lamp1 proteins in macrophages	59
Figure 3	Nramp1 association with latex bead-containing phagosomes	63
Figure 4	Nramp1 and Lamp1 colocalization to the membrane of latex bead-containing phagosomes	66
Figure 5	Purification of Nramp1-positive phagosomes	70
Figure 6	Kinetics of Nramp1 protein delivery to the maturing phagosome	74
Chapter 3		
Figure 1	Nucleotide sequence of the mouse <i>Nramp2</i> cDNA	99
Figure 2	Southern blot analysis of the mouse <i>Nramp1</i> and <i>Nramp2</i> genes	102
Figure 3	Deduced amino acid sequence of the Nramp2 protein and alignment with the mouse Nramp1 protein	105
Figure 4	Northern blot analysis of <i>Nramp2</i> mRNA expression in normal tissues	109
Figure 5	Mapping of the <i>Nramp2</i> gene to mouse chromosome 15	113

Chapter 4

Figure 1	Specificity and immunoreactivity of affinity purified anti-Nramp1 and anti-Nramp2 antisera	139
Figure 2	<i>Nramp2</i> mRNA and protein expression in primary cells and cultured cell lines	142
Figure 3	Subcellular localization of Nramp1 and Nramp2 in transfected CHO cells	147
Figure 4	Colocalization of Nramp2 with transferrin in transfected CHO cells	149
Figure 5	Colocalization of Nramp2 with transferrin in RAW macrophages	151
Figure 6	Subcellular localization of endogenous Nramp2	154
Figure 7	Nramp2 association with phagosomes	158
Figure 8	Schematic representation of Nramp2 and Nramp1 function	163

List of Tables

	Page
Chapter 1	
Table I Nramp homologs	37
Chapter 3	
Table I The binding protein-dependant transport system inner membrane component signature in bacterial and eukaryotic transporters	119

Acknowledgements

I would like to express my heartfelt gratitude to Philippe Gros. He has been an excellent mentor who teaches by example, not only with his scientific acuity, but also with his integrity, dedication, and compassion. I also thank him for the opportunity to contribute to such an exciting project. As for the past and present members of the lab, I have learned from and laughed with so many great people that there is not room to mention them all by name. I am especially grateful to those who helped me regain my perspective on days when things weren't working. Special mention also goes to Normand Groulx, for keeping the lab in good working order despite the fact that there were twenty people going around leaving messes and breaking things.

I would like to also thank my "vice-mentors", Sergio Grinstein and Michel Desjardins, who shared with me their knowledge, expertise and reagents. I am grateful to Diane Gingras, David Hackam, and Elia Ali-Jaoude, who all spent time with me on the confocal microscope. I thank Susan Gauthier for teaching me how to handle mice and to Tony Kwan for his tireless patience in answering all my computer questions.

François Canonne-Hergaux, Nada Jabado, Marc-Etienne Rousseau, and Greg Govoni proofread sections of this thesis and offered their insightful suggestions, and Marc-Etienne Rousseau translated the abstract. I was financially supported during my studies with a studentship from the Medical Research Council of Canada and a President's Dissertation Fellowship from McGill, with the occasional subsidy from my mother who also provided unlimited moral support and encouragement.

Objectives of the presented work

In 1993, at the start of this thesis project, the work of many years had just culminated with the identification of the *Nramp1* gene as a determinant of natural resistance to infections³¹. Though the gene was found to encode a phagocyte-specific protein that was mutated in susceptible mice, there was little data to indicate its mechanism of action. The predicted secondary structure of the protein was reminiscent of an ion channel or transport protein but the amino acid sequence bore no significant homology to any previously described protein. It was hypothesized that the protein was involved in movement of an unidentified substrate, but there was no additional data to facilitate further elucidation of *Nramp1* function. Therefore, the objective of the present thesis project was to garner information that could give insight into the biochemical function and mechanism of action of *Nramp1*.

The studies described in the first part of this thesis (Chapter 2) were aimed at determining the site of *Nramp1* action within cells. Shortly after the identification of *Nramp1*, there were many conflicting hypotheses on the effector mechanisms of the encoded protein. Some predicted that Nramp1 would act at the nuclear envelope to regulate translocation of DNA binding proteins into the nucleus²¹². Others proposed that it exerted its action at the plasma membrane playing a role in signal transduction leading to macrophage activation^{213,214}. The localization of the protein to the phagosomal membrane supported the hypothesis that Nramp1 acted by altering the vesicular milieu within the phagosome by transporting a substrate across the phagosomal membrane.

Clues to the nature of the substrate transported by Nramp1 have eventually come from the analysis of Nramp-homologous proteins. *Nramp2* was the first *Nramp1*-homologous gene identified (Chapter 3), and was of particular interest since it was paralogous with *Nramp1* i.e. it was a homologue co-expressed in the same species, rather than an orthologue expressed in other species. The co-expression of two mammalian Nramp proteins suggested that they could either transport the same substrate at different sites, or transport different substrates by a similar mechanism. Comparative analyses of tissue distribution of the two genes' expression and subcellular localization of the two proteins were aimed at discerning between these two hypotheses (Chapters 2,3,4).

Finally, other groups' identification of divalent cations as substrates for Nramp2 and other Nramp-homologous proteins allowed for the synthesis of all the previous data, and lead to the unifying theory described at the end of Chapter 4. This theory hypothesizes that Nramp1, like Nramp2, transports iron and other divalent cations, but it transports them at the phagosomal membrane. This transport is predicted to deplete the phagosome of ions necessary for microbial proliferation.

Chapter 1

Introduction and Literature Review

1.1 The genetic approach to the study of host defense

Infectious diseases are a major health problem that account for one third of the world's mortality ^{1,2}. The recent emergence of antibiotic-resistant parasites and the resulting failure of conventional anti-microbial therapies have increased the severity of the problem and revealed the need for a greater understanding of host-pathogen interactions ³. Components of defense to infection can manifest themselves as genetic determinants conferring innate resistance or susceptibility to infection in human populations ⁴ or in experimental animal models of infection, such as the laboratory mouse ⁵. Characterizing the genes and proteins implicated in these natural resistance phenomena and elucidating the mechanisms involved can provide insight into host interactions with pathogens as well as shed new light on basic cellular functions.

In humans, the search for individual genes that control variable disease outcome is difficult since many traits do not follow simple Mendelian genetics and the number of affected cases and well-matched controls is often limiting (reviewed in ^{6,7}). A simpler approach is to first identify genes important in mouse models of disease, and then to determine their involvement in disease onset, progression and outcome in human populations (reviewed in ⁸). Genetic analysis of mouse models of infectious diseases provides many advantages when compared with gene discovery in humans. Animal studies facilitate establishment of uniform and controlled experimental conditions with respect to strain, dose, time, and route of inoculation of the pathogen, which minimizes phenotypic heterogeneity due to non-genetic factors. Similarly, the effects of environmental conditions and prior exposure or vaccination can be ruled out.

Genetically, inbred strains of mice are a unique resource that provides an unlimited

number of identical individuals that are homozygous at each locus. When differences in resistance or susceptibility to infection between different mouse strains are identified, informative crosses can be set up in a prospective, directed fashion to identify and eventually isolate the loci involved. This is in direct contrast to genetic studies in humans, where linkage analysis is always, by its nature, retrospective. Another significant advantage of using the mouse as a model system is the feasibility of introducing germ line mutations, which allows direct assessment of infection and resulting disease in presence or absence of the chosen gene product. Finally, once host resistance genes have been identified in mice, their human counterparts can easily be isolated, and their relevance in human disease examined.

Genetic studies of mouse models of disease have led to the mapping of numerous loci involved in host resistance to infection with various microbes, including bacterial, protozoan and helminthic parasites, and viruses⁹. However, since many of the resources and tools that facilitate these studies are still evolving, the number of loci for which the corresponding gene has been identified and cloned remains small. The identification and characterization of *Nramp1* serves as a paradigm for the successful use of this approach to gain novel insight into mechanisms of host defense.

1.2 The *Bcg/Ity/Lsh* locus and the *Nramp1* gene

It was first demonstrated in 1933 that resistance of mice to infection with *Salmonella* was controlled by genetic factors¹⁰. However, it was not until the 1970s that systematic studies on what we now know as *Nramp1* began. In 1974, infection of a panel of inbred mouse strains with *Salmonella typhimurium* revealed that all inbred strains were

either sensitive to infection with less than 10^2 bacteria or resistant to infection with greater than 10^5 , with no strains of intermediate resistance ¹¹. A similar phenomenon was reported for *Leishmania donovani* with resistant strains showing a less than 8-fold increase in the number of parasites in the liver two weeks after infection, while the increase in susceptible strains was 100-fold ¹². Surprisingly, the strain distribution of resistance and susceptibility was the same for both pathogens, leading to the hypothesis that the resistance to both *Salmonella* ("*Ity*") and *Leishmania* ("*Lsh*") could be conferred by the same gene with a general role in controlling resistance to intracellular infections ¹². Mendelian segregation analyses ^{13,14}, and genetic mapping studies ^{15,16} supported this notion, with resistance in both cases segregating as a dominant gene on mouse chromosome 1. Resistance of mice to *Mycobacterium bovis* BCG ¹⁷ and *Mycobacterium lepraemurium* ¹⁸ were subsequently found to follow the same inbred strain distribution pattern as *Ity* and *Lsh*, suggesting a single locus or group of tightly linked loci with an even broader role in resistance to intracellular pathogens. Indeed, the mode of inheritance ¹⁹, and chromosomal localization of *Bcg* ²⁰ was also shown to be identical to that of *Ity* and *Lsh*.

Experiments *in vivo* determined that the cell type expressing the phenotypic difference at *Bcg/Ity/Lsh* was bone marrow-derived, radiation-resistant, and sensitive to the macrophage poison silica ²¹⁻²⁴. Furthermore, *in vitro* studies with explanted cell populations showed differences in the capacity of macrophages from resistant and susceptible mice to restrict growth of intracellular *Salmonella* ²⁵, *Mycobacterium* ^{26,27}, and *Leishmania* ²⁸. Together these results suggested that the inherited resistance to all of

these pathogens was a result of a single gene conferring enhanced bacteriostatic or bactericidal mechanisms in the mature macrophages of resistant mice.

Due to the absence of a known gene product or simple assay for gene function, positional cloning was utilized to isolate the *Bcg/Ity/Lsh* gene. This approach involved following the inheritance of resistance to infection in comparison to the inheritance of known markers throughout the genome in close to 1500 backcross and recombinant inbred mice to generate a high resolution linkage map in the vicinity of the *Bcg*²⁹. This genetic map was then converted to a physical map by isolation and characterization of overlapping DNA fragments which covered the entire genetic interval³⁰. Once the physical interval had been cloned, transcription units were isolated from the interval by exon amplification and these were further analyzed as candidates for *Bcg*. Among six candidates identified in the cloning of *Bcg*, one was a novel gene expressed exclusively in spleen and liver and enriched in macrophage populations derived from them. This gene was given the name *Nramp1* (natural resistance associated macrophage protein 1)³¹. The *Nramp1* gene encodes a highly hydrophobic protein of predicted molecular mass 60kDa with characteristics of an integral membrane protein, including 10-12 putative transmembrane (TM) domains, and a glycosylated extracytoplasmic loop³¹.

Sequencing of the *Nramp1* mRNA from 27 *Bcg^r* and *Bcg^s* inbred mouse strains revealed that susceptibility to infection was associated with a single nucleotide change resulting in a non-conservative glycine to aspartic acid substitution within a predicted TM domain of the protein³². Although the addition of a charged residue into a transmembrane domain is predicted to disrupt the secondary structure of the protein, direct evidence was required to confirm that the mutation in *Nramp1* was the determinant

of susceptibility to infection in *Bcg^S* mice. To formally demonstrate this, a transgene containing the resistance allele of *Nramp1* (*Bcg^R*, G169) was introduced onto the genetic background of a susceptible mouse strain (*Bcg^S*, D169), and resistance to infection with *Mycobacterium* and *Salmonella* was conferred³³. In the converse experiment, gene targeting in embryonal stem cells was utilized to create a mouse mutant with a homozygous null allele at *Nramp1*. Although the mutant *Nramp1^{-/-}* mice created on the 129sv background (*Bcg^R*) had normal appearance and longevity, they no longer possessed natural resistance to *Mycobacterium*, *Salmonella* and *Leishmania*³⁴. Together, these experiments proved definitively that the various phenotypes described for the *Bcg*, *Ity*, and *Lsh* loci are the result of a common genetic defect at *Nramp1*. Additionally, the *Nramp1^{-/-}* mice were no more susceptible to infection with *Mycobacterium*, *Salmonella*, and *Leishmania* than *Bcg^S*, (D169) mice, demonstrating that the D169 allele of *Nramp1* is functionally null³⁴.

1.3 *NRAMP1* and its role in human disease

The *Nramp1* gene was shown to be evolutionarily conserved, with a homologous gene in humans designated *NRAMP1*^{31,35}. The emerging role of *NRAMP1* in human diseases confirms the utility of the *Bcg* mouse model for its corresponding human diseases. The association of human *NRAMP1* polymorphisms with disease susceptibility has been most extensively studied in leprosy. Although *NRAMP1* alleles do not contribute to disease susceptibility in certain populations analyzed³⁶⁻³⁸, positive results were obtained in a large study of susceptibility to leprosy in South Vietnam³⁹. In this

study, segregation analyses were conducted on 285 Vietnamese and 117 Chinese families with leprosy. There was evidence of a co-dominant major gene in the Vietnamese families but no evidence for a major gene in the Chinese families. In the Vietnamese families alone, linkage was observed for both intragenic *NRAMP1* ($p < 0.05$) and extended *NRAMP1* haplotypes ($p < 0.02$). These results support the hypothesis that *NRAMP1* or a gene closely linked to it plays a role in susceptibility to leprosy in the Vietnamese families.

The association of *NRAMP1* polymorphic variants with susceptibility to another mycobacterial infection was demonstrated in a case-control study of tuberculosis in the Gambia, West Africa⁴⁰. In this study, the distribution of 4 polymorphic alleles of *NRAMP1* was determined in 410 adults with smear-positive pulmonary tuberculosis, as well as in 417 ethnically matched healthy controls. Patients with polymorphisms in intron 4 and in the 3' untranslated region of the gene were particularly over-represented in the tuberculous population, as opposed to those with most common *NRAMP1* genotypes ($p < 0.001$). The authors concluded that genetic variations at *NRAMP1* affect susceptibility to tuberculosis in West Africans. Together, these data show that human *NRAMP1* may be an important determinant of susceptibility or progression of at least two major infectious diseases caused by *Mycobacterium*.

A promoter polymorphism has been identified in *NRAMP1* that was shown *in vitro* to result in a higher expression level of the gene, both in the absence of stimuli and after activation with IFN- γ and bacterial lipopolysaccharide⁴¹. This led to the hypothesis that while a deficit of *NRAMP1* activity could lead to susceptibility to infection, an excess

of *NRAMP1* activity could lead to autoimmune or inflammatory disease. One disease that was examined in relation to this hypothesis was rheumatoid arthritis, a chronic inflammatory disease. In a study of affected sib pairs from 61 multicase rheumatoid arthritis families from England's Arthritis and Rheumatism Council (ARC) national repository, a bias towards transmission of this polymorphic allele to affected offspring was observed ($p=0.048$). However, more recent studies of 200 multicase rheumatoid arthritis families from the same ARC repository as well as 85 probands from twins studies and 96 unaffected controls reported no evidence for increased sharing of *NRAMP1* alleles in affected sib pairs and excluded the possibility of a major genetic effect of *NRAMP1* in these families ^{42,43}.

The hypothesis of *NRAMP1* involvement in inflammatory bowel disease was also examined. Inflammatory bowel disease includes Crohn's disease and ulcerative colitis, and has been suggested to be caused by a hyperactive immune response towards normal intestinal flora ⁴⁴. In one study an association of a region spanning *NRAMP1* with Crohn's disease was observed. Out of 103 Crohn's patients and 98 unrelated controls, a particular extended haplotype spanning *NRAMP1* was present in 15% of the patients but in only 5% of controls ($p = 0.001$) ⁴⁴. However, when the analysis was done using alleles of *NRAMP1*, no significant associations were observed. This may have been limited by the lack of informative polymorphisms at *NRAMP1* in this study. In a separate study with 270 healthy controls, 74 Crohn's patients, 72 cases of ulcerative colitis, and 40 cases of sclerosing cholangitis, no association was seen between *NRAMP1* alleles and any form of inflammatory bowel disease ⁴⁵.

Several general caveats of human genetic studies may put the above results into context. For studies that indicate a positive association or linkage, it cannot be ruled out that this linkage or association is due to the proximity of *NRAMP1* to another gene conferring resistance or susceptibility to disease. This can be especially significant in the absence of corroborating functional data, such as the identification of a mutation or deletion in *NRAMP1* that would result in a functional impairment in affected individuals. Indeed, the gene encoding the IL8 receptor is tightly linked to *NRAMP1* (<150 kb, 46). IL8 is a chemokine secreted by monocytes and macrophages that acts to recruit and activate neutrophils, so it is implicated in the same types of pathways as *NRAMP1*. Additionally, false positive results can occur in case-control association studies if the controls are not ethnically matched to the cases. On the other hand, negative results in these types of studies may be due to a lack of informative polymorphic markers around *NRAMP1*, reducing the power to detect an effect of *NRAMP1*. The number of probands can also limit the power of these analyses. In addition, *NRAMP1* might determine disease susceptibility in one population, but a similar phenotype of susceptibility to disease in another population might be controlled by another locus (genetic heterogeneity). Future studies may clarify the role of *NRAMP1* in mycobacterial and inflammatory disease, and may determine if *NRAMP1* plays a role in human susceptibility to other infectious agents as well, including *Salmonella*, *Leishmania*, and other species under control of *Nramp1* in mice.

1.4 *Nramp1* expression in professional phagocytes

Detailed studies in mice and humans have revealed a striking pattern of tissue and cell specific expression of *Nramp1*/*NRAMP1* mRNAs. In a panel of normal mouse tissues, *Nramp1* mRNA was detected exclusively in the spleen and liver, and enriched in macrophage populations derived from these organs³¹. Using a panel of bone marrow-derived cell colonies corresponding either to undifferentiated progenitors or to mature lymphoid, erythroid and myeloid lineages, *Nramp1* mRNA was shown to be exclusively expressed in mature myeloid monocyte/macrophage and granulocytic cells⁴⁷. Using the murine macrophage cell line RAW264.7 as a model, both bacterial lipopolysaccharide (LPS) and interferon- γ (IFN- γ) were shown to up-regulate *Nramp1* mRNA expression, providing evidence that *Nramp1* levels are increased during macrophage activation in response to infectious and inflammatory stimuli⁴⁷.

In humans, *NRAMP1* gene expression is detected in lungs, liver and spleen, but is most abundant in peripheral blood leukocytes. Studies in purified blood cell populations showed that polymorphonuclear leukocytes are by far the major site of *NRAMP1* expression, followed to a lesser degree by monocytes. In addition, Northern blot analysis of mRNA from cultured cells demonstrated that increased *NRAMP1* expression was associated with differentiation towards mature macrophages and granulocytes⁴⁸. Therefore in both humans and mice, *Nramp1*/*NRAMP1* expression is restricted to professional phagocytes, and is higher in fully differentiated phagocytes than in immature progenitor cells.

1.5 Characterization of the Nramp1 protein

Western blot and immunoprecipitation analyses of both endogenous and transfected protein using polyclonal antisera directed against the N- and C-terminal portions of Nramp1 revealed Nramp1 as an integral membrane protein that migrates as a broad band with an apparent molecular mass of approximately 90-100 kDa⁴⁹. Almost 50% of this apparent mass has been shown to be due to extensive glycosylation with complex oligosaccharides, sensitive to digestion with the glycosidase PNGaseF⁴⁹. Additionally, incubation of macrophages with ³²P-orthophosphate resulted in a strong labeling of the protein, indicating that Nramp1 is phosphorylated *in vivo*⁴⁹. The mechanism and function of this phosphorylation has yet to be determined, although the Nramp1 primary amino acid sequence contains consensus sites for phosphorylation by protein kinase C and casein kinase II³¹.

Surprisingly, when immunoprecipitation was performed on macrophages from resistant (*Bcg^r*, G169) and susceptible (*Bcg^s*, D169) inbred mouse strains, no specific band corresponding to the mature Nramp1 protein was detected in macrophages from susceptible mice⁴⁹. Furthermore, mature Nramp1 protein is not detectable in Western blots of membrane preparations of macrophages of susceptible mice⁵⁰. In both instances the protein is readily detected in preparations from genetically resistant mice. The reason for this absence of mature protein in the G169D mutation is unknown, but could be due to misfolding and/or aberrant targeting, with most of the protein accumulating in the endoplasmic reticulum or Golgi apparatus resulting in rapid degradation. Such a situation has previously been noted for mutants in other membrane proteins such as CFTR^{51,52} and P-glycoprotein⁵³.

Immunofluorescence studies in primary macrophages from normal and *Nramp1*^{-/-} mutants together with studies in RAW264.7 transfectants expressing an epitope-tagged *Nramp1* have shown that *Nramp1* is not expressed at the plasma membrane, but rather is restricted to a subcellular membranous compartment of these cells (Chapter 2). Double-label immunofluorescence studies demonstrated that *Nramp1* colocalizes with *Lamp1* (lysosomal-associated membrane protein 1) in a late endocytic compartment (late endosome/lysosome), and becomes associated with the membrane of the phagosome during phagosomal biogenesis (this will be discussed in detail in Chapter 2).

1.6 Functional studies

1.6.1 Historical perspective

Before the identification and cloning of *Nramp1*, models for the study of *Bcg/Ity/Lsh* function were limited to the pre-existing inbred mouse strains, congenic mouse strains, and a set of immortalized bone marrow macrophage cell lines derived from one of the congenic mice strains and a non-congenic control⁵⁴. Because inbred mouse strains have innumerable genetic differences that are not related to *Nramp1*, they are not the ideal system in which to examine the specific effects of *Nramp1*. In order to limit non-*Nramp1* genetic differences, a congenic mouse strain was made in BALB/cJ (*Bcg*^f) mice carrying a portion of chromosome 1 from DBA/2 (*Bcg*^R) mice, spanning from isocitrate dehydrogenase (*Idh1*) to peptidase 3 (*Pep3*)⁵⁵. This genetic interval was originally estimated to be 30 cM, but newer mapping data from the Mouse Genome Database lists the interval as 41.2 cM⁵⁶. This interval contains a number of genes including those encoding cell surface molecules implicated in T cell activation (CD28,

CD152), cytokines (IL10), and cytokine/chemokine receptors (IL8RB, CXCR2, CXCR4), a lysosomal protease (cathepsin E), and signaling molecules (PLC δ , PTPRN) ⁵⁶. With an interval this large containing many genes that could be implicated during infection, it is still not possible to attribute any phenotypic differences between the congenic strains to *Nramp1* in particular. The same limitation applies to a second congenic strain (B10.A) was independently derived in C57BL/10 (*Bcg*^f) mice carrying a portion of chromosome 1 from A/J (*Bcg*^R) mice ⁵⁷. Immortalized cell lines were derived from bone marrow macrophages from B10.A congenic mice and non-congenic C57BL/10 controls using a recombinant retrovirus expressing v-myc and v-raf ⁵⁴, and have been used for many studies on *Nramp1* function. In addition to the non-*Nramp1*-related genetic differences discussed above, these cell lines may have additional differences resulting from their derivation from single cells out of a population known to be heterogeneous ^{58,59}. Studies using these systems must be interpreted with caution, and with awareness of their limitations.

1.6.2. Transfection studies

Since the identification and cloning of *Nramp1*, studies have been published using transfected macrophage cell lines that reveal pleiotropic consequences of *Nramp1* expression. Stable transfectants of myc-epitope-tagged, wildtype (G169) *Nramp1* were made in RAW 264.7 macrophages, a cell line derived from BALB/c mice and therefore endogenously expressing the mutant D169 allele of *Nramp1*. The expression and proper targeting of the transfected protein was verified by Western blot and immunofluorescence using an anti-myc tag antibody. During a 24 hour *in vitro* infection with *Salmonella*

typhimurium, the *Nramp1* (G169)-transfected clones inhibited the intracellular bacterial replication, whereas in control cells the bacteria replicated freely⁶⁰. Thus, the transfected cDNA was shown to confer greater bacteriostatic activity to the macrophages. In other studies, RAW 264.7 cells were transfected with either the wildtype G169 or mutant D169 allele of *Nramp1*. Although protein expression was not determined, clones expressing the wild-type *Nramp1* mRNA were reported to display increased superoxide anion production after PMA stimulation, increased production of nitrite, increased uptake of ³H-L-arginine (a precursor for NO production), a modest increase in class II MHC surface expression, and increased presentation of 1 out of 4 antigens tested to antigen-specific T-cells, when compared to the clones transfected with the mutant allele^{61,62}. From these studies it was concluded that expression of the G169 allele of *Nramp1* leads to a higher state of macrophage priming for activation. Notably, the endosomal and lysosomal environment could have a direct effect class II-associated antigen presentation, since these antigens are derived from the contents of phagocytic vesicles⁶³. However, the link between *Nramp1* and the other phenomena observed in this study is not clear, and awaits further investigation.

1.6.3. Studies in *Nramp1*^{-/-} mice

Since *Nramp1*^{-/-} mice and their wildtype littermates are genetically identical except for the presence or absence of a functional *Nramp1* protein, they comprise the best system in which to assess the affects of *Nramp1*. Studies in these mice have demonstrated that when compared to their *Nramp1*^{+/+} (wildtype) littermates, *Nramp1*^{-/-} mice are susceptible to *Toxoplasma gondii*, and *Mycobacterium avium* indicating that

Nramp1 plays a role in the defense against these pathogens in addition to the previously described ones (reviewed in ⁶⁴). However, the effect of Nramp1 on infection is not universal, as it has been shown to play no role in resistance/susceptibility to *Legionella pneumophila*, *Listeria monocytogenes*, *Pseudomonas aeruginosa*, *Staphylococcus aureus*, and *Bacillus subtilis* (reviewed in ⁶⁴). The observations that *Nramp1* can have no effect on infection with some parasites yet can confer resistance to infection with a group of antigenically and taxonomically unrelated parasites suggests that this group may share a common mode of microbial pathogenesis and may be combated by a common mode of host defense.

1.6.4 *Nramp1* and *Mycobacterium tuberculosis*

The role of *Nramp1* in *Mycobacterium tuberculosis* (MTB) infection remains controversial. As discussed in section 1.3, there is evidence that *NRAMP1* plays a role in susceptibility to tuberculosis in some human populations ⁴⁰. In mice, studies of inbred and congenic strains showed that at certain time points after intravenous infection with fewer than 10^3 MTB strain Erdman, the titre of bacilli in the spleens and lungs of *Bcg^S* strains was 1.5-10 fold higher than the amount found in *Bcg^R* strains ⁶⁵. *In vitro* studies of resident peritoneal macrophages from *Nramp1^{-/-}* and control *Nramp1^{+/+}* mice showed that upon infection with MTB strain H37Rv, *Nramp1^{+/+}* macrophages produced more TNF- α and nitrites than their *Nramp1^{-/-}* counterparts ⁶⁶. This could be predicted to result in more killing of MTB bacilli in resistant mice. Recently, however, *in vivo* studies demonstrated that *Nramp1^{-/-}* mice are no more susceptible to infection after intravenous injection of 10^3 and 10^4 *Mycobacterium tuberculosis* strain H37Rv than their *Nramp1^{+/+}*

littermates. Susceptibility was measured by cfu (colony-forming unit) determination in infected organs, and by survival time in the animals that were injected with the higher dose of MTB ⁶⁷. Further investigation is clearly necessary in order to reconcile the seemingly contradictory results of these studies. Perhaps the differences observed *in vitro* are not enough to protect the animal from succumbing to the *in vivo* infection under the experimental conditions used. Indeed, the 129Sv *Nramp1*^{+/+} mice used in the infection study have previously been categorized as susceptible to MTB infection under these conditions, suggesting the presence of other genes controlling infection in these studies ⁶⁸. It is also important to note that intravenous injection of thousands of bacilli is not considered the best model for human tuberculosis, which is usually initiated by the inhalation of very few mycobacteria (see section 1.7). *In vivo* experiments in the *Nramp1*^{-/-} and control *Nramp1*^{+/+} mice using a lower initial inoculum of bacilli introduced by inhalation will be necessary to obtain definitive data on the role of *Nramp1* in mouse tuberculosis.

1.6.5 *Nramp1* and Phagosomal Acidification

Microorganisms are normally internalized by macrophages and sequestered into membrane-bound vacuoles termed phagosomes. In most instances, the phagosome matures from a plasma membrane-derived envelope into an effective microbicidal organelle through fusion with early endosomes, late endosomes and lysosomes, thereby acquiring lytic enzymes and becoming acidic through acquisition of the vacuolar H⁺-ATPase ⁶⁹⁻⁷³. It has previously been shown that many mycobacterial species, including *M. tuberculosis*, *M. bovis*, and *M. avium*, survive intracellularly by prematurely arresting

the process of phagosomal maturation ⁷⁴⁻⁷⁸ and reside within compartments with attenuated acidity ^{72,79,80}. Although the procedures and results for specific markers vary from study to study, the consensus is that these mycobacterial phagosomes retain the ability to fuse with early endosomes but are unable to fuse with lysosomes (reviewed in ⁸¹). This defect is observed only with live mycobacteria, and is abrogated when the mycobacteria are heat killed before phagocytosis ⁷², killed *in situ* ⁸², or upon activation of the host macrophage ⁸³.

The mycobacterial factors and mechanisms mediating inhibition of fusion have not been fully characterized. Two structurally related mycobacterial components, sulfatide (multiacylated trehalose sulfate), and cord factor (trehalose dimycolate), have been implicated in inhibition of phagosome-lysosome fusion ^{84,85}. Incorporation of cord factor, a glycolipid component of the mycobacterial cell wall, into phospholipid vesicles inhibits their homotypic Ca^{2+} -dependant fusion ⁸⁵, suggesting that if mycobacteria could transfer cord factor into the host phagosomal membrane, it could act at this location to inhibit phagosome/lysosome fusion. Recent video microscopy studies have documented trafficking of mycobacterial lipids throughout host cell membranes, and preliminary evidence suggests that cord factor is among the lipids involved, offering a possible explanation of how inhibition of phagosome-lysosome fusion is achieved by mycobacteria ⁸⁶.

The emerging evidence, however, suggests that the mycobacterial capacity to inhibit phagosome-lysosome fusion is reduced if not abrogated in the presence of a functional host cell *Nramp1*. Using electron microscopy of bone marrow-derived macrophages from BALB/c.*Bcg*^R congenic mice and BALB/c control mice, deChastellier

87 first demonstrated that lysosome fusion with *Mycobacterium avium*-containing phagosomes (measured by the presence of acid phosphatase in the phagosome) was twice as frequent in *Bcg^R* macrophages than in *Bcg^S* ones. These results have now been corroborated using wildtype and *Nramp1^{-/-}* mice 88. Furthermore, studies using microscopic imaging technology to examine the properties of phagosomes in wildtype and *Nramp1^{-/-}* peritoneal macrophages have uncovered a similar effect during BCG infection 72. In these studies, peritoneal macrophages were isolated and fed inert latex beads, heat-killed BCG, or live BCG mycobacteria. The pH inside phagosomes was measured by conjugation of pH-sensitive dyes to the particles before phagocytosis followed by microfluorescence ratio imaging of the particles within the phagosomes. While the phagosomes containing heat-killed BCG or latex beads were found to acidify fully and to the same extent in both wild-type and *Nramp1^{-/-}* macrophages (pH 5.5), phagosomes containing live BCG displayed attenuated acidification in the *Nramp1^{-/-}* macrophages (pH 6.5), yet acidified normally in the wildtype macrophages (pH 5.5). Further investigation revealed that the decreased acidification of the BCG-phagosomes in the *Nramp1^{-/-}* macrophages was correlated with decreased fusion of these phagosomes to the late-endocytic compartments, as determined by quantification of Lamp2 (a late endosomal/lysosomal marker) around the BCG-phagosome. The decreased acidification of the BCG-phagosomes in the *Nramp1^{-/-}* macrophages was also associated with decreased vacuolar H⁺-ATPase activity.

The effect of Nramp1 on phagosomal acidification is not global, as acidification of latex bead or dead BCG containing phagosomes proceeds identically in the presence or absence of Nramp1 72. Are other microbes under control of *Nramp1* inhibited from

replicating by a similar effect of *Nramp1* on their phagosomal pH? Such a scenario is unlikely, since *Mycobacterium lepraemurium* has been shown to reside in fully matured, acidified phagosomes under the same experimental conditions where phagosomal maturation was inhibited by BCG⁷⁶. In addition, *Nramp1* controls replication during *in vitro*²⁸ and *in vivo*³⁴ infection with *Leishmania donovani* amastigotes, which are also known to reside in fully acidified phagosomes⁸⁹(see section 1.7).

1.7 Pathogenesis of *Nramp1*-controlled diseases in mice and humans

Although the microbes affected by *Nramp1* are taxonomically and antigenically unrelated, they do share some common features of pathogenesis. A strong correlation can be noted between the cellular (in macrophages) and subcellular (at the phagosome) localization of *Nramp1* and the known sites of microbial proliferation during the course of these diseases. The time course of *Nramp1* action, plus the functionality of *Nramp1* in isolated macrophage populations *in vitro* establishes that *Nramp1* acts in the pre-immune stage of infection, without the requirement for pathogen-specific T or B cells. However acquired immunity is eventually important for successful resolution of the intracellular infections that are under *Nramp1* control. Another common feature shared by these pathogens is a large variability of disease onset or clinical severity seen in human infections, which may be attributed in part to genetic variation of the host. Details of the interaction of the host with some of microbes under control of *Nramp1* are reviewed below.

1.7.1 *Mycobacterium* species

Tuberculosis is caused by a group of closely related acid-fast, weakly Gram positive bacilli known as the *Mycobacterium tuberculosis* complex. This group consists of *M. tuberculosis* (MTB), the most common causative agent of tuberculosis, *M. bovis*, *M. africanum*, and *M. microti*⁹⁰. BCG (Bacillus Calmette-Guerin) is an attenuated strain of *Mycobacterium bovis* that was developed for use in vaccination against tuberculosis and leprosy, and is not normally lethal to humans or mice⁹⁰⁻⁹². However, BCG causes disease in approximately 1 in 10⁶ people following vaccination⁹². These rare cases often have some form of deficiency in their innate or acquired immunity that compromises their ability to fight off infection, for example mutations in the interferon gamma receptor⁹³, IL12 receptor^{94,95}, or in the NADPH oxidase system that produces reactive oxygen species⁹⁶.

In mice, the kinetics of BCG infection have been well documented^{97,98}. After intravenous inoculation, BCG localizes to the liver, spleen, and lungs. In the pre-immune phase of infection (lasting approximately three weeks), BCG multiplies in macrophages of the spleen and liver. The amount of replication is inversely proportional to the dose of the injected BCG, meaning a low dose of BCG will multiply more than a high dose. Since *Nramp1* acts to control bacterial replication at this stage, the effect of *Nramp1* is more pronounced when mice are given a low initial dose of bacilli, and can lead to a two to three log difference in the spleen-associated bacteria. In the late phase of infection, susceptible strains progressively resolve the infection through T cell dependent macrophage activation, resulting in granuloma formation^{34,98,99}. T cells are necessary for resistance in the late phase of BCG infection, but are not involved in the *Nramp1*-

mediated phenotype, since athymic nude AKR mice control the replication of BCG in the first three weeks of infection, but allow bacterial proliferation at later time points ²³.

Human tuberculosis is transmitted almost exclusively from person to person by inhalation of the infectious agent in aerosolized droplet nuclei ⁹⁰. If the bacteria reach the terminal bronchioles and alveoli, where they are engulfed by local alveolar macrophages, bacilli may multiply and lead to a focus of infection. From the lung, the bacilli are carried to the lymph nodes, where they may also gain access to the bloodstream, leading to a disseminated infection ⁹⁰. The virulence of MTB seems to be related to its ability to inhibit phagosome-lysosome fusion and survive within macrophages ¹⁰⁰. Cell-mediated immunity is also crucial for controlling MTB infection: if successful, granulomas form from activated macrophages and serve to "wall off" the infected area and create an unfavorable environment for mycobacterial replication (low oxygen tension, low pH) where the bacilli may eventually die or persist latently. Without cell-mediated immunity, the disease will spread and progress, as is seen in AIDS patients, who have a very high rate of reactivation of latent tuberculosis, with an accelerated clinical course and poor prognosis ⁹⁰. In the general population, only 10% of people infected with MTB ever develop the disease ⁴⁰. Racial variation in tuberculosis susceptibility ^{101,102} and studies in twins ¹⁰³, strongly suggest that genetic factors play a role in tuberculosis susceptibility. As discussed in section 1.3, *NRAMP1* may be one of these genetic factors ⁴⁰.

Leprosy is caused in humans by *M. leprae*, an obligate intracellular parasite. *M. leprae* is thought to enter the body through the skin or upper respiratory tract after contact with infected persons, however it is often difficult to define the conditions that lead to

onset of disease since the incubation time is long (2-5 years) ¹⁰⁴. Infection with *Mycobacterium leprae* leads to chronic infectious disease with a broad spectrum of clinical manifestations, ranging from tuberculoid leprosy, characterized by small, localized lesions containing a small number of mycobacteria to lepromatous leprosy, with gross physical disfigurement, a high body burden of macrophage-associated mycobacteria, and high mortality rate. It has long been suspected the genetic make-up of the host affects the clinical severity of the disease ¹⁰⁵⁻¹⁰⁷. *NRAMP1* has been implicated in susceptibility to leprosy in humans, suggesting that it might be involved in controlling the replication of *M. leprae* within macrophages, leading to variable numbers of mycobacteria in the host ³⁹. The clinical disease severity of leprosy may also be affected by cell-mediated immune responses, as tuberculoid patients are known to have effective cell mediated immunity, whereas lepromatous patients are anergic ¹⁰⁴.

Mycobacterium lepraemurium is the causative agent of mouse leprosy. It is an obligate intracellular parasite that infects macrophages of the reticuloendothelial system, where it resides in fully matured, acidified phagosomes. In contrast to BCG, infection with *M. lepraemurium* is progressive and fatal regardless of the strain of the mouse ¹⁸. Even so, in *M. lepraemurium* infections, the effect of *Nramp1* is evident in the survival time, parasite doubling times, and spleen weights, which are favorable in resistant mice ^{18,108}.

1.7.2 *Leishmania*

Leishmaniasis can be divided into the clinical categories of cutaneous, mucocutaneous, and visceral disease, with visceral being the most severe. *Leishmania*

donovani is almost exclusively associated with visceral leishmaniasis rather than cutaneous or mucocutaneous, although only approximately 1 in 6.5 people infected will develop disease ¹⁰⁹. The reasons for this are unknown: genetic factors such as *NRAMP1* could be involved. Visceral leishmaniasis, also known as kala azar, is a generalized infection of the lymphoreticular system, causing fever, hepato- and splenomegaly, anemia, progressive emaciation, and often death. Humans are infected with *Leishmania* via an insect vector, the phlebotomine sandfly. *Leishmania* exists as a flagellated promastigote in the sandfly but transforms to a nonflagellated amastigote in human macrophages ¹⁰⁹. While promastigotes survive inside macrophages by inhibiting phagosome-lysosome fusion ¹¹⁰, amastigotes proliferate inside fully acidified phagolysosomes ⁸⁹. From the primary site of infection, amastigotes spread through the reticuloendothelial system to the spleen, liver, bone marrow, and lymph nodes. There is then a huge influx of macrophages to the liver and spleen which causes the enlargement of these organs associated with the disease. The disease usually lasts several years, although acute cases may lead to death within 5 months ¹⁰⁹.

L. donovani causes visceral leishmaniasis-type disease in mice as well.

Experimental infections are generally initiated by intravenous injection of amastigotes. In mice the outcome of *Leishmania donovani* infection depends on *Nramp1* controlling early parasite replication in the liver ³⁴. Some *Nramp1*-sensitive mice are still able to recover from *Leishmania donovani* infection by mounting an efficient cell-mediated immune response, control of which is linked to the H-2 haplotype ¹¹¹.

1.7.3 *Salmonella*

Typhoid fever is described as a severe systemic infection of the reticuloendothelial system, which is associated with a large variety of early symptoms (headache, fever, chills, anorexia, weakness), and the later symptoms of abdominal pain and fever (reviewed in ^{112,113}). It is caused by *Salmonella typhi*, a primate-specific pathogen that does not infect laboratory animals. However, infection of mice with the closely related *Salmonella typhimurium* is considered a model for typhoid fever. *S. typhimurium* are facultative intracellular bacteria with a wide host range that cause gastroenteritis in human hosts, but severe systemic infections in mice.

Humans contract *Salmonella typhi* infections through fecally contaminated food or water. The disease is therefore most common in areas of the world where sewage disposal and water purification is poor. 1-6% of typhoid patients become chronic carriers of the bacteria, acting as reservoirs for the spread of disease. *Salmonella* penetrate the intestinal barrier through ileal Peyer's patches and quickly gain access to the regional lymphatics, where they are engulfed by phagocytes. In experimental infections of mice, *Salmonella* are often directly injected into the bloodstream. Whether infection is through the gastrointestinal tract or direct intravenous injection, *Salmonella* quickly find their way to the reticuloendothelial system, where they are engulfed and carried through the blood and lymphatics to the liver and spleen. The bacteria multiply rapidly within phagocytes and cause enlargement of the spleen and liver due to influx and hyperplasia of cells. (reviewed in ¹¹³).

Salmonella enter macrophages and other cells through a process distinct from classical receptor-mediated phagocytosis termed invasion and form characteristic

"spacious phagosomes", also called Salmonella-containing vacuoles (SCVs) ¹¹⁴⁻¹¹⁶. SCVs interact with the endocytic network in an atypical way that diverges from the normal degradative pathway of the host cell, but has not yet been completely characterized. The SCV acquires some markers of late endosomes and lysosomes (Rab7, Lamp1), yet stays negative for others (mannose-6-phosphate receptor) ^{116,117}. While some groups have reported rapid fusion with lysosomes and full acidification of the SCV ^{118,119}, others have reported delayed or attenuated acidification ^{120,121}. The most recent data indicates that inhibition of phagosome-lysosome fusion by *Salmonella* is necessary for virulence. SpiC is a *Salmonella typhimurium* effector protein that is translocated from the SCV to the host cell cytosol, where it causes a significant decrease in intracellular vesicle trafficking, including decreased fusion of the SCV with endosomes and lysosomes ¹²². SpiC is required for successful infection of macrophages *in vitro* ¹²², and is most likely required for virulence *in vivo* ^{123,124}.

Susceptible mice with *Nramp1* mutations succumb very quickly to *Salmonella typhimurium* infection. Differences are seen early on in infection in the numbers of bacteria in the liver and spleen of resistant versus susceptible mice ⁵⁰. Susceptible mice die within one week of inoculation, whereas *Nramp1*^{+/+} mice are able to control replication of the bacteria and successfully clear the infection ³⁴. It has not yet been determined whether *NRAMP1* has an analogous effect on replication of *Salmonella typhi* in human infections, although this question is of obvious clinical importance. *Salmonella* seems to be unique among the *Nramp1* affected microbes in that both cell-mediated and humoral responses seem to be important in the anti-*Salmonella* immune response ¹¹³. This may be due to extracellular growth of the bacteria.

1.8 Modifiers of *Nramp1*

As described above, infection is a complex process involving many serial steps of pathogenesis. In order to accomplish resistance to infection, the host must successfully combat the pathogen at each of these serial steps. Each step, in turn, is comprised of many genes and gene products acting sequentially or synergistically. Therefore, although it is true that bacterial replication in the early phase of intracellular infections is strictly controlled by *Nramp1*, there exist numerous examples of mice or humans with resistance alleles at *Nramp1* that are nonetheless susceptible to infection. *Nramp1* function can therefore be considered necessary, but not sufficient for resistance to infection. Other genes involved in *Nramp1*-moderated infections are discussed below.

C3H/HeJ mice (*Nramp1*^{+/+}) are killed by *Salmonella typhimurium* within the first week after infection, regardless of the inoculum size¹²⁵, due to a mutation in the *Tlr4* gene^{126,127}. *Tlr4* encodes a member of the Toll family of transmembrane proteins, which includes the IL-1 receptor and *Drosophila* Toll, which is implicated in sensitivity to fungal infections in fruit flies. *Tlr4* is involved in signal transduction after binding of bacterial LPS to CD14 molecules on the plasma membrane of cells, leading to transcription of inflammatory cytokines.

CBA/N mice have an X-linked immunodeficiency that causes reduced numbers of peripheral B cells, and abnormal characteristics of those that are present. This leads to impaired humoral immunity, resulting in susceptibility to some bacterial pathogens, including *Salmonella typhimurium*¹²⁸. The immunodeficiency of CBA/N mice is considered a model for human X-linked Agammaglobulinemia (XLA), both of which are

caused by mutations in *Btk*, a novel src-like tyrosine kinase involved in B cell maturation 129-132.

Finally, the wild-derived inbred mouse *Mus musculus molossinus* (MOLF/Ei) is extremely susceptible to *S. typhimurium* infection, despite resistance alleles at *Nramp1*, *Lps*, and *Btk*. The molecular basis of susceptibility in MOLF/Ei mice is not yet known, although a genome-wide scan using F2 C57BL/6J and MOLF/Ei intercross mice identified two new loci affecting survival time³⁴⁴.

Lyst is mutated in Chediak-Higashi syndrome (CHS) in humans, and in the *beige* mouse, a model for CHS. CHS is a rare autosomal recessive disorder that involves, among other symptoms, a marked increase in susceptibility to infection. Although the exact biochemical function of *Lyst* is still under investigation, it is involved in intracellular trafficking in the endocytic and exocytic pathways, and biogenesis of lysosomes. Mice with the *bg* mutation have defective cytotoxic T-cells, neutrophils and natural killer cells, and are susceptible to a variety of pathogens, including *Leishmania donovani* 133.

The genes described above were all identified by positionally cloning the locus causing a susceptibility phenotype. In contrast to the "reverse genetics" approach of positional cloning, where the phenotype is known and the gene is pursued, many groups have used "forward genetics" to create a defect in a known gene in order to investigate the resulting phenotype. This approach has been used to confirm the roles of many genes that were previously suspected to be involved in resistance to infections (reviewed in 134). The roles of inducible nitric oxide synthase (iNOS), interferon γ receptor, and IL-

12 in resistance of mice to infection with *Mycobacterium* and *Leishmania* have been demonstrated in this way 135-140.

1.9 The *Nramp* gene family and divalent cation transport

1.9.1 *Nramp2*

The biochemical mechanism of *Nramp1*, including the possible substrate transported by this protein remains to be determined. However, important clues have come from the recent discovery and study of additional *Nramp* genes. The third and fourth chapters of this thesis describe the identification and characterization of a second mammalian *Nramp* gene, *Nramp2*. *Nramp2* encodes a protein that is highly homologous to *Nramp1* (64% identity, 78% similarity) which, in contrast to phagocyte-specific *Nramp1*, is ubiquitously expressed (Chapter 3). The function of *Nramp2* was also unknown until recently, when two independent reports showed by very different methods that *Nramp2* functions as a transporter of divalent cations, including iron. In the first study, *Nramp2* was isolated by expression cloning from a rat cDNA library in *Xenopus* oocytes in a screen for iron transport proteins¹⁴¹. The goal of this study was to identify the transporter responsible for absorption of non-heme iron from the diet. The cDNA library used in these studies was prepared from the duodenum of iron-starved rats, where high iron transport activity had previously been described by physiological means^{142,143}. A single cDNA was isolated that led to a 200-fold increase in iron uptake compared to control uninjected oocytes. This cDNA was found to encode rat *Nramp2* (designated DCT1 in this report). Expression of *Nramp2/DCT1* in oocytes was shown to mediate electrogenic transport of Fe^{2+} , Mn^{2+} , Zn^{2+} and other divalent metals, but not Ca^{2+}

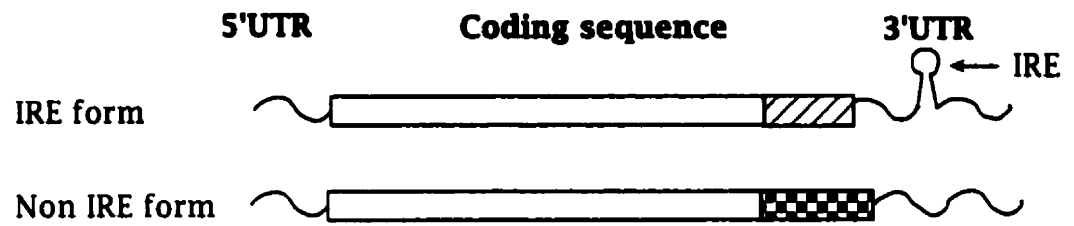
or Mg^{2+} . The transport was pH-dependent, with maximum activity at pH 5.5. mRNA expression studies in this report confirmed ubiquitous expression of *Nramp2*, and demonstrated a striking upregulation of the mRNA levels in the proximal intestine following chronic iron depletion ¹⁴¹.

Comparison of the isolated rat cDNA sequence to the mouse *Nramp2* sequence revealed that the predicted amino acid sequence of DCT1 was almost identical to mouse *Nramp2*, except at the extreme C-terminus, where the sequence diverged, but was homologous to the published C-terminal sequence of human NRAMP2. Analyses by other groups revealed that in mouse, rats, and humans, two alternatively-spliced isoforms of the *Nramp2* cDNA exist, with different predicted C-terminal tails ^{144,145}. In the newly identified splice isoform, the last 25 amino acids of the protein are replaced by a novel sequence of 18 amino acids. In addition, this splice form contains a putative iron-response element (IRE) in its 3'-untranslated region ¹⁴¹ (Figure 1). IREs are found in the untranslated regions (UTRs) of mRNAs encoding proteins involved in iron metabolism. These IREs mediate changes in protein levels in response to iron availability. When iron is scarce within cells, IRE-binding proteins (IRP1 and IRP2) are available to bind IREs. Binding of IRPs to IREs in the 5'UTR of messages such as that encoding ferritin causes a decreased translation of the message. Conversely, protein binding to IREs in the 3'UTR of mRNAs like the one encoding the transferrin receptor causes an increased half-life of the mRNA. When sufficient iron is present, IRP1 is inactivated and IRP2 is degraded. In this way, the coordinate regulation of iron uptake (transferrin receptor) and storage (ferritin) in response to iron availability is achieved (reviewed in ^{146,147}).

Figure 1 *Splice forms of Nramp2 mRNA.*

(A). Schematic representation of the alternative splice forms of *Nramp2*, showing the divergent C-terminal coding sequence and the putative iron response element (IRE) in the 3'UTR. The non-IRE form is the one described in Chapter 3 of this thesis, the IRE form was first described by Gunshin et al.¹⁴¹. (B). C-terminal amino acid sequences encoded by the two splice forms of mouse *Nramp2* mRNA, indicating the divergent amino acids (boxed).

A



B

IRE form GLSFLDCGRS **VSISKVLLSEDTSGGNIK** 561
Non IRE form GLSFLDCGRS **YRLGLTAQPELYLLNTVDADSVVSR** 568

In a simultaneous publication, a mutation in *Nramp2* was identified as the cause of iron deficiency in a mouse model of microcytic anemia, the *mk* mouse ¹⁴⁸. The *mk* mutant arose spontaneously in breeding stocks at the Jackson lab, where it was recognized as anemic due to its pale color and small size, and was subsequently maintained by breeding onto several genetic backgrounds ¹⁴⁹. Two other alleles of *mk* arose independently ¹⁴⁸. The *mk* mouse mutant is characterized by microcytic, hypochromic anemia: small red blood cells of abnormal morphology with a very low hemoglobin content, and increased numbers of reticulocytes (red blood cell precursors) and spleen enlargement due to increased hematopoiesis ¹⁴⁹. The *mk* mouse has poor viability before birth, manifested by fewer *mk/mk* offspring than predicted by Mendelian genetics, and increased mortality 1-3 weeks after birth ¹⁵⁰. There is an absence of stainable iron in the tissues ¹⁵¹, and decreased iron uptake from the gastrointestinal tract has been described using everted intestinal loops ¹⁵².

A *Nramp2* mutation is also the cause of disease in a radiation-induced rat mutant with a *mk*-like phenotype, the Belgrade (*b*) rat ¹⁴⁵. Like the *mk* mouse, the *b* rat exhibits hypochromic anemia, and deficient iron uptake in the intestine ¹⁵³. Both the *mk* mouse and the *b* rat carry the same mutation in *Nramp2*, a guanine to adenosine transition, causing a Glycine to Arginine substitution in the fourth predicted transmembrane domain of the protein (G185R). Transient transfection studies in 293T cells demonstrated that overexpression of the wildtype (G185) *Nramp2* protein caused a marked increase in Fe^{2+} uptake. When the mutated form of the protein (D185) was expressed, the Fe^{2+}

uptake was only slightly higher than in the control cells ¹⁵⁴. Polyclonal antisera were raised against the mouse Nramp2 protein (Chapter 4), and using this antisera, Nramp2 was localized to the brush border at the apical membrane of enterocytes in the proximal duodenum of mice ¹⁵⁵. This has previously been identified as the site of iron uptake in the intestine ^{142,143,156,157}. Together, the results of Gunshin ¹⁴¹, Fleming ^{145,148}, and Canonne-Hergaux ¹⁵⁵ provide compelling evidence that *Nramp2* is responsible for the intestinal absorption of non-heme iron. While the intestinal uptake of ferrous iron has been previously characterized at the physiological level, the molecular basis of this transport has long been an unanswered question.

Dietary iron exists in two forms, conjugated to heme, which is taken up with the porphyrin ring intact, and non-heme. Heme iron accounts for approximately one-third of all absorbed iron, the remaining two-thirds is non-heme. ^{147,158,159} Currently, it is widely accepted that Nramp2 is the intestinal transporter of non-heme iron ¹⁶⁰⁻¹⁶². The intestinal transporter of heme has not been characterized, but is independent of the non-heme transport system ^{158,159}. For simplicity, for the remainder of this thesis, "iron transport" will refer to transport of non-heme iron, unless otherwise specified.

Intestinal absorption of iron and other metals can be divided into three phases, uptake at the apical membrane of enterocytes, intracellular transport, and transfer across the basolateral membrane into the blood ^{158,159}. Uptake takes place at the brush border (apical) membrane of enterocytes of the upper portion of intestinal villi ^{156,157}. The phenotype of *mk* mice and *b* rats, as well as the localization of Nramp2 protein to this exact site ¹⁵⁵ are consistent with Nramp2 being involved in the uptake step. The

mechanisms of intracellular and basolateral transport of iron and other metals are not well understood at this time ^{161,162}, and are beyond the scope of the present work. The uptake of iron at the intestinal lumen proceeds without conjugation of iron to transferrin (reviewed in ¹⁶⁰), but requires reduction of ferric iron (Fe^{3+}) to the ferrous form (Fe^{2+}) ^{163,164}. Reductase activity is associated with the cell surface of enterocytes and other cells, although the enzyme involved has not been cloned ^{163,165}. Other divalent metals, such as Co^{2+} , Mn^{2+} and Zn^{2+} interfere with intestinal uptake of iron ¹⁶⁶⁻¹⁶⁹. These observations are all consistent with the known transport characteristics of Nramp2.

Nramp2 is not just implicated in iron transport at the intestine, since *mk* and *b* also exhibit defective iron transport in erythrocyte precursor cells known as reticulocytes ^{170,171}. The defect in reticulocytes has been extensively studied in *b* rats. As opposed to iron uptake in the intestine, which does not involve transferrin conjugation of iron, at least on the luminal side ¹⁶⁰, reticulocytes normally acquire iron via the transferrin cycle ¹⁷²: Iron-bound transferrin binds to cell surface receptors and the complex is internalized by endocytosis. As the pH of the endocytic vesicle is lowered, transferrin loses its affinity for iron, and the iron dissociates. Normally, iron is retained in the cell while transferrin is recycled back to the cell surface (see Chapter 4, figure 8). Studies using ⁵⁹Fe-¹²⁵I-labelled transferrin revealed that binding and uptake of transferrin were normal in the *b* rat, but instead of being retained, iron was recycled back to the cell surface along with the transferrin in *b* reticulocytes ^{171,173}. The transport activity of Nramp2, and the observed defect in the transferrin cycle of *b* reticulocytes suggests that Nramp2 may be the transporter responsible for translocating iron across the endosomal membrane into the cytosol. The colocalization of Nramp2 with transferrin in recycling

endosomes provides further support for this hypothesis (Chapter 4). Again, the molecular basis of this transport activity had long been an enigma.

Ultimately, accumulating evidence suggests that *Nramp2* may play a very broad role in the transport of iron and other metals in many tissues. Most tissues express transferrin receptors and are thought to acquire iron through the transferrin cycle¹⁴⁷. The implication of *Nramp2* in the transferrin cycle strongly suggests that it is involved in iron uptake in most tissues. This is in agreement with the ubiquitous expression of *Nramp2* observed (Chapter 3, 141). Indeed, *in vivo* studies using injected isotopic iron revealed decreased iron uptake from ⁵⁹Fe-¹²⁵I-labelled transferrin in *b* brain, liver, bone marrow, and heart, as well as decreased transport of ⁵⁹FeCl₃ across the intestine¹⁵³. When ⁵⁹Fe-¹²⁵I-labelled transferrin was injected into pregnant heterozygous female rats, homozygous *b* embryos took up 60% less iron than their heterozygous womb-mates. Additionally, skin fibroblasts prepared from *b* rat embryos display impaired uptake of ⁵⁹Fe-transferrin *in vitro*¹⁷³. While most physiological uptake of iron is transferrin-mediated, in states of iron overload or in artificially manipulated experimental conditions, uptake of non-transferrin bound iron (NTBI) can occur as well¹⁷⁴. This has been described in several cell types including fibroblasts, erythroleukemia cells, hepatoma cells, and reticulocytes. The properties of this transport system include competition by Cu²⁺, Mn²⁺, Cd²⁺, Ni²⁺ and Zn²⁺, and optimum activity at pH 5.5^{174,175}. These properties concur with those observed for *Nramp2*-mediated transport in *Xenopus* oocytes¹⁴¹. Furthermore, reticulocytes from *b* rats have been shown to have impaired uptake of non-transferrin-bound ferrous iron (NTBI) in addition to the defect in uptake of transferrin-conjugated iron^{173,176}. This suggests that transport through *Nramp2* is a

mechanism shared by the transferrin-dependent and independent iron uptake pathways in reticulocytes and other cells. Under physiological conditions Nramp2 is activated by the low pH inside acidified endosomes. By using an uptake medium at pH 5.5, Nramp2 molecules are (anomalously) activated at the plasma membrane, bypassing the need for endocytosis, and resulting in NTBI uptake.

In addition to the defects in iron metabolism, *b* rats are reported to have abnormalities in manganese metabolism¹⁷⁷ and *mk* mice show signs of zinc deficiency¹⁴⁵. Given the broad substrate range of Nramp2 as demonstrated in *Xenopus* oocytes¹⁴¹, it is not surprising that animals with *Nramp2* defects lack other divalent metals in addition to iron. Together, these results suggest that *Nramp2* plays a central role in the uptake of iron and other divalent metals, and provides a common link between many previously described modes and sites of iron transport: transferrin-dependent and transferrin independent, in reticulocytes, the intestine, and peripheral tissues¹⁷⁴.

1.9.2 *Nramp* homologs

Nramp homologs encoding conserved proteins have been identified in many phylogenically distant organisms through various genome sequencing projects, as well as by conventional cloning methods. *Nramp* homologs have been described in mammals, fish, insects, nematodes, plants, yeast, and bacteria^{178,179}. Some of these homologs are described in Table I.

The remarkable degree of sequence conservation among *Nramp* family members is suggestive of a parallel conservation of function. Recent studies provide strong support for this proposal. Zebrafish with mutations in an *Nramp*-homologous gene (*cdy*)

PROTEIN	ORGANISM	CLASSIFICATION	% IDENTITY* (to mNramp1)	SUBSTRATE (demonstrated/implied) [†]	MUTANT PHENOTYPE
mNramp	<i>M. musculus</i>	Animalia (chordata)	100%	Fe^{2+} Mn^{2+}	susceptibility to infection
mNramp2	"	"	64%	Fe^{2+} Zn^{2+} Mn^{2+} Co^{2+} Cd^{2+} Cu^{2+} Ni^{2+} Pb^{2+}	anemia
cdy	<i>D. rerio</i>	Animalia (chordata)	unknown	Fe^{2+}	anemia
malvolio	<i>D. melanogaster</i>	Animalia (arthropoda)	60%	Fe^{2+} Mn^{2+}	taste behaviour defect
CeNramp1, 2	<i>C. elegans</i>	Animalia (nematoda)	49-52%	unknown	unknown
OsNramp1,2,3	<i>O. sativa</i>	Plantae	31-46%	"	unknown
EIN2	<i>A. thaliana</i>	"	20%	"	ethylene insensitive
Smf1,2	<i>S. cerevisiae</i>	Fungi	24-25%	Mn^{2+} Cd^{2+} Cu^{2+} Co^{2+}	no growth on EGTA no growth at alkaline pH
yfeP	<i>E. coli</i>	Monera (eubacteria)	32%	Fe^{2+} Mn^{2+} Zn^{2+} Cd^{2+} Ni^{2+}	no growth in iron-free medium (hflB1 strain)
BRAMP	<i>M. bovis</i>	Monera (eubacteria)	29%	unknown	unknown

* % identity was calculated from an alignment of full length protein sequences in ClustalW and therefore may be lower than values previously calculated using the hydrophobic cores only.

† demonstrated substrate refers to those identified in isotope uptake or electrophysiological transport experiments, implied substrate is from complementation studies or mutant phenotype (see text)

have hypochromic microcytic anemia very similar to that seen in the *mk* mouse and the *b* rat, suggesting that fish *Nramp* functions as an iron transporter analogously to *Nramp2* 180. Yeast have two *Nramp* homologs, *SMF1* and *2*, and combined loss-of-function at both loci leads to hypersensitivity to EGTA as well as hypersensitivity to alkaline pH. *SMF1* was recently shown to function as a transporter of Mn^{2+} , Cu^{2+} and Cd^{2+} , and *SMF2*, a transporter of Co^{2+} 181-184. Mammalian *Nramp2*, but not *Nramp1*, was found to complement both the hypersensitivity to EGTA and hypersensitivity to alkaline pH characteristic of the *SMF1/SMF2* mutant yeast, demonstrating that the structural similarity between the mammalian and yeast *Nramp* proteins results in a functional similarity as well 185. Complementation by *Nramp2* was specific and required a functional protein, as independent mutations at residues highly conserved in the *Nramp* family abrogated *Nramp2* complementation. Since Mn^{2+} was the only divalent cation capable of completely suppressing both the EGTA and pH phenotypes, these results suggest that *Nramp2* can transport Mn^{2+} in yeast 185.

Other studies support a conservation of divalent cation transport function between *Nramp* proteins. The fruit fly *Nramp* homolog, known as *malvolio*, has been shown to be important for taste discrimination behavior in the fly 186. Whereas wild type flies will avoid media containing 100 mM sodium chloride and strongly favor media containing sugars, flies with a mutation in *malvolio* show an increased acceptance of salt, and a greatly reduced preference for sugars. However, when the flies are fed with media supplemented with excess Fe^{2+} or Mn^{2+} for a minimum of 2 hours before testing,

normal taste behavior is restored¹⁸⁷. This implies that malvolio is important for $\text{Fe}^{2+}/\text{Mn}^{2+}$ metabolism in the fly, and that these ions are somehow involved in taste perception in *Drosophila*.

Recent data has shown that divalent cation transport function is conserved in one of the Nramp proteins that is the most phylogenically distant from mammalian Nramp2. *YfeP* is a *Nramp* homolog in the Gram negative bacteria *Escherichia coli*. Elimination of *YfeP* by targeted disruption had no effect on wild-type *E.coli* under standard nutrient conditions. However, when the mutation was introduced onto the background of the metal-dependant *hflB1* strain, growth on media containing Fe^{2+} -chelators was abrogated. Additionally, expression of *yfeP* protein was shown to promote uptake of $^{55}\text{Fe}^{2+}$ and $^{54}\text{Mn}^{2+}$ that could be competed by excess non-radioactive Fe^{2+} , Zn^{2+} , Mn^{2+} , and Cd^{2+} .¹⁸⁸ The fact that *Nramp2* and its distant relative *YfeP* both encode divalent metal transporters supports the assertion that more closely related *Nramp* homologs whose functions have yet to be demonstrated (such as *Nramp1*) most likely encode divalent cation transporters as well. Indeed, overexpression of human *NRAMP1*, driven by the strong, ubiquitous promoter of *hsp70*, has recently been shown to rescue the taste defect in *mvl* mutant flies¹⁸⁹. The fact that human *NRAMP1* expression and $\text{Fe}^{2+}/\text{Mn}^{2+}$ supplementation result in similar phenotypic rescue in this system provides preliminary evidence that *NRAMP1* may act as a transporter of these metals, in analogy to other members of the Nramp family^{187,189}.

The most recently described member of the Nramp family, and the one with the least homology to other Nramp proteins is *EIN2*, from the plant *Arabidopsis thaliana*¹⁹⁰. *EIN2* was isolated from a screen for mutants that were insensitive to ethylene, a

hormone that regulates plant growth, development, and responsiveness to a variety of stresses. *EIN2* encodes a protein of 1294 amino acids, the first 461 of which are 20% identical to Nramp1 and are predicted to have a typical "Nramp-type" secondary structure with twelve transmembrane domains. The C-terminal 833 amino acids are predominantly hydrophilic with no significant homology to any known proteins. Many other loci involved in the ethylene signaling pathway have previously been cloned and characterized, including ethylene receptors, protein kinases, and transcription factors. The exact role of EIN2 in the ethylene signaling pathway is unknown, but whereas expression of the full length protein in a mutant background rescues ethylene insensitivity, overexpression of the C-terminal alone, but not the full length protein, constitutively activates most but not all ethylene responses in adult plants. Based on this observation, as well as the known activity of other Nramp proteins, it was proposed that the N-terminal of EIN2 acts as a sensor that somehow regulates the signaling activity of the C-terminal portion of the protein in response to divalent cations. Further experiments will presumably test this prediction.

In summary, Nramp proteins from phylogenically distant organisms from mammals to bacteria share a common function of divalent metal transport. Thus, it is likely that other more closely related Nramp proteins share this function as well. The most distantly related family member, EIN2, may have developed the divergent function of acting as a sensor rather than transporter of these metals, though this remains to be proven.

Chapter 2

The Nramp1 protein is recruited to the membrane of the phagosome

Abstract

The *Nramp1* locus (*Bcg*, *Ity*, *Lsh*) controls the innate resistance or susceptibility of mice to infection with a group of unrelated intracellular parasites which includes *Salmonella*, *Leishmania*, and *Mycobacterium*. *Nramp1* is expressed exclusively in professional phagocytes and encodes an integral membrane protein that shares structural characteristics with ion channels and transporters. Its function and mechanism of action remain unknown. The intracellular localization of the *Nramp1* protein was analyzed in control 129/sv and mutant *Nramp1*^{-/-} macrophages by immunofluorescence and confocal microscopy and by biochemical fractionation. In colocalization studies with a specific anti-*Nramp1* antiserum and a panel of control antibodies directed against known cellular structures, *Nramp1* was found not to be expressed at the plasma membrane but rather localized to the late endocytic compartments (late endosome/lysosome) of resting macrophages in a *Lamp1*-positive compartment. Double immunofluorescence studies and direct purification of latex bead-containing phagosomes demonstrated that upon phagocytosis, *Nramp1* is recruited to the membrane of the phagosome and remains associated with this structure during its maturation to phagolysosome. After phagocytosis, *Nramp1* is acquired by the phagosomal membrane with time kinetics similar to *Lamp1*, but clearly distinct from those of the early endosomal marker *Rab5*. The targeting of *Nramp1* from endocytic vesicles to the phagosomal membrane supports the hypothesis that *Nramp1* controls the replication of intracellular parasites by altering the environment of the microbe-containing phagosome.

Introduction

In mice, resistance or susceptibility to infection with a number of antigenically and taxonomically unrelated intracellular parasites is determined by alleles of the chromosome 1 locus *Bcg*, also known as *Ity* or *Lsh*. Infections under the control of *Bcg* include several mycobacterial species (*M. bovis*, *M. avium*, *M. lepraemurium*), *Salmonella typhimurium* and *Leishmania donovani* ^{13,14,19,108,191}. The genetic control is expressed phenotypically as a rapid microbial replication during the early phase of infection in reticuloendothelial (RE) organs of susceptible (*Bcg^S*) mice, as opposed to absence of such multiplication in resistant (*Bcg^R*) animals ¹⁹. While in the case of non-virulent infections (*Mycobacterium*, *Leishmania*), onset of specific immune response clears the infection in susceptible animals, the highly virulent pathogen *Salmonella* leads to a fulminant and rapidly lethal infection in susceptible animals. *In vivo* experiments have shown that the cell population(s) responsible for phenotypic expression of *Bcg* is bone marrow derived, radiation-resistant, and sensitive to the phagocyte poison, silica ²³. Furthermore, explanted macrophages from *Bcg^R* and *Bcg^S* mice show different capacities to restrict the growth of *Mycobacteria*, *Salmonella*, and *Leishmania in vitro* ^{25-28,192}. Together, these results indicate that the macrophage is the cell type expressing the genetic difference at *Bcg*, in agreement with the intracellular nature of infectious agents affected by *Bcg*. The physiological role of *Bcg* within phagocytes is unknown, but its ability to affect the replication of such a divergent group of parasites supports a pivotal role in anti-microbial defenses of these cells.

Using positional cloning, we have recently isolated a candidate for *Bcg* designated *Nramp1* (Natural resistance associated macrophage protein 1) ³¹. *Nramp1* mapped within the minimal genetic and physical intervals defined for *Bcg*, and the expression of its mRNA was restricted to RE organs and to phagocytic cells derived from them. The predicted amino acid sequence of *Nramp1* identifies an integral membrane protein composed of 12 predicted transmembrane (TM) domains, a glycosylated extracytoplasmic loop, and several putative phosphorylation sites in predicted intracellular loops. Sequence analysis of *Nramp1* shows that susceptibility to infection in *Bcg^S* inbred strains is associated with a single non-conservative G169D substitution in the predicted TM4 of the protein ³². In addition, creation of a null allele at *Nramp1* by homologous recombination abrogates the natural resistance of *Bcg^R* mice to infection with *Mycobacterium*, *Salmonella*, and *Leishmania* ³⁴. Finally, transfer of the G169 allele of *Nramp1* in transgenic animals of susceptible background (*Bcg^S* ; *Nramp1^{D169}*) restores resistance to infection with intracellular parasites ³³. Together, these results demonstrate that *Nramp1*, *Bcg*, *Ity*, and *Lsh* are the same gene.

Recently, we have isolated a second mammalian *Nramp* gene, *Nramp2*, that encodes a highly similar protein (77% similarity) ^{35,193}. As opposed to its phagocyte-specific *Nramp1* counterpart, *Nramp2* is expressed fairly ubiquitously in most tissues tested. Database searches and additional cloning experiments have shown that *Nramp* comprises a very ancient family of proteins with highly conserved members in invertebrates (*C. elegans*, *D. melanogaster*), plants (*O. sativa*, *A. thaliana*), fungi (*S. cerevisiae*), and even bacteria (*M. leprae*) ^{178,179}. This family is defined by a highly conserved hydrophobic core composed of 10 TM domains, including several invariant

charged residues in TM domains, and helical periodicity of sequence conservation which predicts a helical bundle within the membrane with a conserved charged interior and a semi-conserved hydrophobic exterior. This type of structural organization is typical of families of ion transporters and channels¹⁷⁸. In addition, an invariant sequence motif in the Nramp family shows striking similarity with the ion permeation path of mammalian voltage-gated K⁺ channels (TMT-4X-G-D/Q-4X-GF)¹⁹⁴. Together, these observations suggest that *Nramp1* may be a macrophage-specific ion transporter, and that its substrate may play a key bacteriostatic or bactericidal role in these cells. Interestingly, the yeast *Nramp* homolog *SMF1* was recently proposed to encode a manganese transporter¹⁸².

Some of the key unresolved issues concerning *Nramp1* and its role in host resistance to infection include its unknown biochemical function, putative substrate, and how its action affects the intracellular survival of microbes ingested by professional phagocytes. It would also be important to understand how *Nramp1* affects the replication of antigenically unrelated microbes (*Mycobacterium*, *Salmonella*, *Leishmania*) that have devised different strategies to evade the microbicidal arsenal of phagocytes (see Discussion; reviewed in¹⁹⁵), and why mutations at *Nramp1* are seemingly without effect on the replication of other intracellular infections such as *Listeria* and *Legionella*¹⁹⁶.

In this study, we have used specific anti-*Nramp1* antibodies to analyze the subcellular localization of the *Nramp1* protein in macrophages by immunofluorescence and confocal microscopy, using a series of markers corresponding to known membranous compartments within this cell. We have determined that *Nramp1* is not present in the plasma membrane of these cells but is rather found in the late endosome fraction. Moreover, upon phagocytosis, *Nramp1* gets recruited to the membrane of the phagosome

during the course of its maturation from early plasma-membrane derived phagosome to phagolysosome, and therefore becomes intimately associated with the membranous compartment containing the ingested parasites.

Materials and Methods

Isolation and Culture of Macrophages

129/sv mice were purchased from Taconic Farms (Germantown, NY), and 129/sv mice bearing a null mutation at the *Nramp1* locus (129/sv *Nramp1*^{-/-}) were created as described by Vidal et al.,³⁴. Mice were maintained and handled according to regulations of the Canadian Council on Animal Care. Resident peritoneal macrophages were isolated from either 129/sv mice or from 129/sv *Nramp1*^{-/-} mutants by peritoneal lavage as described previously¹⁹⁷. Briefly, mice were sacrificed and the peritoneal cavity washed with 10 ml of warm RPMI (Gibco/BRL) using a 10 ml syringe fitted with a 18G needle. Resident cells were pelleted (1000 g, 5 min), resuspended in complete RPMI supplemented with 10% heat-inactivated (56°C, 30 min.) fetal bovine serum (Gibco), and plated onto glass coverslips. After incubation overnight at 37°C in 5% CO₂, non-adherent cells were eliminated by three washes with warm phosphate buffered saline (PBS; 137 mM NaCl, 2.7 mM KCl, 1.5 mM KH₂PO₄, 8.1 mM Na₂HPO₄, pH 7.4), and adherent macrophages were placed in complete RPMI medium. Macrophages were used for immunofluorescence or phagocytosis assays no longer than 24-48h after isolation.

Antibodies

A rabbit anti-mouse *Nramp1* polyclonal antiserum was raised against a fusion protein containing amino acids 514 to 548 of *Nramp1* (carboxy terminal domain) fused in frame to a 27 kDa segment of glutathione S-transferase (GST), and expressed in *Escherichia coli*, as described elsewhere⁴⁹. The immunoglobulin fraction of the

hyperimmune rabbit antiserum was concentrated by ammonium sulfate precipitation; further purification of the anti-Nramp1 antibody was achieved by absorption of the anti-GST fraction of the antiserum to Sepharose beads coupled to GST. Coupling of GST to cyanogen bromide activated Sepharose beads, absorption of the antiserum and further concentration of the anti-Nramp1 antibody were essentially as described ¹⁹⁷. The rat anti-Lamp1 monoclonal antibody (late endosome, early lysosome) has been described previously ¹⁹⁸; the rabbit anti-Calnexin (endoplasmic reticulum; ¹⁹⁹) and anti-MG160 ^{200,201} polyclonal antibodies were generous gifts of Dr. J.J.M. Bergeron (Anatomy, McGill University); crude or affinity purified rabbit anti-Cathepsin D (lysosome) and anti-Cathepsin B (lysosome, ²⁰²) polyclonal antisera were generous gifts of Dr. John Mort (Shriner's Hospital, Montreal); crude or affinity-purified rabbit polyclonal anti-Rab5 (early endosome; ²⁰³) and anti-Rab7(late endosome; ²⁰⁴) were kind gifts from Drs. Philippe Chavrier and Stephane Meresse respectively (Centre d'Immunologie, INSERM-CNRS, Marseille, France); finally, the mouse monoclonal antibody 9E10 ²⁰⁵ directed against a short antigenic epitope of the c-Myc protein was purchased from Babco (Berkeley, CA). Secondary antibodies Texas red-conjugated goat anti-rabbit, FITC-conjugated goat anti-rat, and Rhodamine-conjugated goat anti-mouse were purchased from Jackson ImmunoResearch Laboratories (Bio/Can Scientific, Mississauga, ON). All antibodies were used at dilutions indicated in the Figure legends.

Immunofluorescence

Cells grown on glass coverslips were fixed with 4% paraformaldehyde in PBS for 30 min at 4°C. After three washes in PBS, cells were then permeabilized by treatment

with 0.05% NP-40 in PBS with 1% BSA (Bovine Serum Albumin, Fraction V, Boehringer Mannheim) and 5% normal goat serum (Gibco). Cells were washed again with PBS, and blocked for 1 hour at room temperature in PBS containing 1% BSA, 10% normal goat serum and 10% normal mouse serum (omitted for experiments with the mouse monoclonal antibody 9E10). The normal goat and mouse sera were heat inactivated (50°C, 30 min) prior to use. The cells were incubated with the primary antibody diluted in blocking solution (dilutions are indicated in figure legends) for 1 hour at room temperature, followed by three washes in PBS containing 1% BSA, and 0.2% tween-20. Incubations for the secondary antibodies were done in a similar fashion, and were followed by a final wash in PBS. The coverslips were then mounted onto glass slides in ImmuMount (Shandon, Pittsburgh, PA). Immunofluorescence was analyzed with either a Zeiss Axiophot microscope using the 63X oil immersion objective, or an Olympus fluorescence microscope using the 40X and 100X oil immersion objectives. Certain colocalization studies were performed using a Bio-Rad scanning confocal fluorescence microscope and digitizing equipment (Bio-Rad, Hercules, CA).

Phagocytosis and Kinetic Studies of Phagosome Maturation

For phagocytosis experiments, resident peritoneal macrophages were fed a meal of latex beads (3µm diameter, diluted 1:25 in warm RPMI medium from stock suspension; Sigma, St-Louis MO), and the internalized latex beads were used to follow the steady-state or kinetics of association of various protein markers with the maturing phagosome. For colocalization studies of Nramp1 and Lamp1 proteins at steady state, macrophages were incubated with medium containing beads for one hour, washed in

PBS, and incubated in bead-free medium for 1 hour to allow maturation of the phagosome into phagolysosome. Cells were then processed for immunofluorescence as described above. For kinetic experiments, macrophages were incubated with latex bead-containing medium for 5 min at 37°C, followed by five washes with PBS (at 4°C) to remove uninternalized beads. The chase period was initiated by incubating the cells with RPMI medium pre-warmed at 37°C, and at pre-determined times during the incubation at 37°C, cells were fixed, stained with specific antibodies, and processed for immunofluorescence. To determine the percentage of phagosomes positive for the markers analyzed, macrophages were initially examined under phase contrast to locate cell-associated latex beads. These cell-associated beads were then examined under fluorescence for the presence or absence of immunospecific label around the bead-containing phagosome. A minimum of one hundred beads were scored for the presence of pairs of endosomal or lysosomal markers for each time point. At least two independent experiments were carried out for each pair of markers and averages were calculated and shown.

Isolation of Phagosomes from RAW 264.7 macrophages

The mouse monocyte-macrophage cell line RAW 264.7 was obtained from the American Type Culture Collection and grown in Dulbecco's Modified Eagle's Medium supplemented with 10% heat-inactivated FCS (Gibco), 20 mM HEPES pH 7.6, and 2 mM L-glutamine. An expression plasmid was constructed using the mammalian expression vector pCB6²⁰⁶ with an insert containing the entire coding region of mouse *Nramp1* cDNA modified by the addition of four consecutive antigenic peptide epitopes

(EQKLISEEDL) derived from the human c-Myc protein, fused in-frame at the carboxy terminus of Nramp1 (pCB6-Nramp1). pCB6-Nramp1 was introduced in RAW264.7 macrophages by electroporation: 700 μ l of cells at a density of 2×10^7 cells/ml in complete medium was mixed with 40 μ g of the purified plasmid in an electroporation cuvette. Cells were electroporated at a setting of 960 μ F and 300 mV on a BioRad GenePulser. Electroporated cells were plated in complete growth medium and selection in geneticin (G418, 0.5 mg/ml final concentration; GIBCO/BRL) was initiated 48 hours later. Stable transfectants (G418^R) were isolated after 14 days of selection. G418^R colonies were individually picked, expanded in culture, and tested for expression of the c-Myc epitope tagged Nramp1 protein by immunofluorescence, using either the anti-Nramp1 antibody GST-54N⁴⁹ or the anti-c-Myc epitope monoclonal antibody 9E10²⁰⁵. Expression of the c-Myc tagged Nramp1 protein in these cells was further verified by immunoprecipitation, using the anti-Nramp1 antiserum GST-54N, according to a protocol and experimental conditions previously described by our group⁴⁹. One RAW264.7 G418^R clone positive for Nramp1 protein expression and showing levels of expression comparable to those observed for the wild type protein in resident macrophages was selected for further immunofluorescence studies and biochemical characterization of purified phagosomes.

Phagosomes were isolated from the RAW cells and RAW transfectants by a modification of a method described previously⁶⁹. Ten sub-confluent 150 mm dishes of each cell line were fed with a 1:200 dilution of blue-dyed latex beads (0.8 μ m, Sigma) in culture medium for 1 hour at 37°C in 5% CO₂. The cells were then washed in PBS, and incubated one hour in complete culture medium at 37°C in 5% CO₂, to allow phagosome

maturation. Cells were then scraped into PBS + 0.5% BSA + protease inhibitors (1 µg/ml leupeptin, 1 µg/ml aprotinin, 1 µg/ml pepstatin, 100 µg/ml PMSF, all Boehringer Mannheim) and recovered by centrifugation (2000 g, 5 min). The cell pellets were washed and resuspended in homogenization buffer (8.5% sucrose, 3 mM imidazole, pH 7.4) and homogenized by passage through a 22G needle until 90% of the cells were broken, with most of the nuclei remaining intact as monitored by light microscopy. Nuclei and unbroken cells were pelleted and the supernatant loaded onto a sucrose step gradient as follows: the supernatant was brought up to 40% sucrose by addition of 62% sucrose, and loaded on top of a 1 ml 62% sucrose cushion. Layers of 2 ml of 35%, 25% and finally 10% sucrose (all sucrose solutions w/w in 3mM Imidazole, pH 7.4 + protease inhibitors) were sequentially added to the top of the tube, and the gradients were centrifuged at 100,000 g for 1 hour at 4°C (SW41; Beckman, Palo Alto, CA). Phagosomes were recovered from the 10 - 25% sucrose interface, washed with PBS containing protease inhibitors, and recovered by a final centrifugation at 40,000 g in an SW41 rotor at 4°C. The final pellets were resuspended in 2 X Laemmli sample buffer²⁰⁷. Phagosomes prepared by this protocol have been previously shown to be free of endoplasmic reticulum (endoplasmin, BiP and calnexin) and Golgi apparatus (galactosyl transferase) contaminants⁶⁹.

Immunoblotting Analysis of Phagosomes

Equal amounts of phagosomal proteins from each cell line were separated by SDS-PAGE on 7.5% gels and transferred onto nitrocellulose filters as described previously²⁰⁸. The filters were blocked in TBST (100mM Tris/Cl pH 8, 0.9% NaCl,

0.1% Tween-20) + 1% BSA and Nramp1 was revealed using the anti-Myc mouse monoclonal antibody 9E10. Controls in this experiment included the anti-Lamp1 rat monoclonal antibody, and a rabbit anti-Rab7 antiserum followed by incubation with goat secondary antibodies conjugated to horseradish peroxidase (Amersham, Buckinghamshire, UK). Chemiluminescence was used for detection of immune complexes on the filter (ECL, Amersham).

Results

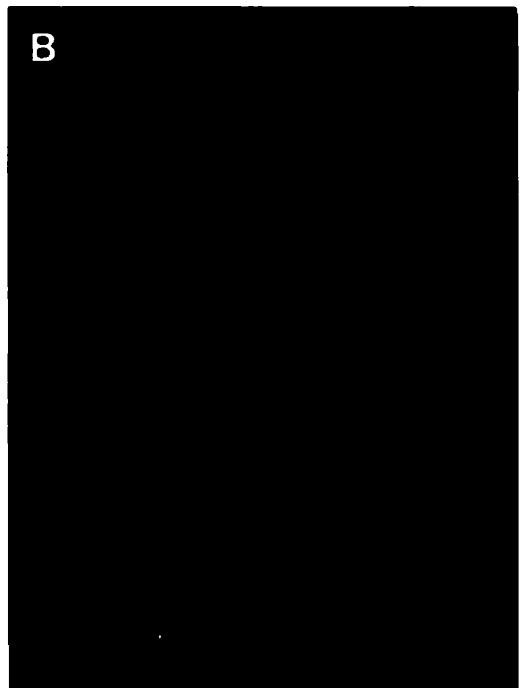
Nramp1 is localized to an intracellular compartment in macrophages

As a first step towards elucidating the biochemical function of *Nramp1*, and how it may affect replication of intracellular parasites, we set out to establish the subcellular localization of the protein. Studies of mRNA distribution in normal tissues and cell types identified expression restricted to reticuloendothelial organs and to mature macrophages derived from them ³¹. Consequently, peritoneal macrophages from 129/sv mice, a strain that bears the wild type allele at *Nramp1* (*Nramp1*^{G169}, *Bcg*^r) were chosen for these studies. Peritoneal macrophages 1) express many markers of fully mature phagocytes ²⁰⁹, 2) are positive for *Nramp1* mRNA ⁴⁷, 3) experiments *in vitro* show that mutations at *Nramp1* affect the capacity of these cells to control the replication of intracellular parasites ^{25-28,192} 4) they are easy to obtain in small numbers. Finally, we have created a 129/sv mouse strain that bears a null mutation at *Nramp1* (*Nramp1*^{-/-}), therefore providing an ideal control for subcellular localization studies in 129/sv macrophages ³⁴.

We have previously reported the production of a series of specific rabbit anti-*Nramp1* polyclonal antisera ⁴⁹, including the GST-35C serum raised against a protein comprising the C-terminal 35 residues of *Nramp1* fused to glutathione-S-transferase (GST). In immunoprecipitation and immunoblotting experiments using extracts from macrophages, this serum identified *Nramp1* as an integral membrane phosphoglycoprotein of 90-95 kDa ⁴⁹, in agreement with structural and functional features predicted from the sequence of *Nramp1* cDNA ³¹. GST-35C was used to localize the *Nramp1* protein in macrophages by indirect immunofluorescence (Fig. 1). In

Figure 1 *Subcellular localization of the Nramp1 protein in macrophages*

Peritoneal macrophages from normal 129/sv mice (A) and from 129/sv *Nramp1*^{-/-} mutants (B) were harvested by peritoneal lavage, cultured for 48 hr, and analyzed by indirect immunofluorescence with an anti-Nramp1 rabbit polyclonal antibody (GST-35C, used at 1:50 dilution) raised against the 35 C-terminal residues of Nramp1. The secondary antibody was a goat anti-rabbit antiserum conjugated to Texas Red (used at 1:200 dilution). Cells in panels A and B were processed identically, and equal exposure times were used for photography.



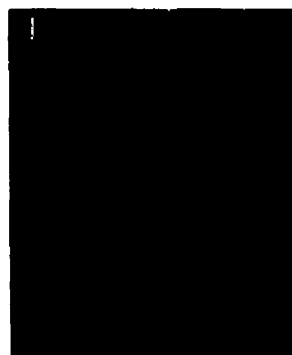
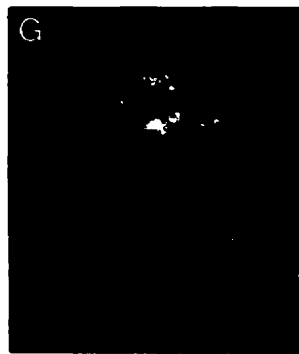
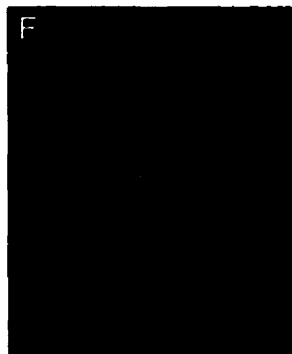
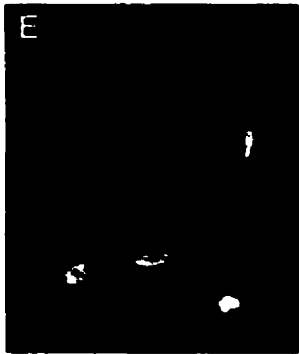
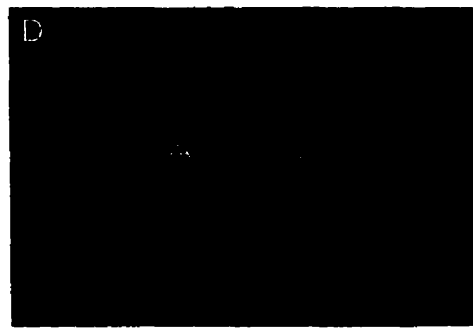
129/sv macrophages (Fig. 1A), we observed a strong intracellular vesicular staining pattern that was intense in the perinuclear region but also extended throughout the length of the long cellular processes. This staining was specific and absent in macrophages from control *Nramp1*^{-/-} mutants (Fig. 1B). A similar staining pattern was observed using an unrelated anti-Nramp1 antiserum directed against the 53 N-terminal residues of the protein (data not shown). Finally, we did not detect any Nramp1 staining associated with either the plasma membrane or the nuclear membrane, indicating that Nramp1 expression is restricted to a subcellular, probably membranous compartment.

Colocalization of Nramp1 with the late endosomal/lysosomal marker Lamp1

We set out to identify the subcellular compartment of macrophages positive for Nramp1 protein expression. For this, we compared the pattern of Nramp1 staining obtained by immunofluorescence to that produced in the same cells by markers of discrete intracellular membrane compartments. The fluorescent signal produced by GST-35C (Nramp1) was found to be distinct from those produced by antibodies against the membrane protein MG160 (Golgi apparatus medial cisternae; perinuclear and asymmetric staining; Fig. 2E), the integral membrane protein and molecular chaperone Calnexin (endoplasmic reticulum; cytoplasmic reticulated network and nuclear envelope; Fig. 2H), or the soluble cysteine proteases cathepsin B and D (lysosomes; strong punctate staining uniformly distributed; Fig. 2G, 2J, respectively). On the other hand, the Nramp1 staining shared some similarity with that produced by antibodies against the membrane associated small GTP binding proteins Rab5 (early endosome; punctate reticular with small vesicles; Fig. 2F), and in particular Rab7 (late endosome; punctate reticular; Fig. 2I). However,

Figure 2 *Colocalization of the Nramp1 and Lamp1 proteins in macrophages*

Peritoneal macrophages were isolated from normal 129/sv (A, C, E-J) and 129/sv *Nramp1*^{-/-} mutants (B, D) and processed for double indirect immunofluorescence with the rabbit anti-Nramp1 antiserum GST-35C (A, B; 1:50 dilution) and a rat anti-Lamp1 monoclonal antibody (C, D; 1:10 dilution). Both cell populations were processed identically and equal exposure times were used for photography. Macrophages from 129/sv mice were also reacted with antibodies directed against MG160, a medial Golgi marker (E; 1:500 dilution); Rab5, an early endosomal marker (F, 1:200 dilution); Cathepsins B and D, lysosomal proteases (G,J, respectively; 1:200 dilution); Calnexin, a protein expressed in the endoplasmic reticulum and nuclear envelope (H; 1:100 dilution); and Rab7, a late endosomal marker (I; 1:200 dilution).



we observed an even more striking similarity between the Nramp1 pattern and that of a marker for the late endosomal and early lysosomal compartments, Lamp1 (Fig. 2C, 2D). The possible colocalization of Lamp1 and Nramp1 in this compartment was further investigated by double immunofluorescence on the same preparations of macrophages from either wild type 129/sv (Fig. 2A, 2C), or *Nramp1*^{-/-} mutant mice (Fig. 2B, 2D), using rat anti-Lamp1 (Fig. 2C, 2D) and rabbit anti-Nramp1 antibodies (Fig. 2A, 2B). We observed complete colocalization of the Nramp1 and Lamp1 proteins to the same type of subcellular structures in the 129/sv macrophages (Fig 2A, 2C). Control macrophages from *Nramp1*^{-/-} mice stained normally for Lamp1, but did not show any staining for Nramp1, establishing that the observed colocalization of Nramp1 and Lamp1 was not due to cross-reactivity of the secondary antibodies or other procedural artifacts (Fig 2B, 2D). Together, these results indicate that Nramp1 is expressed in the late endosomal/early lysosomal compartment of macrophages.

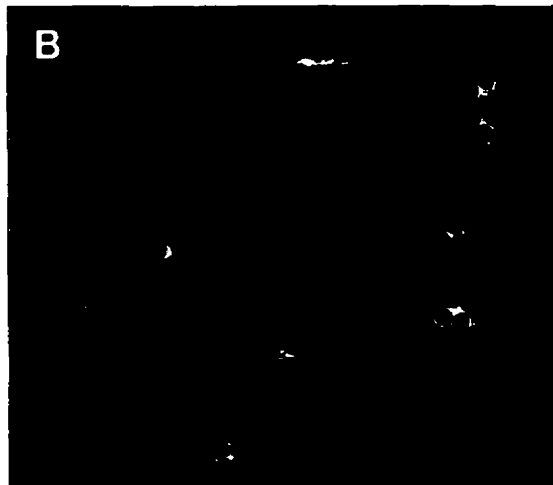
Nramp1 becomes associated with the phagosome after phagocytosis

Our localization of Nramp1 to the late endocytic compartment is exciting, since this compartment plays a major role in the ultimate destruction of internalized microbial targets by macrophages. Indeed, most intracellular parasites enter the macrophage by active phagocytosis; the resulting plasma membrane-derived phagosome then acquires various cytotoxic and cytostatic properties (low pH, oxygen radicals, proteolytic enzymes) through a maturation process consisting in a series of complex fusion events involving endosomal and lysosomal partners. Consequently, our localization of Nramp1 to the late endocytic/lysosomal compartment would suggest that Nramp1 may become

associated with the phagosomal membrane during maturation, and be intimately associated with invading parasites. To test this prediction, we monitored a possible association of Nramp1 with latex bead-containing phagosomes. Latex beads are inert spherical particles of defined size that are readily phagocytosed by macrophages; they serve as excellent phagosome markers for microscopy analysis and for biochemical purification of these organelles. Latex bead phagosomes show normal fusogenic properties and have been extensively used to establish the kinetics of delivery of various endosomal and lysosomal markers to the maturing phagosome^{69,70,210}. Normal (129/sv) and *Nramp1*^{-/-} mutant macrophages were harvested and fed latex beads for 1 hr.. The cell monolayers were washed extensively to eliminate unphagocytosed beads, followed by a further 1 hr. incubation to allow phagosome maturation. The cells were then fixed, and analyzed for subcellular distribution of Nramp1 protein; individual fields were photographed under phase contrast (Fig. 3A, 3C), and examined by immunofluorescence for Nramp1 staining (Fig. 3B, 3D). In 129/sv macrophages showing internalized beads (Fig. 3A, 3B), Nramp1 was concentrated primarily around the beads with a striking ring-like staining, strongly suggesting that Nramp1 was now localized in the phagosome membrane. Beads located outside the cells (arrow in Fig. 3A), and a small percentage of cell-associated beads remained negative for Nramp1. This suggests that the striking Nramp1 staining found associated with the majority of internalized beads was due to the presence of Nramp1 protein acquired during latex bead phagosome maturation, as opposed to an optical artifact of the beads on the previously noted intracellular Nramp1 staining background (Fig. 1A). Cells without beads showed typical Nramp1 staining. Finally, *Nramp1*^{-/-} macrophages showed no obvious defects in

Figure 3 *Nramp1* association with latex bead-containing phagosomes

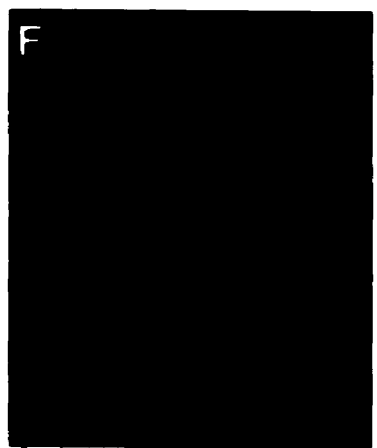
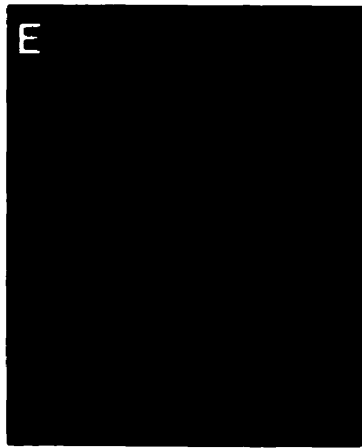
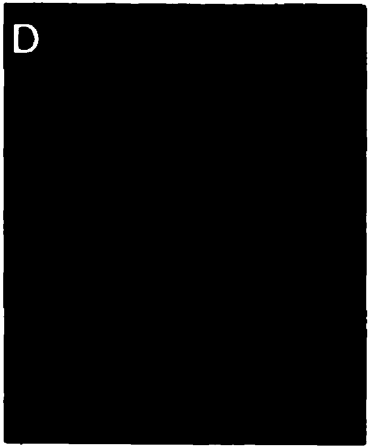
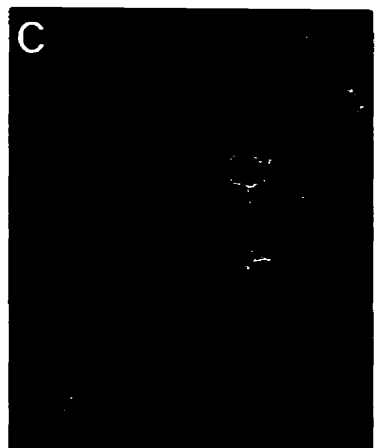
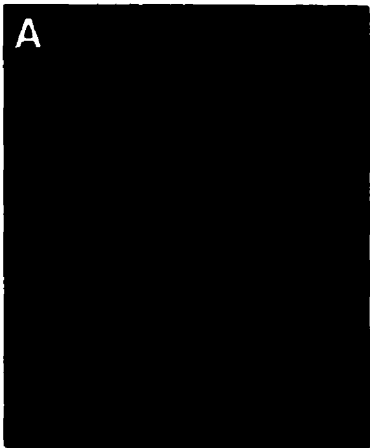
Normal 129/sv (A, B) and mutant 129/sv *Nramp1*^{-/-} (C, D) macrophages were harvested, cultured for 48 hr., and fed a meal of latex beads for 1 hr. at 37°C. The cells were washed free of unphagocytosed beads, and further incubated for 1 hour to allow phagosome maturation. The cells were then fixed and subjected to indirect immunofluorescence with the anti-Nramp1 antiserum (see legend to Figure 1). Phase contrast (A, C) and immunofluorescence micrographs (B, D) of the same fields of cells are shown. The position of an uninternalized latex bead is indicated by the arrow in panel A.



their ability to phagocytose latex beads (Fig. 3C), but the cells and latex bead phagosomes remained negative for Nramp1 (Fig 3D).

In the next set of experiments, double immunofluorescence and confocal microscopy were used to further validate the initial results of immunofluorescence, and to ascertain that Nramp1 is delivered to the phagosomal membrane during phagocytosis. Confocal microscopy permits microscopic analysis of individual cell sections, allowing accurate localization of proteins to subcellular membranous compartments (reviewed in 211). Normal 129/sv and *Nramp1*^{-/-} mutant macrophages were fed a meal of latex beads as above, and phagosome maturation was allowed to take place. Cells were then fixed, and stained with both anti-Nramp1 (coupled to Texas Red, red signal), and anti-Lamp1 antiserum (coupled to FITC; green). Cells were examined by confocal microscopy and separate images from the same field were created for the Nramp1 staining (red, Fig. 4A, 4D) and the Lamp1 staining (green, Fig. 4B, 4E). In 129/sv macrophages, a striking ring-like staining concentrated at the periphery of individual latex beads was observed for both markers (Fig. 4A, 4B); similar images were obtained at different planal sections of the same cells (data not shown). These results indicate that both proteins become associated with the phagosomal membrane after phagocytosis and maturation. Superimposition of the Nramp1 and Lamp1 images in 129/sv macrophages indicate almost complete overlap of both markers in individual latex bead phagosomes (yellow, Fig. 4C), suggesting similar kinetics of delivery of both proteins to the phagosomes. Latex bead phagosomes from control *Nramp1*^{-/-} macrophages were positive for Lamp1 but remained negative for Nramp1 (Fig. 4D, 4E, 4F).

Figure 4 *Nramp1 and Lamp1 colocalization to the membrane of latex bead-containing phagosomes.* Macrophages from normal 129/sv mice (A-C) and from 129/sv *Nramp1*^{-/-} mutants (D-F) were fed a meal of latex beads and further incubated to allow phagosome maturation (see legend to Figure 3). The samples were then subjected to double indirect immunofluorescence with the rabbit anti-Nramp1 antibody (GST-35C) revealed by a Texas Red coupled secondary antibody, and with the rat anti-Lamp1 antibody revealed by an FITC coupled secondary antibody. Slides were analyzed by confocal laser scanning microscopy on Bio-Rad equipment, for optical sections of 0.2µm. Red identifies Nramp1 positive structures (A, D), and green identifies Lamp1 positive structures (B, E). In panels C and F, images in A+B and D+E have been superimposed; the yellow color identifies colocalization of the Nramp1 and Lamp1 proteins to the same structures.



Detection of Nramp1 in purified phagosomes

In order to provide direct biochemical evidence for the association of Nramp1 with the phagosomes, we proceeded to purify these organelles from macrophages, followed by immunoblotting for detection of Nramp1 protein. We have previously described a method for the isolation of latex bead phagosomes by subcellular fractionation and discontinuous density gradient centrifugation; such latex bead phagosomes are free of contaminants from the Golgi (galactosyl transferase) or the endoplasmic reticulum (endoplasmin, BiP and calnexin) ^{69,70}. Since purification of phagosomes by this method requires large number of macrophages (1-2 x 10⁸), mouse peritoneal macrophages cannot be used as starting material (1-5 x 10⁶/mouse). For these studies, we created a mouse macrophage cell line that expresses high levels of a transfected wild type *Nramp1*^{G169} allele. RAW264.7 is a mouse monocyte-macrophage cell line derived from BALB/c (*Bcg*^S), thus homozygous for the *Nramp1*^{D169} mutation which is phenotypically expressed as the absence of mature protein caused by improper maturation resulting in its rapid degradation ⁴⁹. RAW264.7 macrophages were transfected with the mammalian expression pCB6 which contains a *neo* gene and an expression cassette that uses cytomegalovirus regulatory elements to direct high levels expression of cloned cDNAs ²⁰⁶. Wild type *Nramp1*^{G169} cDNA was modified at its C-terminus prior to insertion in pCB6, by the in-frame addition of four copies of the antigenic c-Myc epitope EQKLISEEDL ²⁰⁵. This construct was transfected into RAW264.7 cells, transfectants were selected in geneticin, and initially screened for Nramp1 protein expression by immunoprecipitation using the mouse monoclonal 9E10 directed against the c-Myc epitope present in the tagged protein (data not shown).

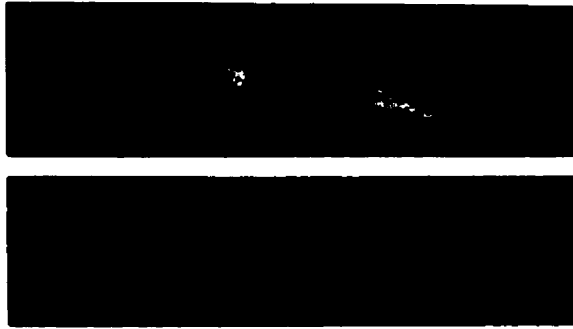
Several positive clones were identified and one of them showed levels of Nramp1 protein expression similar to that seen for the endogenous protein in wild type 129/sv peritoneal macrophages. Immunofluorescence with the 9E10 antibody on transfected RAW264.7 cells expressing the tagged *Nramp1* cDNA showed bright intracellular signal with a vesicular and pseudo-reticular staining (Fig. 5A, upper panel), similar to that seen for 129/sv macrophages analyzed with the Nramp1 antiserum 35C-GST (Fig. 1A). This signal was specific and absent from untransfected RAW264.7 cells (Fig. 5A, lower panel). The RAW264.7 *Nramp1* transfectants and RAW264.7 controls were then used as starting cells for the production and isolation of latex bead phagosomes⁶⁹. Phagosomes were then analyzed for expression of the Nramp1/c-Myc tagged protein by immunoblotting with the 9E10 antibody (Fig. 5B, upper panel). Phagosomes from *Nramp1* transfectants expressed a single broad immunoreactive species of molecular mass 85-90 kDa, that was absent from phagosomes of untransfected RAW cells; The molecular mass and electrophoretic mobility of this tagged protein are in good agreement with that of Nramp1 expressed in wild type peritoneal macrophages⁴⁹. Control immunoblotting experiments with an antiserum directed against the late endosomal marker Rab7 identified equal amounts of an immunoreactive 23 kDa protein in phagosome preparations from control RAW cells and from RAW cells expressing the Nramp1/c-Myc protein (Fig. 5B, lower panel). Similar amounts of Lamp1 were also detected in both preparations by immunoblotting (data not shown). These control experiments indicate equal protein loading in each lane and equal transfer of endosomal and lysosomal markers to latex phagosomes prepared from both types of cells.

Figure 5 *Purification of Nramp1-positive phagosomes*

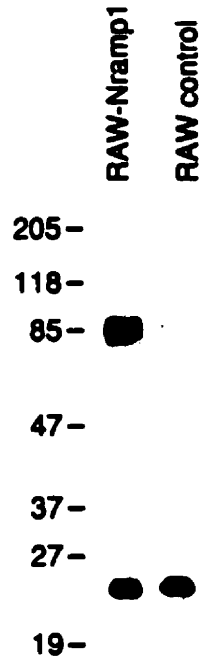
(A) *Characterization of RAW264.7 macrophages expressing a transfected Nramp1^{G169} cDNA.* RAW-Nramp1 is a clone of the macrophage cell line RAW 264.7 that has been transfected with a pCB6 expression vector containing a full length *Nramp1^{G169}* modified by the in-frame addition of four antigenic c-Myc epitopes of sequence EQKLISEEDL. RAW-Nramp1 cells (upper panel) and their untransfected RAW264.7 counterparts (lower panel) were analyzed by indirect immunofluorescence using the mouse monoclonal 9E10 directed against the introduced c-Myc epitope (used at a 1:50 dilution). Both cell populations were treated identically and equal exposure times were used for photography.

(B) *Immunoblotting of latex bead-containing phagosomes isolated from RAW264.7 cells and from RAW-Nramp1 transfectants.* Latex bead-containing phagosomes were purified from cell homogenates by subcellular fractionation on sucrose density gradients as described in Materials and Methods. Equal amounts of phagosomal proteins from each cell line were separated by SDS-PAGE on a 7.5% gel. Proteins were transferred to nitrocellulose and the Nramp1-c-Myc fusion protein was revealed using the anti-c-Myc epitope monoclonal antibody 9E10 (upper panel). Equal loading of proteins on the gel, equal transfer to the membrane and delivery of late endosomal markers to the latex phagosomes were verified by immunoblotting with polyclonal antisera against Rab7 (lower panel) and Lamp1 (data not shown). The position of molecular mass markers (in kDa) is indicated on the left side of the immunoblot.

A



B



Together, results presented in Figs. 3, 4, and 5 establish that the Nramp1 protein is initially present in the late endosomal/lysosomal compartment, and is recruited to the phagosome upon maturation of this organelle which occurs after the initial phagocytic event.

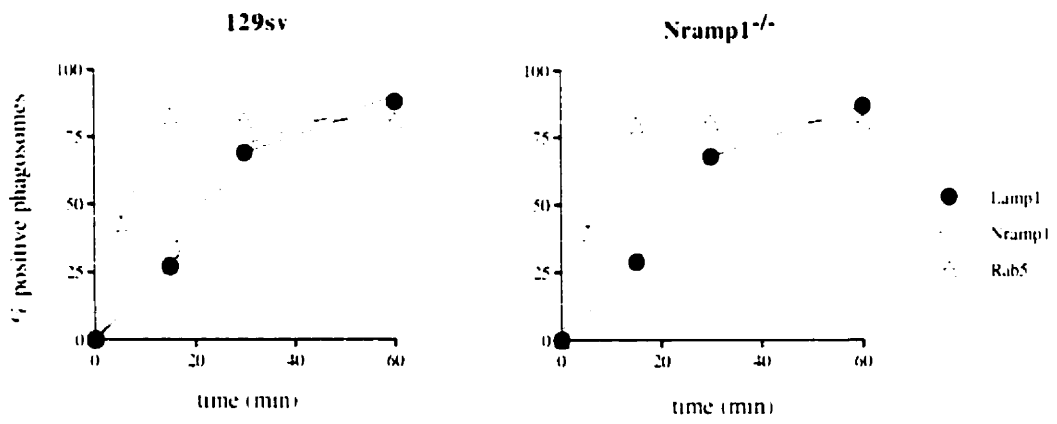
Kinetics of Nramp1 delivery to the maturing phagosome.

We next wished to establish the kinetics of delivery of the Nramp1 protein to the phagosome, and initiate studies to determine if the absence of Nramp1 protein in macrophages may affect the fusogenic properties of this organelle. Therefore, we determined the kinetics of Nramp1 delivery to the phagosome, and compared it to that of an early endosomal marker Rab5, and that of a late endosomal/early lysosomal marker Lamp1. These kinetics were then compared for normal 129/sv macrophages and for *Nramp1*^{-/-} mutants. Peritoneal macrophages were first incubated with latex bead-containing medium for 5 minutes at 37°C to allow phagocytosis, followed by extensive washing of the monolayer at 4°C to eliminate non-phagocytosed beads and synchronize subsequent maturation of the latex bead phagosomes. Cells were then returned to 37°C to initiate maturation, and at pre-determined times, cells were fixed and analyzed by immunofluorescence. To determine the percentage of phagosomes positive for the markers analyzed, macrophages were initially examined under phase contrast to locate cell-associated latex beads (assumed to be phagosomes). These cell-associated beads were then examined under fluorescent light for the presence or absence of immunospecific signal at the periphery of the bead (latex bead phagosome). In 129/sv

macrophages, acquisition of Nramp1 staining by phagosomes was linear over the first 30 min. with 63% of phagosomes labeled, and ultimately 85% of phagosomes becoming positive after 60 min. (Fig. 6A). The kinetics of Nramp1 association (rate and final percentage) were found to be identical to that independently determined for Lamp1 (also plotted in Fig. 6A). Additional experiments where phagosomes were immunostained for both Nramp1 and Lamp1 simultaneously showed that the vast majority of individual phagosomes were either positive for both Nramp1 and Lamp1 or negative for both markers, and this at all times examined (data not shown). By contrast, the kinetics of association of the early endosomal marker Rab5 with latex bead phagosomes were very different. Rab5 was delivered much more rapidly, with 40% of the latex bead phagosomes positive after 5 minutes of maturation, and with a maximum plateau reached at 15 min. where 81% of the phagosomes were positive for this marker (Fig. 6A). Together, these results indicate that Nramp1 and Lamp1 are delivered to the phagosome membrane concurrently. When these studies were repeated with macrophages from *Nramp1*^{-/-} mutant mice, no significant differences were observed between the 129/sv and *Nramp1*^{-/-} mice with respect to the acquisition of Rab5 and Lamp1 during phagosome maturation (Fig 6B). These results together with those shown in Figure 5B suggest that at this level of resolution, the absence of Nramp1 protein does not grossly affect the fusogenic properties of the phagosome to either Rab5, Rab7 or Lamp1 positive structures.

Figure 6 *Kinetics of Nramp1 protein delivery to the maturing phagosome*

Macrophages from normal 129/sv mice (left panel) and from 129/sv *Nramp1*^{-/-} mutants (right panel) were fed a meal of latex beads for 5 min., washed at 4°C, and further incubated to initiate phagosome maturation. At pre-determined times, cells were fixed and analyzed by immunofluorescence for subcellular localization of Nramp1 (□), the late endosomal/early lysosomal marker Lamp1 (●), and the early endosomal marker Rab5 (Δ). The percentage of phagosomes positive for each marker was determined after examination of the cells, first under phase contrast to locate cell-associated latex beads, then under fluorescence for the presence or absence of immunospecific signal at the periphery of the bead. A total of 100 beads were counted for each marker and at each time point. The average of values from two independent experiments are shown.



Discussion

At the cellular level, mutations at *Nramp1* cause a loss of natural resistance to infections which is phenotypically expressed as uncontrolled intracellular replication of these microbes in macrophages of the reticuloendothelial system during the early phase of infection ¹⁹. We have previously established that *Nramp1* mRNA expression is restricted to phagocytes ³¹; since *Nramp1* mutations affect the intracellular growth of antigenically and taxonomically unrelated microbes, the *Nramp1* protein must therefore play a key role in the microbicidal activity of these cells. This role, however, has so far remained elusive. Identifying the subcellular localization of the *Nramp1* protein in macrophages may provide important clues on the physiological process associated with *Nramp1* and underlying resistance/susceptibility, but also on the puzzling lack of immediate relationship between microbial infections afflicting these cells and controlled by *Nramp1*.

Although the highly hydrophobic nature of the *Nramp1* polypeptide predicted from cDNA sequencing was clearly suggestive of a membrane protein ³¹, the nature of the cellular membrane compartment expressing *Nramp1* has remained controversial. While some have predicted that *Nramp1* may localize to the nuclear envelope and regulate translocation of DNA binding proteins into the nucleus ²¹², others have proposed that it may exert its action at the plasma membrane playing a role in signal transduction leading to macrophage activation ^{213,214}. On the other hand, we had proposed that *Nramp1* may be found at the phagosome membrane, possibly interacting with different intracellular parasites transiting through this compartment ^{31,178}. To

address these issues, we have recently generated a series of specific anti-Nramp1 antibodies, and shown that Nramp1 behaves as an integral membrane protein, resistant to urea extraction⁴⁹. Nramp1 is phosphorylated in macrophages and is also heavily glycosylated with up to 40% of its mass accounted for by the post-translational addition of two complex carbohydrate side chains of the tri- or tetra-antennary type⁴⁹. In the present study, we have used these antibodies for double immunofluorescence and confocal microscopy to analyze the subcellular distribution of Nramp1 in populations of macrophage from normal mice (129/sv) and from animals bearing a null *Nramp1* allele³⁴. These experiments have established that Nramp1 is expressed neither at the plasma membrane nor at the nuclear membrane, but is rather found in an intracellular compartment. Colocalization studies using antibodies directed against known markers of specific subcellular membranous compartments have identified the Nramp1 positive compartment as late endosome/lysosome. Additional cell fractionation experiments and immunofluorescence analyses using phagosomes containing latex beads further showed that Nramp1 is recruited to the phagosomal membrane during the phagosome maturation which follows the initial phagocytic event. The time kinetics of Nramp1 acquisition by maturing phagosomes is similar to kinetics of acquisition of Lamp1, another late endosomal/ lysosomal marker, and are clearly distinct from that of Rab5, an early endosomal marker.

Having localized Nramp1 to the late endosomal /early lysosomal compartment of resting macrophages, and having established that Nramp1 is recruited to the phagosome, we can focus on the known physiological role of these subcellular compartments in pathogenesis of intracellular infections, and evaluate possible site and mechanism of

action of Nramp1 during these events. A large body of data indicate that these compartments are essential effectors in the intracellular destruction of ingested parasites by macrophages. Most intracellular parasites enter host macrophages via a phagocytic event, resulting in initial encapsulation of the microbe in a plasma membrane-derived structure, the early phagosome ²¹⁵. Phagosomes themselves have little microbicidal activity, and this activity is delivered to the phagosome through a maturation process that involves a series of complex fusion events, with ultimate fusion to terminal lysosomes to form the phagolysosome ^{69,216,217}. Plasma membrane molecules are removed from the early phagosome via recycling, while new soluble or membrane-associated proteins are provided either directly by the biosynthetic pathway or indirectly, by fusion to endocytic organelles including early and late endosomes, and the lysosome. The acquisition or loss of specific phagosomal membrane proteins such as Rabs and SNAREs is believed to be responsible for selection of the correct fusogenic partner for the subsequent steps in maturation (reviewed in ²¹⁸). Phagosome maturation results in strong intravesicular acidification caused by recruitment of the membrane bound subunits of the vacuolar H⁺/ATPase, appearance of microbicidal function through delivery of the lysosome proteolytic arsenal, generation of reactive oxygen radicals via activation of the NADPH-dependent oxidase system, release of lactoferrin and other bactericidal or bacteriostatic molecules (reviewed in ²¹⁹).

On the other hand, intracellular parasites have developed competing mechanisms to circumvent or resist the cytotoxic response of macrophages, and the dynamic balance between the two competing systems determines either successful destruction of the invading microbe or intracellular survival with successful replication and parasitism.

Microbial tactics for intracellular survival include lysis of the phagosomal membrane and escape to the cytoplasm, inhibition or delay in phagosome maturation and/or acidification, and survival within the fused phagolysosome (reviewed in 195). In fact, the detailed characterization of the strategy used by specific microbes for intracellular survival in macrophages has proven important to elucidate normal cytotoxic mechanisms of these cells. Likewise, mutations in host genes (such as *Nramp1*) that affect intracellular survival of a selected group of parasites can uncover a key macrophage effector mechanism particularly effective against this selected group. Mutations at *Nramp1* have a dramatic effect on the growth rate of *Leishmania donovani*, several species of *Mycobacterium* (*M. bovis*, *M. intracellulare*, *M. avium*, *M. lepraemurium*), *Salmonella typhimurium*, and *Brucella abortus* in RE organs; However, they do not affect the growth of other intracellular parasites such as *Listeria monocytogenes*, and *Legionella pneumophila* ⁶⁴. A rapid review of the intracellular survival strategies adopted by these microbes, contrasted with the subcellular localization and kinetics of association with the phagosome determined in this study for *Nramp1*, may provide clues on the temporal and site-specific mode of action of *Nramp1*.

L. donovani phagosomes mature to phagolysosome in a seemingly normal fashion, with the acquisition of lysosomal markers, and strong acidification of the parasitophorous vacuole; *L. donovani* survives this harsh intracellular environment through synthesis of superoxide dismutase (SOD) that neutralizes reactive oxygen species, acid phosphatase and proteases that inactivate or degrade lysosomal enzymes, when activated by acidic pH (reviewed in 220). On the other hand, *M. tuberculosis* (MTB) blocks acidification of the phagosome by preventing fusion of the phagosome to

vacuolar H⁺/ATPase positive vesicles⁸⁰. The exclusion mechanism is controversial but appears selective as MTB containing phagosomes do become positive for lysosomal glycoproteins (lgps)⁷⁸. Finally, *S. typhimurium* are taken up within specialized "spacious phagosomes" similar to macropinosomes¹¹⁴. These phagosomes acquire lgps and lysosomal acid phosphatase (LAP), yet have no mannose-6-phosphate receptors, (late endosome marker) and show decreased levels of the lysosomal protease CathepsinD¹¹⁶. It is believed that the *S. typhimurium* -containing phagosome acquires its lgps and LAP through fusion of vesicles distinct from lysosomes, perhaps arising directly from the trans-Golgi network. Phagosomes containing *S. typhimurium* have also been shown to have greatly decreased fusion with late endocytic compartments and to exhibit delayed and attenuated acidification¹⁹⁵. Thus, although these three types of intracellular parasites have evolved different mechanisms to evade macrophage effector functions, they all transit through and remained associated with the phagosome, and this phagosome seems to fuse to some but not all endosomal or lysosomal vesicles. One common characteristic of phagosome containing these parasites is that they all seem to acquire, at some stage, the late endosomal/ early lysosomal marker Lamp1^{80,116,117,220,221}. As we have shown that Nramp1 and Lamp1 co-localize within the cell (Fig.2, 3), and are delivered to latex bead-containing phagosomes with identical kinetics (Fig. 6), we predict that the phagosomal membrane enveloping these parasites also acquires Nramp1. This would place Nramp1 in close proximity of those intracellular parasites under its genetic control.

Conversely, *Legionella pneumophila* enters the macrophage through the formation of a unique "coiled phagosome" and replicates within a characteristic

ribosome-dotted vacuole that does not fuse with endosomes or lysosomes. It does not acidify nor does it become positive for endosomal or lysosomal markers, including Lamp1 ²²¹. Hence, it appears that Nramp1 may not be delivered to the specialized vacuole containing intracellular *L. pneumophila*. In the case of *Listeria monocytogenes*, once in the phagosome, *L. monocytogenes* secretes an enzyme (listeriolysin) that lyses the phagosomal membrane within 20 minutes of phagocytosis, thus allowing escape to and replication in the cytosol ²²². Interestingly, we have observed that 20 minutes after phagocytosis, only approximately 30% of the phagosomes examined by immunofluorescence are positive for Nramp1 (Fig. 6). Thus, it seems that *L. monocytogenes* may escape from the phagosome before a significant amount of Nramp1 is delivered to that site. Therefore, the lack of effect of *Nramp1* mutations on infections with *L. monocytogenes* and *L. pneumophila* is consistent with the unique intracellular behavior of these bacteria and of the phagosomes containing them.

We propose that Nramp1 is targeted to the membrane of the maturing phagosome, and either directly or indirectly modifies the intraphagosomal environment to affect replication of intracellular parasites. Nramp1 could do this indirectly by affecting the fusogenic properties of the maturing phagosome; however, results shown in Figures 5 and 6 indicate that latex bead-containing phagosomes from wild type 129/sv or *Nramp1*^{-/-} mutants show very similar kinetics of acquisition for early and late endosomal markers. Therefore, we favor a more direct transport mechanism that might involve the delivery of a cytotoxic or cytostatic agent to the phagosome, or the elimination of a factor that is essential for proliferation of the parasite at that site.

The nature of the putative transport mechanism of Nramp1 and its possible substrate(s) remain unknown. However, the discovery and characterization of Nramp homologs in phylogenically distant organisms have pointed at possible candidate transport activities. The high degree of sequence similarity amongst *Nramp* family members (*D. melanogaster*, 70% similarity; *C. elegans*, 67%; *O. sativa*, 61%; *S. cerevisiae*, 41%)¹⁷⁸ suggests parallel functional conservation. Detailed analyses of the primary and secondary sequence features of the *Nramp* family has identified as the common structural unit of this family, a core hydrophobic domain that shares characteristics previously noted in families of ion transporters and channels. These include i) high degree of sequence conservation of the 10 TM domains forming this core, ii) helical periodicity of sequence conservation in TM segments, predicting a helical bundle inserted in the membrane with a conserved polar interior and a semi-conserved hydrophobic exterior, iii) direct primary amino acid sequence similarity between the most highly conserved segment of the *Nramp* family (TM8-TM9 intracellular loop), and the highly conserved region of voltage-gated K⁺ channels of the *shaker* type (TMT-4X-G-D/Q-4X-GF)¹⁷⁹. Therefore, structural considerations suggest that the *Nramp* family may form a new group of ion transporters or channels.

Null mutations have been obtained and characterized for the *Nramp* homologs of *D. melanogaster* and the yeast *S. cerevisiae*. *Drosophila* with a non-functional *Nramp* homolog *malvolio* (*mvl*) gene have defects in the pathway involved in integration and processing of gustatory information. The *mvl* gene is expressed in the central nervous system, peripheral neurons, and macrophages¹⁸⁶. No information is currently available on the molecular mechanism of action of *mvl*. The yeast *Nramp* homologs, *SMF1* and

SMF2, were originally isolated in a screen for suppressors of the *mif* mutation (mitochondrial import factor), a lethal mutation that causes a defect in protein import and translocation across the mitochondrial membrane. *SMF1/SMF2* complement only the T_5 allele but not a null allele of *mif*, suggesting indirect complementation as opposed to functional redundancy between *mif* and *SMF1/SMF2* ¹⁸¹. Independently, *SMF1* was recently identified in a screen for survival to otherwise lethal concentrations of the metal chelating agent EGTA ¹⁸². It was shown that deletion of *SMF1* results in decreased cellular uptake of Mn^{2+} whereas overexpression of the gene results in increased Mn^{2+} uptake by cells. The protein encoded by *SMF1*, Smf1p, is located on the yeast plasma membrane, and was proposed to function as a Mn^{2+} transporter. [Complementation of *mif* mutant is explained by the fact that Mif encodes a Mn^{2+} -dependent signal peptidase]. It is tempting to suggest that other *Nramp* family members may also be involved in the transport of divalent cations such as Mn^{2+} . Mn^{2+} , Mg^{2+} , Cu^{2+} , Zn^{2+} or other divalent cations are essential cofactors for many metabolic enzymes, and alterations in their availability could have pleiotropic effects. Considering our localization of Nramp1 to the phagosomal membrane, it is tempting to speculate that Nramp1 protein could eliminate Mn^{2+} or other divalent cations from the phagosomal interior, as suggested by Supek et al. ¹⁸². Mn^{2+} is an essential cofactor for certain isoforms of superoxide dismutase (SOD), an enzyme that neutralizes reactive oxygen species. Indeed, *S.typhimurium*, *M. tuberculosis*, *M. bovis* and *L. donovani* all encode their own SOD, suggesting that this enzyme plays an important role in the intracellular survival strategies of these microbes. Eliminating this response through removal of an essential cofactor would result in a net enhancement of the bactericidal activity of the macrophage. Finally, the recent discovery

of *Nramp* homologs in several species of *Mycobacterium* (P. Gros, unpublished), including *M. leprae*¹⁷⁹ suggest that bacteria may have evolved a parallel transport system, possibly competing for the same substrate as the phagosomal Nramp1. The proposal that mammalian *Nramp1* and bacterial homologs function as transporters of similar types of substrates (such as Mn^{2+}) is currently being tested.

The localization of the Nramp1 protein to the phagosomal membrane described in the previous chapter puts forth the hypothesis that Nramp1 alters the intraphagosomal environment by transporting a substrate across the phagosomal membrane. The following two chapters of the thesis describe investigations that were initiated with the general goal to gaining more insight into *Nramp1* function. These studies involved the identification and characterization of *Nramp2*, a second *Nramp* gene co-expressed in mammals. Although the investigations of Chapter 3 were actually initiated before those in Chapter 2, they are presented in this order since the data from Chapters 3 and 4 has directly contributed to the expansion and refinement of the hypothesis of Nramp1 function arrived at in Chapter 2.

Nramp2 was the first *Nramp1*-homologous gene identified, and is of particular interest since it is a paralog of *Nramp1* i.e. it is a homolog co-expressed within the same species. The co-expression of two mammalian Nramp proteins suggests that they could either transport the same substrate at different sites, or transport different substrates by a similar mechanism. Comparative analyses of tissue distribution and subcellular localization of the two proteins were aimed at discerning between these two alternatives. Although the substrates transported by Nramp1 remain to be definitively demonstrated, the most compelling clues to date have come from the analysis of Nramp2 as well as other Nramp-homologous proteins^{148,182}. Other groups' eventual identification of divalent cations as substrates for Nramp2 and other Nramp-homologous proteins represent one the most significant contributions to date towards our understanding of

Nramp1 function. This illustrates the utility of the characterization of homologous genes as a means to gain insight into a particular gene of interest.

Chapter 3

Identification and Characterization of a Second Mouse *Nramp* Gene

Abstract

The *Nramp* gene was isolated as a candidate for the host resistance locus *Bcg/Ity/Lsh* which controls natural resistance of mice to several types of infections. We have isolated by cross-hybridization cDNA clones corresponding to a second mouse *Nramp* gene, that we designate *Nramp2*. Nucleotide and predicted amino acid sequence analyses of full length cDNA clones for *Nramp2* indicate that this novel *Nramp* protein is closely homologous to the previously described *Nramp*, and that the two genes form part of a small gene family. The two *Nramp* genes encode integral membrane proteins which share 63% identical residues and an overall homology of 78%. They share very similar secondary structure, including identical hydropathy profiles and predicted membrane organization, with a minimum of 10 and most likely 12 transmembrane domains, a cluster of predicted N-linked glycosylation sites, and a consensus transport motif. Analysis of the distribution of *Nramp2* mRNA transcripts in normal mouse tissues by Northern blotting revealed that the *Nramp2* gene produces several mRNAs, including prominent 3.3 and 2.3kb species generated by the use of alternative polyadenylation signals. In contrast to the previously described macrophage specific *Nramp* gene, *Nramp2* mRNAs were found to be expressed at low levels in all tissues tested. Using a polymorphic (GT)₂₆ dinucleotide repeat identified in the 3' untranslated region of the mRNA, we have mapped the *Nramp2* gene to the distal part of mouse chromosome 15 between markers *D15Mit41* and *D15Mit15*, with the gene order and intergene distance (in cM): Centromere- 56.1- *D15Mit41*- (1 -- 1) -*Nramp2*- (5 -- 2) - *D15Mit15*.

Introduction

In the mouse, innate resistance to infection with unrelated intracellular parasites such as *Mycobacterium bovis* (BCG) ¹⁷, *M. intracellulare* ¹⁹², *M. lepraemurium* ¹⁰⁸, *Salmonella typhimurium* ¹⁴, and *Leishmania donovani* ¹³ is controlled by the expression of a single dominant gene on mouse chromosome 1 alternatively designated *Bcg* ²⁰, *Ity* ¹⁴, or *Lsh* ¹³. Detailed *in vivo* ^{19,23} and *in vitro* studies ^{25-28,192} have established that *Bcg* affects the capacity of the host macrophages to control the intracellular replication of these antigenically unrelated microbes, during the early pre-immune phase of infection. The molecular mechanism by which *Bcg* modulates the innate bactericidal function of the tissue macrophage remains to be elucidated. In the absence of a known gene product or biochemical assay for the gene, we have used a positional cloning approach to clone *Bcg*. By using a large number of polymorphic DNA markers and informative backcross progeny, we have first defined a maximal genetic interval of 0.3 cM for *Bcg* on mouse chromosome 1 ^{29,223,224}. Using pulse field gel electrophoresis and fluorescence *in situ* hybridization to interphase nuclei, we have constructed a physical map of the *Bcg* region and have delineated a maximal physical interval of 1 Mb for the gene ³⁰. A genomic DNA domain of 400 kb was cloned in YAC and cosmid clones and 7 candidate transcription units were identified in the region by exon trapping ²²⁵. One of these genes encoded a mRNA which was exclusively expressed in reticuloendothelial organs such as spleen and liver, and was greatly enriched in tissue macrophages ³¹. This gene was designated *Nramp* for Natural Resistance Associated Macrophage Protein.

Nucleotide and predicted amino acid sequence analyses indicated that the *Nramp* gene most likely encoded an integral membrane protein composed of a minimum of 10

transmembrane (TM) domains. A cluster of predicted N-linked glycosylation sites was situated within the predicted extracytoplasmic domain delineated by TM 5 and 6. The Nramp polypeptide was also found to contain a sequence motif known as the "binding protein dependent transport system inner membrane component signature" in the intracytoplasmic loop flanked by predicted TM 6 and 7³¹. This motif was originally detected in one of the intracytoplasmic loops of the membrane subunits of periplasmic transport systems of Gram negative bacteria^{226,227} and in a few eukaryotic proteins³¹. It is believed to mediate interaction between the peripheral ATP binding units and the membrane anchors of these transporters to energize transport of structurally unrelated substrates²²⁷. The Nramp protein was found to share similarity, including the presence of the transport motif, with a eukaryotic nitrate/nitrite transport system of *Aspergillus nidulans*²²⁸, raising the possibility that Nramp may be involved in the metabolism or transport of these inorganic anions³¹. This is of particular interest since nitrate and nitrite are oxidation products of nitric oxide, a major anti-microbial effector molecule of macrophages^{229,230}. Nucleotide sequencing of *Nramp* cDNA clones and detailed haplotype mapping in 27 inbred mouse strains of distinct *Bcg* genotypes indicated that 1) all *Bcg^S* mouse strains shared a common haplotype for the portion of chromosome 1 overlapping *Bcg*, and 2) susceptibility was associated with a single non-conservative glycine to aspartic acid substitution within the second TM domain of the protein³². Finally, the glycine residue mutated in *Bcg^S* strains was found to be precisely conserved in the human, rat and chicken homologs of *Nramp*³².

During the characterization of mouse *Nramp* cDNA and genomic clones, it became evident that *Nramp* was not a single gene but was a member of a small family of closely related genes which included a minimum of two members in humans and mice and three members in chicken and swine ¹⁹⁶. In order to gain insight in the function and mechanism of action of the Nramp protein, we have set out to clone and characterize other members of the *Nramp* family.

Materials and Methods

Isolation of Nramp2 cDNA clones

Screening of human cDNA libraries with a full length mouse *Nramp1*³¹ under conditions of low stringency resulted in the identification of two classes of positive cDNA clones: some corresponding to human *NRAMP1* and a cross-hybridizing clone with a distinct restriction map. Partial sequence analysis of this clone revealed that it corresponded to a novel *Nramp* gene which was different from the mouse *Nramp1*³¹ or human *NRAMP1*²³¹ genes. Therefore, this clone was designated *NRAMP2* (Vidal et al., unpublished). A cDNA subfragment from this clone (position 519 to 825 of mouse *Nramp1* sequence, Genbank # L13732) was used to isolate full length cDNA clones for the corresponding mouse *Nramp2* gene. A total of 5×10^5 independent phage clones from a cDNA library (selected for insert size larger than 2.3 kb) constructed from the mouse pre-B cell line 70Z/3 in bacteriophage vector lambda gt11 were screened to identify *Nramp2* clones. For this, duplicate sets of filters (Hybond N, Amersham) were pre-hybridized at 42°C for 16 h in a solution containing 50% formamide, 5X SSC (1X SSC is 0.15M NaCl, 0.015M sodium citrate), 1% sodium dodecyl sulfate (SDS), 10% dextran sulfate, 0.02 M Tris pH 7.5, 1X Denhardt's (0.1% Bovine Serum Albumin, 0.1% ficoll, 0.1% polyvinylpyrrolidone) and 200 µg/ml heat denatured salmon sperm DNA. Hybridization was for 16h at 42°C in the same buffer containing a [³²P]-labeled human *NRAMP2* hybridization probe (1×10^5 cpm/ml). The probe was labeled to high specific activity ($1-2 \times 10^9$ cpm/µg DNA) by random priming using [^αP³²]-dATP (DuPont-NEN, specific activity 3000 Ci/mmol), random hexamers, and the Klenow fragment of DNA

polymerase I²³². The filters were washed to a final stringency of 0.5 X SSC, 0.5% SDS at 65°C, and exposed to Kodak XAR films for 48h with an intensifying screen. Phage pools from the positive clones were used to prepare plate lysates and DNA from these mass populations was purified, digested with *EcoR* I, and analyzed by Southern blotting. Positive phage clones fell into three populations, based on insert size, and DNA inserts from each population were subcloned into the *EcoR* I site of pBluescript and M13mp19 for further restriction mapping and nucleotide sequencing.

Nucleotide Sequence Analysis

The complete nucleotide sequence of the *Nramp2* cDNA clones was carried out by the dideoxy chain termination method of Sanger et al.²³³, using modified T7 DNA polymerase and either double stranded DNA templates (pBluescript) or single stranded DNA templates from M13mp19 recombinant phage clones. Oligonucleotide primers used for sequencing were derived either from the plasmid sequence near the cloning site, or from the cDNA insert sequence using a bi-directional walking strategy. The nucleotide sequence of the full length *Nramp2* cDNA was obtained from both strands of the same clone and/or from the same strand of independent overlapping clones. Computer assisted analyses of the nucleotide and predicted amino acid sequences were performed on the VAX/VMS server and computer of the Université de Montréal using the UWGCG software package (University of Madison, Wisconsin, USA)²³⁴ and with the DNA Strider package²³⁵. Sequence data from this article has been deposited with the Genbank data library under Accession No. L33415.

RNA and DNA Hybridization Studies

Normal mouse organs were frozen in liquid nitrogen and homogenized to a fine powder using a mortar and pestle cooled to -60°C . Total RNA was extracted with either Guanidinium hydrochloride (6M) or a Lithium Chloride (3M)/ Urea (6M) mixture and purified by ethanol precipitations and phenol and chloroform extractions, as described previously^{236,237}. The polyadenylated fraction of the RNA was isolated by chromatography on Oligo dT cellulose (Pharmacia-LKB). Ten μg of poly A+ RNA from each organ was electrophoresed in 1% agarose gels containing 0.66 M formaldehyde in 1X MOPS buffer (40 mM morpholinopropanesulfonic acid, 10 mM sodium acetate, 10 mM EDTA, pH 7.2), and transferred to a hybridization membrane (Genescreen Plus, New England Nuclear) by capillary blotting in 10 X SSC. Following baking at 80°C for 2 h, the membranes were pre-hybridized at 65°C for 16 hr in a solution containing 1M NaCl, 1% SDS, 10% dextran sulfate and heat denatured salmon sperm DNA (100 $\mu\text{g}/\text{ml}$). Hybridization was performed for 24 h in the same buffer containing 1×10^6 cpm/ml of a series of hybridization probes labeled to high specific activity ($1-2 \times 10^9$ cpm/ μg DNA) with [^{32}P] α -dATP by random priming²³². The membranes were washed up to a final stringency of 0.5 X SSC, 1% SDS at 65°C (45 min.), and exposed to Kodak XAR films at -80°C with an intensifying screen. The hybridization probes were striped from the blot by three consecutive washes in 0.1 X SSC, 0.1% SDS at 90°C .

Genomic DNA was isolated from frozen mouse livers by proteinase K treatment, phenol and chloroform extractions, and precipitation with ethanol²²³. Genomic DNA

was digested with restriction enzymes (5 units / μ g DNA), under conditions recommended by the supplier of enzyme. The fragmentation products were separated by electrophoresis in agarose gels containing TAE (40 mM Tris-acetate, 20 mM sodium acetate, 20 mM EDTA, pH 7.6), and transferred to a hybridization membrane (Hybond N, Amersham) by capillary blotting in 20 X SSC. Prehybridization and hybridization conditions for Southern blots were identical to those used for RNA blots except that the solution consisted of 50% formamide, 5 X SSC, 1 X Denhardt's, 0.5% SDS, 10% dextran sulfate, and 10 mM TRIS, pH 8 and the temperature of hybridization was 42°C.

Chromosome Mapping

Genomic DNA was isolated from frozen livers of mouse strains C57BL/6J, DBA2/J, AKR/J, and A/J and tested for the presence of polymorphic differences at the *Nramp2* locus. Oligonucleotide primers (forward primer: 5'-AGGTGTCTCCAGTCTCTACC-3'; pst.2287-2306) and (reverse primer: 5'-GATCCTTGAACCTTACTGGCTG-3'; pst.2467-2487) (Figure 1C) flanking a dinucleotide (GT) repeat identified in the 3' untranslated region of *Nramp2* were used to amplify by PCR the corresponding genomic DNA fragment (SSR) from the various inbred strains. A unique allele of this SSR was identified in AKR/J genomic DNA, and consequently 100 progeny of a (AKR/J X C57BL/6J) F1 X C57BL/6J interspecific backcross ²²⁴ were typed for this polymorphism. This marker has been submitted to the Jackson Lab data base, under the formal designation *D15Mcgl*. For amplification of the SSR, 20 picomoles of one of the reverse primer was end labeled with $\gamma^{32}\text{P}$ -ATP (New England Nuclear, specific activity 8000 Curies/mmmole) in a reaction mixture consisting

of 50 mM Tris pH 9.5, 10 mM MgCl₂, 100 μM Dithiothreitol and T4 Polynucleotide Kinase (1 unit) at 37° for 30 minutes. 0.25 picomoles of the labeled primer was added to a PCR amplification reaction consisting of 50 mM KCl, 10 mM Tris (pH 9.0), 0.1% Triton X-100, 1 mM MgCl₂, 0.12 mM of each dNTP, 0.5 μM of each unlabeled primer , 50 ng of template DNA, and 0.5 units of Taq polymerase (BIO/CAN). Parameters for PCR amplification of the *Nramp2* SSR from genomic DNA were initial denaturation at 94°C for 3 min., followed by 25 cycles at 94°C (30 s), 60°C (30 s), 72°C (1 min), and a single final extension period of 10 min. at 72°C. Oligonucleotide primer pairs *D15Mit15* and *D15Mit41* defining polymorphic SSR's on chromosome 15 were purchased from Research Genetics and PCR amplification from genomic DNA was performed as recommended ²³⁸. Amplification products were analyzed by electrophoresis on 6% denaturing polyacrylamide gels followed by exposure to Kodak XAR film. Genetic linkage and gene order was determined by segregation analysis, minimizing the number of crossovers between individual markers ²³⁹.

Results

Isolation and Characterization of Mouse Nramp2 cDNA Clones

Two sets of experimental evidence suggested that the mouse *Nramp* gene was not unique and might be part of a family of closely related genes. Firstly, Southern blotting analysis of mouse and human genomic DNA under conditions of reduced stringency revealed complex patterns of hybridization suggestive of at least two genes (data not shown). Secondly, screening of human cDNA libraries for the presence of homologous *NRAMP* sequences with a mouse *Nramp* probe yielded two types of hybridizing clones (strongly and weakly hybridizing). Nucleotide sequencing of these clones revealed that the first group (strong hybridization) corresponded to the previously reported mouse *Nramp*²³¹, while the second group showing weaker hybridization signal displayed a more divergent sequence. The corresponding genes were therefore designated *NRAMP1/Nramp1* for the former and *NRAMP2/Nramp2* for the latter human and mouse genes, respectively. To investigate further this novel *Nramp2* gene, we sought to isolate a full length cDNA clone for the mouse gene. For this, a pre-B cell cDNA library was screened with a cDNA subfragment derived from a partial cDNA clone for human *NRAMP2*. Thirty-five positive clones were identified (frequency = 1 in 14,000 or .007% of the mRNA population), and EcoR I digested DNA from primary phage pools was analyzed by Southern blotting. The phage clones could be assembled into three groups of identical clones with insert size: 2.1 (clone 3B), 2.9 (clone 8B) or 3.0 kb (clone 1B) (Figure 1A). It is likely that three original clones gave rise to the thirty-five clones during repeated amplifications of the library (data not shown). Phages from each population were plaque-purified and their inserts subcloned into pBluescript and M13mp19 for

further analysis. Restriction enzyme mapping and partial nucleotide sequencing of the 5' and 3' extremities of these clones revealed that 1) they overlapped and corresponded to the same transcription unit, and 2) clone 1B apparently showed a small 80 bp insertion in its 3' region, when compared to the inserts of clones 3B and 8B (Figure 1A).

Clones 1B and 8B were sequenced in full and the 3' end of clone 3B was also sequenced using successive oligonucleotide primers deduced from the cDNA sequence. The nucleotide sequence of the full length clone (2972 nucleotides), and the oligonucleotide primers used for sequencing are shown in Figure 1B. The first 5' ATG codon was found at nucleotide position 61 of the sequence, followed by an open reading frame (ORF) consisting of 1707 nucleotides capable of encoding a putative polypeptide of 568 amino acids, ending with a TGA stop codon at pst. 1765. Since no in-frame termination codon was found upstream the proposed initiator ATG at pst. 61, it could not be formally established that this upstream segment was indeed untranslated. However, several observations support the notion that this ATG codon is indeed used as the initiator *in vivo*: 1) it is positioned within the optimal sequence context (ACCAUGG) for initiation by eukaryotic ribosomes²⁴⁰, 2) the size of the full length cDNA is compatible with the size of the corresponding mRNAs detected *in vivo* in normal tissues (Figure 4), 3) the polypeptide initiated by this ATG is highly homologous to the mouse Nramp1 protein (Figure 3A). The ORF was followed by a long 3' untranslated region (UTR) of 1206 nucleotides which terminated by a short poly-A tail. This 3' UT included two (GT)_n dinucleotide repeats, a (GT)₁₆ at pst. 2203-2234 and a (GT)₂₆ at pst. 2310-2361 (clone 8B). The 3' UT of clone 1B contained yet an additional copy of the (GT)₁₆; This third repeat most likely arose as a duplication event during the propagation of the cDNA

Figure 1 *Nucleotide sequence of the mouse Nramp2 cDNA*

(A) Schematic representation of the *Nramp2* cDNA, identifying the coding region of the mRNA (thick line), the dinucleotide (GT)_n repeats in the 3' UTR (vertical lines), and the poly A tail. The cDNA clones analyzed in this study are shown immediately below. The additional copy of the shorter repeat identified in clone 1B is also shown. (B) Nucleotide Sequence of mouse *Nramp2* cDNA. Nucleotides are numbered in the 5' to 3' orientation starting with the first nucleotide of the predicted 5' UTR. The coding portion of the mRNA is capitalized, while untranslated nucleotides are in lower case. The proposed initiator ATG codon is identified by an arrow and the termination codon by an asterisk (*). The primers used for direct nucleotide sequencing and for PCR amplification are identified by arrows immediately underneath the corresponding nucleotide sequence. The simple sequence (GT)_n repeats are in bold.

library, since it could not be detected in genomic DNA from either parental mouse strains (C57BL/6J, DBA/2J) from which the 70/Z cell line was derived (data not shown).

Finally, a putative poly-adenylation signal (AATAAA) was found at position 2930, 23 nucleotides upstream from the segment of 20 adenosines at the end of the cDNA insert.

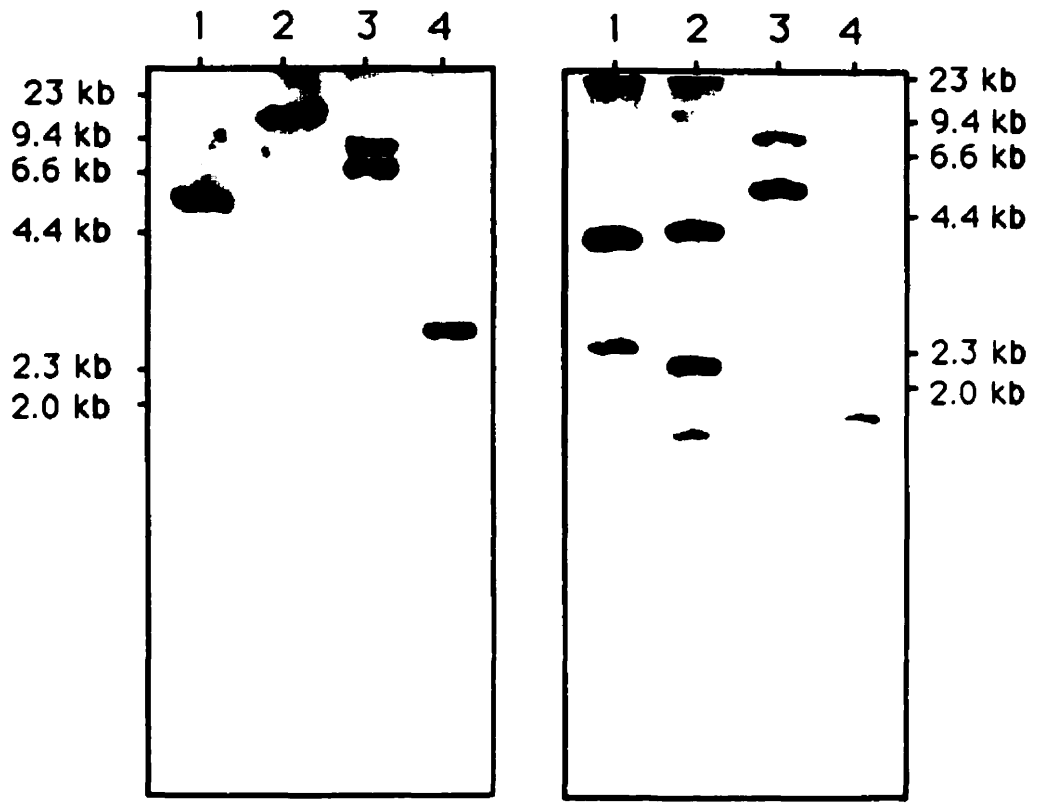
Southern blotting analysis of mouse genomic DNA, using as hybridization probes cDNA subfragments derived from homologous segments of the previously identified mouse *Nramp1* and this new *Nramp2* gene (nt. 519-825, mouse *Nramp1*; nt. 535-841, mouse *Nramp2*), revealed two distinct and non-overlapping patterns of hybridizing fragments for the four restriction enzymes tested (Figure 2). This data clearly indicates that the *Nramp2* cDNA isolated here indeed corresponds to a new gene and was not derived from the *Nramp1* transcription unit.

Analysis of the Predicted Nramp2 Polypeptide

Analysis of the predicted amino acid sequence of the protein encoded by the mouse *Nramp2* cDNA identified a polypeptide chain of 568 amino acids with a minimum molecular mass of 62 kDa (Figure 3A). The *Nramp2* protein was predicted to be highly hydrophobic with characteristics of an integral membrane protein. Indeed, hydrophobic amino acids accounted for 44% of the protein (leucine, 12%; isoleucine, 7%; valine, 10%; alanine, 8%; phenylalanine, 7%), the apolar residue glycine accounted for 8%, while charged residues accounted for only 15% (arginine-4%, lysine-3%, aspartic acid-4%, glutamic acid-4%) of the total amino acid composition (Figure 3A). In addition, hydropathy profile analysis of *Nramp2* using the Kyte-Doolittle algorithm²⁴¹ or the

Figure 2 *Southern blotting analysis of the mouse Nramp1 and Nramp2 genes*

Southern blots containing 5µg of mouse genomic DNA in each lane digested with *BamH* I (lane 1), *EcoR* I (lane 2), *Hind* III (lane 3), or *Pst* I (lane 4) were hybridized with gene-specific cDNA probes from *Nramp1* or *Nramp2*. The probes were derived by PCR using primers (PG03, 5'-GGCTCAGATATGCAGGAAGTC-3') and (MCO6, 5'-GACGATGCCCACTGC-3') to amplify equivalent regions from *Nramp2* (pst 535 to 841) or *Nramp1* (pst 520 to 826) cDNA clones. The *Hind* III fragments bacteriophage lambda were used as molecular size markers (in kb)



Nramp1

Nramp2

calculation of the hydrophobic moment ²⁴² (data not shown) identified a minimum of 10 and a maximum of 12 highly hydrophobic putative transmembrane (TM) domains in the sequence (underlined in Figure 3A). Interestingly, several of the TM domains predicted in the amino terminal half of the protein (TM1, 2, 4, 5) and one (TM9) in the carboxy terminal half contained one charged residue, while TM 3 included 2 such residues. The carboxy and, in particular, the amino terminal segments of the Nramp2 protein contained alternating clusters of negatively and positively charged residues; Such segments are incompatible with membrane insertion, are most likely located in the aqueous phase, and have also been described at the NH₂ terminal region of other integral membrane proteins ²⁴³. The sequence showed four potential N-linked glycosylation signals (N-X-S/T; ²⁴⁴) (psts 33, 336, 337 and 349), three of them (psts 336,337, and 349) clustered within a short segment flanked by the two TM domains delineated by residues 300-319 and 361-380. The "binding-protein dependent transport system inner membrane component signature", is a 20 residue consensus motif that has been detected in the predicted intracellular loop of the membrane subunits of several periplasmic transport systems of Gram negative bacteria ^{226,227}, but has also been described in a few eukaryotic proteins ³¹. This motif was detected at pst. 384 to 403, flanked by the two TM domains defined by residues 361-380 and 412-429 (Figure 3A). Five consensus sites for phosphorylation by protein kinase C (S/T-X-R/K; ^{245,246}; psts 66, 228, 326, 462 and 543), and four consensus for phosphorylation by Casein kinase II (S/T-X-X-D/E) ²⁴⁷ were also found in the predicted Nramp2 protein (psts 39, 49, 189, and 536).

Taken together, these results strongly suggest that like its Nramp1 homolog, Nramp2 is an integral membrane protein with a potential transport function. The

Figure 3 (A) *Deduced Amino Acid Sequence of the Mouse Nramp2 Protein and Alignment with the Mouse Nramp1 Protein.* Amino acids are numbered starting with the predicted initiator methionines of each sequence. Predicted N-linked glycosylation sites identified at psts.321, 335 and 33, 336, 337, 349 in *Nramp1* and 2 cDNAs, respectively (*), the binding protein dependent inner membrane component signature (boxed) and putative transmembrane domains (underlined) are shown. The sequences of *Nramp1* and *Nramp2* were aligned using the "GAP" program of the GCG package and gaps were introduced into the carboxy and amino terminal regions to optimize alignment. Identical residues between *Nramp1* and 2 are indicated by a vertical line (|) and conservative substitutions by two dots (:), according to the Dayhoff (1976) for a relative rate of acceptance of point mutations greater than 40. (B) *Hydropathy profiles of the predicted amino acid sequence of mouse Nramp2 (top) and 1 (bottom).* The profiles were derived with the DNA Strider program, using the algorithm and hydropathy values of Kyte and Doolittle (1982) for a window of 11 amino acids. (C) *Twelve transmembrane domain model of the Nramp2 protein.* Transmembrane domains are shown as cylinders and N-linked glycosylation sites are identified in the fourth extracellular loop.

A

```

Nramp 2  MVLDPKEKMPDDGASGDHGDASLGAINPAYSNSSLPHSTGDSEEPFTTYFDEKIP IPIEEEYSCFSFRKL 70
Nramp 1  ..... MISCKSPPLSRPSYGSI.....SSLRQPAKQFAPCRETYLSEKIP IFSADQXTTFLSRKL 55

Nramp 2  WAFTGPGFLMSIAYLDPGNI ESDLQSGAVAGFKLLWVLLLATIVGLLLQRLAARLGVVTGLHLAEVCHRQ 140
Nramp 1  WAPTORGFLMSIAPLDRNIESDLQAGAVVGFALLWVLLWATVLSLLQRLAARLGVTGKLDSEVTHLV 125

Nramp 2  YPKVPRIIILWLVELAIIGSDMOEVIQSAIAINLLSAGRVPVWGGVLTITADTFVFLFLDKYGLRKL EAF 210
Nramp 1  YPKVPRIIILWLVELAIIGSDMOEVIQSAIAINLLSAGRVPVWGGVLTITADTFVFLFLDKYGLRKL EAF 195

Nramp 2  EGFLITIMALTFGY EYIITVKPSQSQVLRGMFVPSGRCRTPQVDAQVGI V GAVIMPHNMYLHSALVKSRO 280
Nramp 1  EGFLITIMALTFGY EYIITVKPSQSQVLRGMFVPSGRCRTPQVDAQVGI V GAVIMPHNMYLHSALVKSRE 265

Nramp 2  VNRANKQEVREANKYFFIE SCIALVSPFINVFWVSVFAEAPFEKINKQVVEVCKNNSSPH .ADLFFSDN 349
Nramp 1  VNRANKQEVREANKYFFIE SCIALVSPFINVFWVSVFAEAPFEKINKQVVEVCKNNSSPH .ADLFFSDN 335

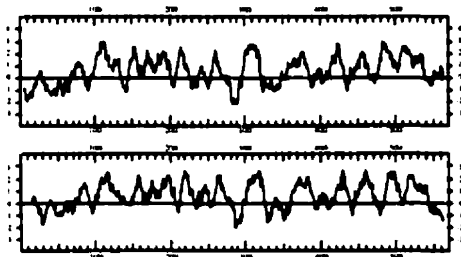
Nramp 2  STLAVDIYKGGVVLGCYEGPAALYIWA VGILAAQSSSTMIGTYSQGFVMEGFLN LKMSRPARVILTRSA 419
Nramp 1  STLAVDIYKGGVVLGCYEGPAALYIWA VGILAAQSSSTMIGTYSQGFVMEGFLN LKMSRPARVILTRSA 405

Nramp 2  I I P T L L V A V P Q D V E H L T G N D F L N V L Q S L Q L P F A L I P I L T F T S L R F V M S E F S N G I G W R I A C G I L V L I V C S 489
Nramp 1  I I P T L L V A V P Q D V E H L T G N D F L N V L Q S L Q L P F A L I P I L T F T S L R F V M S E F S N G I G W R I A C G I L V L I V C S 475

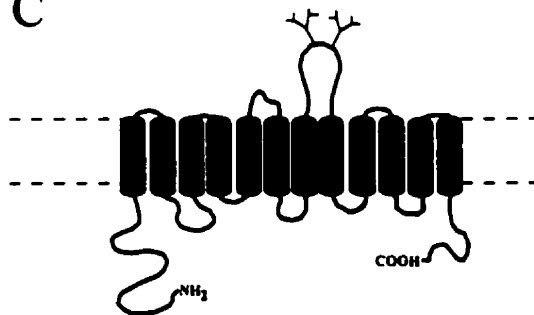
Nramp 2  INMYFVVVVYQELGHVALYVVA AVVSVAYLTEVFYLGWQCLIALGLSFLDCGRSYRLGLTAQPELYLLNT 559
Nramp 1  INMYFVVVVYQELGHVALYVVA AVVSVAYLTEVFYLGWQCLIALGLSFLDCGRSYRLGLTAQPELYLLNT 545

Nramp 2  VDADSVVSR. 568
Nramp 1  SEQFFVQISG 545
  
```

B



C



positioning of 1) the cluster of N-linked glycosylation signals to a putative extracellular domain of the protein, and 2) the consensus transport motif to an intracellular domain, together suggest the following membrane topology for an even number of 10 or 12 TM domains. The amino terminus of the protein would be intracellular, followed by 10 or 12 TM domains arranged in 5 or 6 transmembrane loops, which would position the carboxy terminus to the intracellular phase of the membrane (Figure 3C).

Mouse Nramp1 and Nramp2 Homology

In their region of overlap, the cDNAs for *Nramp1* (Genbank #L13732) and *Nramp2* were found to share 56 % nucleotide sequence identity, with 64% identity in the coding region of the mRNAs and 48% and 38% in the 5' and 3' untranslated regions, respectively (data not shown). This translated at the amino acid level to 63% identical residues and 15% highly conservative substitutions for a total homology of 78% between the two proteins (alignment shown in Figure 3A). Although *Nramp2* was predicted to be 20 residues longer (568) than its *Nramp1* counterpart (548), the two proteins showed superimposable hydropathy profiles (Figure 3B), and shared similar structural features with identical proposed membrane topology. Non-conserved substitutions were not randomly distributed and were concentrated at the amino (residues 1 to 65, 53% identity) and carboxy terminal (residues 528 to 569, 42% identity) segments of the two proteins, where several gaps had to be introduced to optimize alignment. It was within these segments that differences in length of the two proteins could be accounted for. Sequence divergence was also observed in the predicted intra and extracellular loops located in the carboxy terminal half of the two proteins (TM5-12 region) (Figure 3A). The rest of the two polypeptide chains were highly conserved, in particular within the predicted TM

domains with respect to length, position, sequence, including preservation of the charged residues within them. Two large domains of the two proteins showed a remarkably high degree of sequence conservation with greater than 90% amino acid sequence identity (Figure 3A). These included the segment which encompassed predicted TM 1 to 5 (residues 65-229, 92% identity), and the segment that overlapped TM 8-10 and included the "binding-protein dependent transport system inner membrane component signature" (residues 361-461, 91 % identity). This suggests that these two segments play an important structural and/or functional role in the common mechanism of action of these two proteins. Finally, although located within a segment which was not conserved amongst the two proteins, the clusters of glycosylation signals located between TM 7 and 8 were preserved in Nramp1 and Nramp2, also suggesting an important role for processing, stability or targeting of these two proteins. On the other hand, only two of the predicted protein Kinase C sites (pst 66, 543) and one of the Casein Kinase II sites (pst 189) were preserved in both sequences, arguing against an important role for these sites.

Nramp2 mRNA Expression in Normal Mouse Tissues

The polyadenylated fraction of RNA from normal mouse brain, lung, heart, liver, spleen, kidney, intestine and muscle was isolated and analyzed for *Nramp2* mRNA expression by Northern blotting (Figure 4A). *Nramp2* cDNA hybridization probes derived from the coding region of the cDNA detected two major mRNA species of size 3.3 kb and 2.3 kb which were expressed in all tissues tested (Figure 4B). Upon prolonged exposure of the autoradiogram (Figure 4B, and data not shown), additional minor species of size 5 kb (all tissues) and 1.7kb (brain, intestine) were detected. On the other hand, a cDNA probe derived from the 3' UTR of the mRNA immediately downstream the

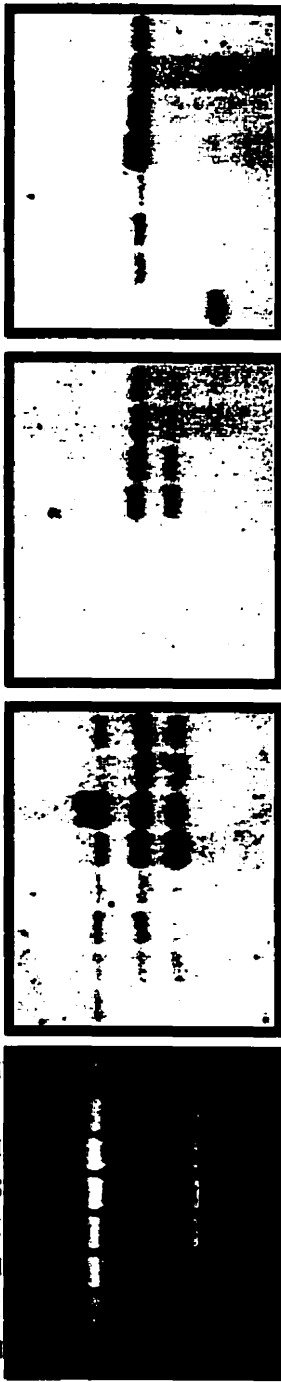
Figure 4 *Northern blot analysis of Nramp2 mRNA expression in normal tissues*

Approximately 10 µg of polyadenylated mRNA from normal mouse tissues was analyzed by Northern blotting using probes derived from position 535 to 841 in the *Nramp2* coding region (panel B), pst. 1785 to 2013 in the 3' UTR (panel C) and pst. 2461 to 2878 in the 3' UTR (panel D). The ethidium bromide staining of the gel is shown in panel A. The positions of 18S and 28S ribosomal RNA is indicated.

AAAAAAAAA



Brain
Lung
Heart
Liver
Spleen
Kidney
Intestine
Muscle



A B C D

termination codon (nt. 1785-2013) detected only the two major hybridizing bands of size 3.3 and 2.3kb (Figure 4C). Finally, hybridization with a distal 3' UTR probe (nt. 2460-2878) detected only the larger 3.3 kb mRNA species in all tissues tested, except brain where the 1.7kb mRNA was prominent (Figure 4C). This suggests that the two major *Nramp2* transcripts differ in length in their 3' untranslated regions. Although this difference has yet to be fully characterized, it is most likely due to alternative use of distinct polyadenylation signals. The size of the *Nramp2* cDNA clone isolated is compatible with the size of these two mRNAs and is therefore likely to be full or close to full length. The origin and nature of the minor 5 kb mRNA remains unclear, but could correspond to a partially processed mRNA or reflect cross-hybridization to related genes transcripts. Finally, the nature of the unique 1.7kb species seen in brain and intestine is unknown but could reflect alternative splicing of the *Nramp2* gene product in these tissues or the cross-hybridization of a different mRNA sharing homology with the 3' UTR of *Nramp2*.

The *Nramp2* mRNA transcripts were found to be ubiquitously expressed in all tissues tested. The apparent variations in the levels of expression detected in the various tissues (Figure 4 B-D) were not likely caused by variations in tissue specific expression but rather seemed to be caused by differences in amounts of mRNA loaded on gel or transferred to the blot, as suggested by ethidium bromide staining of the agarose gel (Figure 4A). The level of *Nramp2* expression was fairly low and its detection by Northern blotting required the use poly A+ RNA. This is in sharp contrast to the *Nramp1* gene previously described by our group which was found to be expressed in a tissue

specific fashion in reticuloendothelial organs, in general, and mature tissue macrophages, in particular ³¹.

Chromosomal Localization of the Mouse Nramp2

In order to map the chromosomal location of the *Nramp2* gene, we tested whether the dinucleotide repeats (GT)_n identified within the 3' untranslated region of the *Nramp2* mRNA were polymorphic in genomic DNA from different inbred strains, and therefore informative for mapping. Oligonucleotide primer pairs flanking the (GT)₂₆ repeat (Figure 1B; nt. 2287 to 2487) were used to PCR amplify the corresponding genomic DNA fragment from inbred strains A/J, AKR/J, C57BL/6J, and DBA/2J. A single fragment of 200 bp was amplified in all inbred strains tested except for AKR/J which produced a 202 bp fragment, suggesting variation by a single GT unit in this strain (Figure 5A). The inheritance pattern of this polymorphism was followed in 100 progeny of a (AKR/J x C57BL6/J) F1 x C57BL6/J intraspecific backcross. The mice showed either a homozygous C57BL6/J pattern or a heterozygous F1 type pattern, depending on the allele inherited from the F1 parent. Since preliminary results from our laboratory suggested the long arm of chromosome 12 as a possible location for the human *NRAMP2* gene ³⁵, we tested the possibility that the mouse *Nramp2* SSR identified in AKR/J and C57BL/6J may co-segregate with dinucleotide repeat markers from mouse chromosomes 10 and 15 which contain groups of loci syntenic with human 12q. This analysis identified co-segregation of the *Nramp2* SSR with markers from the distal portion of mouse chromosome 15 (Figure 5B). In a total of one hundred backcross progeny tested, one crossover was observed between *Nramp2* and *D15Mit41*, while five

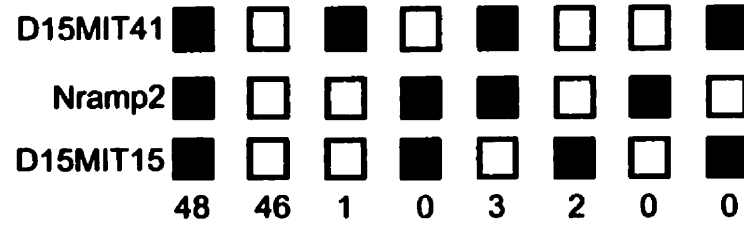
Figure 5 *Mapping of the Nramp2 gene to mouse chromosome 15*

(A) A DNA fragment containing the (GT)₂₆ dinucleotide repeat detected in the 3' UTR of the *Nramp2* cDNA was amplified by PCR from the genomic DNA of several inbred strains of mice (see Materials and Methods) and a unique polymorphic variant (SSLP) was identified in the AKR/J strain (lane 1- AKR/J, lane 2- DBA/2J, lane 3- A/J, lane 4- C57BL/6J). This SSLP was used to map the chromosomal location of the *Nramp2* gene by segregation analysis. (B) Distribution of haplotype for *Nramp2*, *D15Mit15*, and *D15Mit41* in 100 progeny analyzed from a (AKR x C57BL/6)F1 x C57BL/6 backcross. B6 alleles are represented by a black box, AKR alleles by a white box. The number of progeny with each haplotype is shown at the bottom of each column. (C) Schematic representation of the map position of *Nramp2* on mouse chromosome 15. Map positions of the known markers are shown in brackets to the right of the chromosome, and intergene distances deduced from our backcross panel are shown to the left of the chromosome.

1 2 3 4

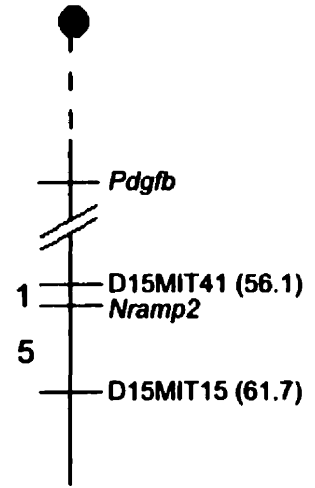


A



B

15



C

crossovers were detected between *Nramp2* and the more distally located marker *D15Mit15* (Figure 5B). Haplotype analysis of these mice for the three markers indicated that the *Nramp2* gene was between *D15Mit41* (proximal) and *D15Mit15* (distal), with the following gene order and intergene distance (in cM): Centromere- *D15Mit41* - (1 \pm 1) cM - *Nramp2* - (5 \pm 2) cM - *D15Mit15* (Figure 5C).

Discussion

Natural resistance to infections with several intracellular parasites is determined by the *Bcg* (*Ity*, *Lsh*) gene¹⁹, for which we have isolated by positional cloning a candidate named *Nramp*³¹. By cross-hybridization, we now have identified cDNA clones corresponding to a novel related gene. Nucleotide sequence analysis of the coding region this gene revealed 64% identity with the previously identified *Nramp* gene, translating into 78% amino acid sequence homology between the two proteins, with identical predicted secondary structure and proposed membrane topology. Based on this high degree of sequence homology, we propose that both form part of a small family of at least two *Nramp* genes in the mouse. We have tentatively given this new gene the appellation *Nramp2*, and have also renamed the previously isolated *Nramp* gene³¹, *Nramp1*. Although the name *Nramp* (Natural Resistance Associated Macrophage Protein) was originally chosen to reflect the association of this gene with the chromosome 1 locus *Bcg*, and its role in resistance to infection, the physiological function of *Nramp2* including a possible role in resistance to infection remain unknown (see below). The high degree of sequence homology between *Nramp1* and *Nramp2* suggests that the two genes have evolved from a common ancestor by gene duplication. After duplication, the two genes have been separated on different chromosomes (*Nramp1*, chromosome 1; *Nramp2*, chromosome 15) and distinct genomic environments, in agreement with their distinct expression profiles in normal tissues. Southern hybridization and cDNA cloning experiments have indicated that highly conserved *Nramp* genes also exist in humans and rats (2 genes), but also in swine and birds (3 genes), suggesting that duplication events occurred prior to mammalian radiation (data not shown). Finally, another group has

reported a possible third *Nramp* gene. Dosik et al. (1994) have identified *Nramp-rs*, a genomic DNA fragment that cross-hybridizes with a *Nramp*-derived probe. This fragment has been mapped to mouse chromosome 17. However, full analysis of *Nramp-rs* and its relationship to the other members of the *Nramp* family awaits the identification and sequencing of a corresponding cDNA.

The ATG codon found at position 61 (Figure 1) is the first in-frame methionine codon identified in the *Nramp2* cDNA and begins an open reading frame encoding a protein of 62 kDa. Although this ATG is positioned within an optimal sequence context for initiation (ACCAUGG)²⁴⁰, we cannot exclude the possibility that the ATG at position 84 could be the initiator ATG. In addition, since no in-frame termination codon could be found upstream the ATG at position 61, the formal possibility exists that an additional ATG exists in yet further upstream 5' sequences not present in our clone. However, the minimum size of the *Nramp2* mRNAs identified by Northern blotting and estimated at approximately 2.3 kb and 3.3 kb. (Figure 4) suggest that our cDNA is close to full-length. Hydropathy profiling using the algorithm of Kyte and Doolittle²⁴¹, and hydrophobic moment analysis suggest that *Nramp2* is a polytopic membrane protein, with a minimum of 10 and possibly up to 12 putative transmembrane (TM) domains. The availability of a full length sequence for mouse *Nramp2* and also human *NRAMP1* proteins²³¹ has allowed us to focus our analysis on the number of putative TM domains in this group of proteins. Although a 10 TM domains configuration was initially proposed for *Nramp1*³¹, two additional amino terminal segments (*Nramp2*; TM 1, residues 55-76; TM 3 residues 141-161) also seem compatible with membrane insertion. Although TM 1 is strongly suggested both by hydropathy and hydrophobic moment

analyses, TM 3 would be thermodynamically less favored because it would require the insertion of two negatively charged amino acids within the membrane. It is interesting to note that putative TM3 has the capacity to form an amphipathic helix positioning both charges on the same phase of the helix. Finally, the sequences of TM1 and TM3 were found to be highly conserved in mouse Nramp1, human NRAMP1²³¹ and mouse Nramp2 (Figure 3), but also in distant members of this emerging gene family that we have identified in lower and higher eukaryotes^{178,179}. Therefore, we have revised the predicted structural model of the Nramp family to include a maximum of 12 putative TM domains (Figure 3C).

Although there is little doubt that both Nramp1 and Nramp2 are integral membrane proteins, their function or mechanism of action remain unknown. A review of some of the structural features identified within these proteins together with an analysis of the pattern of conservation of these predicted domains may help distinguish between their possible common function. A sequence motif known as the "binding protein dependent inner membrane component signature" [(E, Q)(S, T, A)₂ 3X G 6X (L, I, V, M, Y, F, A) 4X (F, L, I, V) (P, K):²⁴⁸] was identified in both proteins (Nramp1, pst. 370 to 389; Nramp2, pst. 384 to 403) within one of the predicted intracellular loops. This motif was originally identified within predicted intracellular loops of the membrane anchors of bacterial periplasmic permeases, where it is believed to participate in the interaction of membrane components with peripheral ATP binding subunits of these transporters^{226,227}. Although both Nramp1 and Nramp2 have conserved this motif in the same segment of the protein, they show a single substitution (Lys to Asn) at the last position of this motif. Although Lys and Pro residues have been assigned at that position

in the consensus motif, substitutions at that (araH, phnM) and other positions (amiC, amiD) seem to be tolerated without loss of function, as exemplified by the combined analysis of bacterial permeases ^{227,249}. A search of the Swiss Prot data base for the presence of this motif, allowing for substitutions at the last position, identified a total of 254 prokaryotic and eukaryotic proteins, 51 of which were membrane proteins; In this latter group of membrane proteins, presence of the motif was associated with transport function in 45 cases (examples are given in Table I). Therefore, it appears that this motif when present in membrane proteins such as Nramp, is associated with an energy dependent carrier function. The sequence of this motif was recently revised to more accurately define the group of bacterial periplasmic proteins by including (L, I, V, M, F, Y) at a position -9, R at the 1st position, G at the 3rd position, (L, I, V, M, F, Y, S, T, A, C) at the 8th position, (S, T) 14th position, (M, F) at the 19th position and an R at the 20th position ²⁴⁹. This sequence diverges from Nramp and other eukaryotic transporters at the -9 position and in some cases at the 8th and 20th positions. The functional consequence of this sequence divergence between prokaryotes and eukaryotes remains unknown.

A possible role of Nramp1 in signal transduction has been proposed independently ²¹³. This proposal was based on the presence of several predicted phosphorylation sites by Protein kinase C (PKC) and of several proline residues clustered within the amino terminal domain ²¹³. Proline rich domains in certain proteins have been proposed to interact with the src homology domain 3 or SH3 domains of other proteins and would therefore be involved in protein-protein interactions during signal transduction. The amino terminal of Nramp1 is rich in prolines (12 in first 100 residues)

Table 1- The binding-protein-dependent transport system inner membrane component signature in bacterial and eukaryotic transporters

	(E,Q)	(S,T,A)	(S,T,A)	3X	G	5X	(L,I,V,M,F,Y,A)	3X	(F,L,I,V)	(P,K)										
HisQ	E	A	A	T	A	F	G	F	T	H	G	Q	T	E	R	R	I	M	F	P
MalF	E	A	S	A	M	D	G	A	G	P	F	Q	N	F	F	K	I	T	L	P
PstA	E	A	A	Y	A	L	G	T	P	K	W	K	M	I	S	A	I	T	L	K
PhnM	E	A	S	R	K	H	G	M	N	V	L	M	G	A	P	N	I	V	R	G
AraH	E	A	A	R	L	A	G	V	P	V	V	R	T	K	I	I	I	F	V	L
Atn1	E	A	A	E	F	I	G	T	S	L	T	E	G	L	T	Q	D	E	F	V
CmA	Q	S	S	R	P	S	G	P	P	S	I	I	A	Y	A	I	P	D	V	E
Nramp 1	Q	S	S	T	M	T	G	T	Y	A	G	Q	F	V	M	E	G	F	L	K
Nramp 2	Q	S	S	T	M	T	G	T	Y	S	G	Q	F	V	M	E	G	F	L	N

Note: all sequences were obtained from the Swiss-Prot database.

and contains a proline rich 20 amino acid segment with similarity to one of the SH3 binding domains of the *Drosophila* dynamin protein *Shibire*²⁵⁰. The sequence motif PGPAPQPXPXR (pst. 22 to 32) was proposed to be the SH3 binding motif of Nramp²¹³. The amino terminal of Nramp2 also contains several prolines (9 in first 100 residues) and one predicted PKC phosphorylation site (Figure 2), suggesting that this region may also contain an SH3 binding motif possibly important for a common mechanism of action of both proteins. However, the observations that the proposed PGPAPQPXPXR motif was 1) not precisely conserved in the human NRAMP1 homolog²³¹, 2) mapped in a region that showed the lowest degree of homology between the human and mouse proteins²³¹, and 3) was also not conserved in Nramp2 (Figure 3) argue against a critical role for this part of the molecule. Therefore, the relevance of this putative SH3 binding domain to Nramp function and proposed role in signal transduction remains unclear.

On the other hand, the position and sequence of TM domains were found to be strictly conserved between Nramp1 and Nramp2. Of particular interest were the findings that all charged residues (Figure 2A: D, pst.86; K, pst.93; D, pst.161; E, pst.164; D, pst.192; E, pst.225; R, pst.416), and prolines (pst.76, 87, 266, 369, 422, 451, 456) mapping within these domains were precisely conserved between the two proteins. This suggests an important role of these residues in common structural/functional aspects of both proteins. Prolines within TM domains have been previously shown to be important functional and structural determinants of integral membrane proteins²⁵¹. Although unusual, charged residues within TM domains can play important role in the overall three dimensional structure of the protein by forming salt bridges, such as in the lactose

permease ²⁵², or can interact directly with substrate ^{253,254}, within the context of a water filled pore. Conservation of such residues is most obvious in channels of transporters acting on small charged molecules such as CFTR, where the positions and identity of charged residues in TM domains has been precisely conserved in mouse and human isoforms of the protein ²⁵⁵. Taken together, these results support the notion that Nramp proteins are membrane transporters.

The genetic analysis of *Nrampl* indicates that it plays an important role in host defenses against infections. Indeed, *Nrampl* maps at the host resistance locus *Bcg/Ity/Lsh*, and is mutated in mouse strains susceptible to infections with intracellular parasites ³¹. In addition, the pattern of *Nrampl* expression is restricted to macrophages, a cell type known to play a pivotal role in host response to infections ³¹. Based in part on the observation that the transport motif detected in Nramp is also present in a nitrate/nitrite transporter from *A. nidulans* (one of seven eukaryotic membrane transporters known to bear this motif), we have previously speculated that in these cells, *Nrampl* may code for a nitrate/nitrite transporter ³¹. Although hypothetical, such a transport function is attractive since nitrite and nitrate are oxidation products of nitric oxide which is synthesized by macrophages and which plays a key effector function in the bactericidal activity of these cells ^{230,256}. Could Nramp2 play an analogous role in host resistance to infections? Preliminary results from this study do not support such a contention: *Nramp2* mRNA expression is ubiquitous and does not seem particularly associated with organs or cell types implicated in host defenses (Figure 4). In addition, *Nramp2* maps on chromosome 15 away from known host resistance genes or mutants. On the other hand, the high degree of sequence similarity between Nramp1 and Nramp2

strongly suggests an underlying functional homology. Both proteins could act on the same type of substrates but in different tissues, like different isoforms of the glucose transporters GLUT 1-5 family (reviewed in ²⁵⁷). With respect to this possibility, it is interesting to note that, in addition to the macrophage specific and LPS inducible nitric oxide synthase (NOS) enzyme, two additional NOS enzymes have been described in endothelial cells and brain ²³⁰. This suggests the possibility that additional transporters of oxidation products of nitric oxide may also exist in non-macrophage cells. Alternatively, Nramp proteins could transport different types of yet to be identified substrates by the same mechanism, similar to the bacterial periplasmic permeases and the mammalian P-glycoproteins family ^{258,259}.

The previous chapter that describes the identification and characterization of *Nramp2* was published in 1995. Some elements of the discussion must be taken in the context of the status of our knowledge of *Nramp1* function at that time. Indeed, it is through studies of *Nramp1*-homologous genes that our knowledge has advanced. Particularly, although consideration of a nitrate/nitrite transport function for both *Nramp* proteins was appropriate at the time, due to the recent identification of divalent cations as substrates of *Nramp2* and other members of the *Nramp* family, such a contention is no longer relevant ^{148,182}. Similarly, although the region between transmembrane domains 8 and 9 is well conserved among *Nramp* proteins, the combined analysis of the region in many *Nramp* family members ¹⁷⁹, as well as further refinement of the consensus sequence in periplasmic transporters ^{249,260}, calls for a re-evaluation of the relationship between the two. Although the region is well conserved in the *Nramp* family it may not be as related, as was once speculated, to the periplasmic transport protein motif. Later analyses uncovered similarity of this region to the ion permeation pathway of voltage-gated potassium channels, and also to a subunit of the vacuolar H⁺-ATPase ¹⁷⁹. However, due to the recent discovery of the most divergent *Nramp* proteins ^{188,190}, even these similarities need to be re-considered. Indeed, the elucidation of the function of this region will only be determined definitively through functional studies.

An aspect of the previous chapter that is interesting in retrospect is the minor 5 kb mRNA species that was observed in the Northern blot experiment. At the time it was stated that the origin and nature of this transcript was unclear and may have resulted from *Nramp2*- related transcripts or a partially processed RNA. This transcript most likely corresponds to the alternatively-spliced IRE form of *Nramp2* identified more recently

(see introduction, 141,145.). Neither the 3.3 or the 2.3 kb mRNA species observed correspond to this form, as they both are recognized by a probe derived from the proximal 3' untranslated region, which is not present in the IRE-containing splice form. On the other hand, the 5 kb species is recognized by the coding region probe, but not by the two probes derived from the 3' untranslated region of the cDNA. The larger size of this mRNA species is also in agreement with the larger size of the IRE-containing mRNA observed in rats (4.5 kb, 141). Indeed, in a recent publication an IRE form-specific probe on Northern blots of mouse intestinal mRNA was used, which recognized RNA species of approximately 4.5-5.5 kb 261.

Having analyzed the expression of *Nramp2* at the mRNA level, the next logical step was to investigate the *Nramp2*-encoded protein. The immediate relevance of these studies was increased due to two breakthrough publications in 1997 identifying a mutation in *Nramp2* as the causative defect in a mouse model of anemia, and demonstrating divalent cation transport function for *Nramp2* (see Chapter 1, 141,148). The well-timed generation of specific antiserum directed against *Nramp2* and the use of this serum to characterize the *Nramp2* protein clarified its role in divalent cation metabolism by establishing the subcellular sites of *Nramp2* activity. This is described in the following chapter.

Chapter 4

The iron transport protein Nramp2 is an integral membrane glycoprotein that colocalizes with transferrin in recycling endosomes

Abstract

The *Nramp* gene family is composed of two members in mammals, *Nramp1* and *Nramp2*. *Nramp1* is expressed primarily in macrophages and mutations at this locus cause susceptibility to infectious diseases. *Nramp2* has a much broader range of tissue expression and mutations at *Nramp2* result in iron deficiency, indicating a role for *Nramp2* in iron metabolism. To get further insight into the function and mechanism of action of *Nramp* proteins, we have generated isoform specific anti-*Nramp1* and anti-*Nramp2* antisera. Immunoblotting experiments indicate that *Nramp2* is present in a number of cell types, including hemopoietic precursors, and is co-expressed with *Nramp1* in primary macrophages and macrophage cell lines. *Nramp2* is expressed as a 90-100kDa integral membrane protein extensively modified by glycosylation (>40% of molecular mass). Subcellular localization studies by immunofluorescence and confocal microscopy indicate distinct and non-overlapping localization for *Nramp1* and *Nramp2*. *Nramp1* is expressed in the lysosomal compartment, while *Nramp2* is not detectable in the lysosomes but is expressed primarily in recycling endosomes and also to a lower extent at the plasma membrane, co-localizing with transferrin. These findings suggest that *Nramp2* plays a key role in the metabolism of transferrin-bound iron, by transporting free Fe^{2+} from across the endosomal membrane and into the cytoplasm.

Introduction

Naturally occurring³² or experimentally induced³⁴ mutations at the *Nramp1* locus *in vivo* impair macrophage function and cause susceptibility to infection with intracellular pathogens such as *Salmonella*, *Leishmania* and *Mycobacterium* in mice. In humans, polymorphic variants at *NRAMP1* are associated with increased susceptibility to tuberculosis and leprosy^{39,40}. Studies *in vitro* in explanted cell populations have indicated that mutations at *Nramp1* affect the ability of the macrophage to restrict the intracellular replication of antigenically unrelated microorganisms. We cloned the *Nramp1* gene (*Natural Resistance Associated Macrophage Protein 1*)³¹ and showed that its mRNA is expressed abundantly in macrophages³¹ and in neutrophils⁴⁸ and is inducible in macrophages by exposure to cytokines and bacterial endotoxin⁴⁷. Predicted amino acid sequence analysis indicates that *Nramp1* has many characteristics of an integral membrane transport protein including twelve putative transmembrane (TM) domains, several predicted N-linked glycosylation sites, and a sequence signature previously identified in a number of eukaryotic and prokaryotic transport proteins³¹. In macrophages, direct biochemical studies have shown that *Nramp1* is a membrane phosphoglycoprotein of apparent mass 90-110 kDa⁴⁹, which is expressed in the Lamp1-positive lysosomal compartment²⁶². Moreover, studies in phagosomes containing either latex beads or intact bacteria have shown that upon phagocytosis, *Nramp1* is recruited to the membrane of the phagosome, where it remains during its maturation to phagolysosome^{60,262}. These findings suggest that *Nramp1* may affect resistance to infection by modulating the intravacuolar milieu of the bacterial phagosome.

We have identified a second *Nramp* gene in mammals, *Nramp2*, which encodes a protein highly similar to *Nramp1* (78% identity) ¹⁹³. As opposed to the phagocyte-specific expression of *Nramp1*, *Nramp2* mRNA expression has been detected in most tissues and cell types analyzed ^{141,193,263}. Recently, it was shown that the *Nramp2* gene is mutated (G185R) in two animal models of iron deficiency, the *mk* mouse ¹⁴⁸ and the *Belgrade* rat ¹⁴⁵. The *mk* mouse displays deficiency in intestinal iron uptake and microcytic anemia ^{145,149,152}. The *Belgrade* rat also shows a defect in intestinal iron absorption ¹⁵³. Moreover, studies in oocytes have shown that *Nramp2* can transport a number of divalent cations such as Fe^{2+} , Zn^{2+} , and Mn^{2+} in a pH-dependent, electrogenic fashion, associated with the symport of a single proton ¹⁴¹. In addition, transient overexpression of the wild type but not G185R *Nramp2* in HEK293T cells results in a robust stimulation of cellular [⁵⁵Fe] uptake ¹⁴⁵. Taken together, these results indicate that *Nramp2* is the transferrin-independent system responsible for dietary iron absorption in the intestine. However, the ubiquitous expression of *Nramp2* mRNA suggests that it may be involved in iron metabolism in other tissues as well. As opposed to *Nramp1*, where the cellular and subcellular localization of the protein have been established, the lack of isoform-specific anti-*Nramp2* antibodies has precluded the identification of the cell type and of the subcellular compartment expressing this protein. Such information is critical to elucidate the role of the *Nramp2* protein in cellular iron metabolism. In particular, the demonstrated H^+ -driven, Fe^{2+} transport activity of *Nramp2*, as well as its expression in a wide variety of tissues, make it a likely candidate not only for transferrin-independent iron absorption in the intestine, but also for the transferrin-dependent uptake of iron in peripheral tissues. It is well established that acidification of the endosomal

compartment causes Fe^{3+} release from transferrin and that reductases then convert the Fe^{3+} to Fe^{2+} , but the mechanism of transport of Fe^{2+} across the endosomal membrane has not yet been elucidated.

Materials and methods

Immunogens

For the production of isoform-specific polyclonal antisera directed against Nramp2, rabbits were immunized with fusion proteins containing Glutathione S-Transferase (GST) fused to a peptide segment derived from the amino terminal region of Nramp2 (residues 1 to 71; for amino acid numbering, see ¹⁹³). This peptide is in a region of the protein that is not conserved in other Nramp family members, including Nramp1 ¹⁷⁸. The GST-Nramp2 fusion protein was constructed in the plasmid vector pGEX (Pharmacia) as follows: The Nramp2 sequence was amplified by PCR using oligonucleotides NF2 (5'-AAAGATCTATGGTGTGGATCC-3') and NR (5'-CTGAATTCGAACGCCAGAGT-3') (nucleotides 1-268), and the full length *Nramp2* cDNA as template. The PCR product was digested with *Bgl* II and *Eco* RI (underlined) and the fragment was subcloned into pGEX digested with *Bam* HI and *Eco* RI to create the in-frame GST fusion protein. Overexpression of the Nramp2-GST fusion protein was carried out in large-scale cultures of *E. coli* and the protein was purified from bacterial lysates using Glutathione-sepharose 4B (Pharmacia), as previously described ²⁶⁴. Purified proteins were analyzed by 7.5% SDS-PAGE, and excised from the gel after light staining with 0.05% Coomassie blue in ddH₂O.

Production of Anti-Nramp2 Antibodies

Polyclonal antibodies were produced in New Zealand White male rabbits as described previously ⁴⁹. A system for affinity purification of the antibodies was devised,

using the same Nramp2 peptide fused to a second fusion partner, dihydrofolate reductase modified by the addition of 8 consecutive histidine residues (his-DHFR). The fusion protein construct was made as described above, except the PCR product was digested with *Eco* RI, the resulting overhangs repaired using the Klenow fragment of DNA polymerase I (Pharmacia) before digestion with *Bgl* II. The digested PCR product was ligated into *Bgl* II and *Sma* I digested pQE40 plasmid vector (Qiagen, Mississauga, Canada). The in-frame his-DHFR-Nramp2 fusion protein construct was transformed into *E. coli* strain M15(pREP4) for expression (Qiagen). Purification was performed on Ni-NTA agarose according to experimental conditions suggested by the manufacturer (Qiagen). The polyclonal antiserum directed against the GST-fusion protein was purified against the his-DHFR-fusion protein by a preparative immunoblot procedure ²⁶⁵. The anti-Nramp1 polyclonal antiserum ⁴⁹ was affinity purified against the corresponding Nramp1-GST fusion protein by the same protocol.

Cell Culture

The mouse monocyte-macrophage cell lines RAW 264.7 and J774a, the mouse Sertoli cell line TM4, and the mouse kidney line mIMCD-3 were obtained from the American Type Culture Collection (ATCC, Manassas, VA). They were cultured in media and under conditions recommended by the ATCC. WEHI 3B (myelomonocyte), WEHI 231 (B lymphocyte), BI 141 (T lymphocyte), and 70Z/3 (pre-B cell) cells were cultured as described previously ²⁶⁶. Chinese Hamster Ovary (CHO) cells LR73 ²⁶⁷ were grown in α -MEM supplemented with 10% fetal calf serum, 2 mM L-glutamine, 50 units/ml penicillin and 50 μ g/ml streptomycin. All media and media supplements were

purchased from Gibco/BRL. Murine macrophages were obtained by peritoneal lavage, as previously described ⁴⁹. We have previously described the production and characterization of RAW macrophages expressing a transfected wild type Nramp1 fused to a cMyc epitope ²⁶². The cMyc-tagged Nramp2 expression plasmid was constructed by excising the Myc-tagged *Nramp2* cDNA from plasmid pBluescript ¹⁸⁵ using *Spe* I and *Eco* RV sites from the polylinker, followed by cloning into the mammalian expression plasmid pCB6 ²⁰⁶. For expression in CHO cells, the same insert was cloned into the expression vector pMT2 ²⁶⁸. CHO cells were transfected by the calcium phosphate co-precipitation method ²⁶⁹. RAW cells were transfected by electroporation as described previously ²⁶². Clones of stable transfectants were selected in geneticin (G418, Gibco, 1 mg crude/ml final) for 10-14 days, picked and expanded individually, and tested for protein expression by immunofluorescence using the anti-cMyc tag monoclonal antibody 9E10 (Babco).

Immunoblotting and Immunoprecipitation

Crude membrane fractions from the various cells were prepared as described previously ²⁴³. Protein concentration of the membrane fraction was determined by the Bradford assay (BioRad). Proteins were separated on SDS-polyacrylamide gels and transferred by electroblotting to nitrocellulose membranes. For experiments where the membrane was to be stripped and reprobed, a polyvinylidene fluoride membrane was used (Westran, Schleicher & Schuell) to reduce protein loss from the membrane during stripping. Equal loading and transfer of proteins was verified by staining the blots with Ponceau S (Sigma). The blots were blocked in TBST (10 mM Tris/Cl pH 8, 150 mM

NaCl, 0.05% Tween-20, pH 8) plus 5% skim milk powder for 1 h at room temperature. Primary antibodies used were as follows: affinity purified rabbit anti-mouse Nramp2 (1:100 dilution); affinity purified rabbit anti-mouse Nramp1 (1:200); mouse monoclonal anti cMyc-epitope tag 9E10 (Babco, 1:100), rat anti-mouse Transferrin receptor (Biosource International, 1:200), rat anti-mouse Lamp1 (1:200). Anti-rabbit, anti-rat and anti-mouse secondary antibodies conjugated to horseradish peroxidase were used at 1:10,000 (Amersham). Chemiluminescence was used for detection of immune complexes on the immunoblot (ECL, Amersham). For immunoprecipitation, CHO cells and Nramp1 and Nramp2 CHO transfectants were metabolically labeled with [³⁵S]-methionine by incubating overnight in 100 μCi/ml of [³⁵S]-methionine (DuPont) in methionine-free DMEM (Gibco BRL) containing 10% heat-inactivated, dialyzed fetal bovine serum, 2 mM L-glutamine and 2 mM HEPES. Immunoprecipitation was performed exactly as described previously ⁴⁹.

Immunofluorescence

Cells were grown on glass coverslips and fixed with 4% paraformaldehyde in PBS for 30 min at 4°C. Immunofluorescence was performed as previously described ²⁶², with the following modifications: incubation with the primary antibody was 1 hour at 20°C for the anti-cMyc mouse monoclonal 9E10 (1:200, Babco), and the anti-Lamp1 rat monoclonal (1:200), or overnight at 4°C for the anti-Nramp2 antiserum (1:800) followed by anti-mouse, anti-rat or anti-rabbit secondary antibodies conjugated to Rhodamine (1:300) or FITC (1:200) (Jackson Immunochemicals). Immunofluorescence was analyzed with a Nikon microscope using the 100X oil immersion objective. Certain

colocalization studies were carried out using a Zeiss laser confocal microscope (Heidelberg, Germany) with a 63X objective. Composites of confocal images were assembled and labeled using PhotoShop, Metamorph and Freehand software. To label the lysosomal compartment, cells were incubated with 1 mg/ml lysine-fixable FITC-dextran (Molecular Probes) in growth medium for 4 h at 37°C in 5% CO₂. After washing, cells were incubated an additional 30 min to chase the dextran from early endosomal to the lysosomal compartments. For identification of the early and recycling endosomal compartment, cells were incubated in serum-free medium containing 50 µg/ml FITC-transferrin (Molecular Probes) for 30 min at 37°C in 5% CO₂. Phagosomes were formed by incubating the cells with 3 µm latex beads (Sigma) diluted 1:200 in complete culture medium for 15 minutes at 37°C in 5% CO₂. After treatments to identify the specific subcellular compartments, cells were fixed in 4% paraformaldehyde and processed for immunofluorescence.

Glycosidase Treatments

Endo-β-acetylglucosaminidase H (Endo H) and peptide *N*-glycosidase F (PNGase F) were obtained from New England Biolabs (NEB). Aliquots of membrane preparations from J774a and CHO cells were denatured before digestion in a buffer containing 0.5% SDS and 0.1 M β-mercaptoethanol for 2 min at 70°C. For Endo H digestion, samples were diluted 2-fold and incubated with 4000 units of Endo H in 50 mM sodium citrate pH 5.5 for 1 h at 37°C. The (-) Endo H controls were treated identically except an equivalent volume of ddH₂O was added in place of Endo H. For PNGase F digestion, samples were diluted 2-fold and incubated in 50 mM sodium phosphate pH 7.5, 1 % NP-40, with 500

units of PNGase F for 1 h at 37°C. The (-) PNGase F controls were treated identically except an equivalent volume of ddH₂O was added in place of PNGase F.

RNA Isolation and Hybridization Studies.

Total cellular RNA was isolated using guanidinium-HCl solubilization and differential ethanol precipitation²³⁷. Twenty µg of total cellular RNA were denatured in a formamide/formaldehyde mixture, and loaded onto denaturing agarose gels containing 0.66 M formaldehyde. Blots were pre-hybridized in a solution containing 10% dextran sulfate, 1M NaCl, 1% sodium dodecyl sulfate (SDS), and heat-denatured salmon sperm DNA (200 µg/ml) at 65°C for 2 to 16 hrs. Hybridization was for 24 hrs at 65°C in the same buffer containing the radiolabeled probe (1 x 10⁶ cpm/ml of hybridization buffer; specific activity 1 X 10⁹ cpm/µg DNA). Blots were washed under conditions of increasing stringency up to 0.1X SSC and 0.1% SDS, at 65°C and then exposed to Kodak XAR film with 2 intensifying screens at -70°C for 18 h to 7 days at -80°C.

Phagosome fractionation

Phagosomes were isolated from J774a cells by a modification of a method described previously²⁶². Ten sub-confluent 150 mm dishes of each cell line were fed with a 1:200 dilution of blue-dyed latex beads (0.8 µm, Sigma) in culture medium for 1 hour at 37°C in 5% CO₂. The cells were then washed in PBS and harvested in the presence of protease inhibitors (1 µg/ml leupeptin, 1 µg/ml aprotinin, 1 µg/ml pepstatin, 100 µg/ml PMSF, all Boehringer Mannheim) and recovered by centrifugation (2000 g, 5 min). The cell pellets were washed and resuspended in homogenization buffer (8.5%

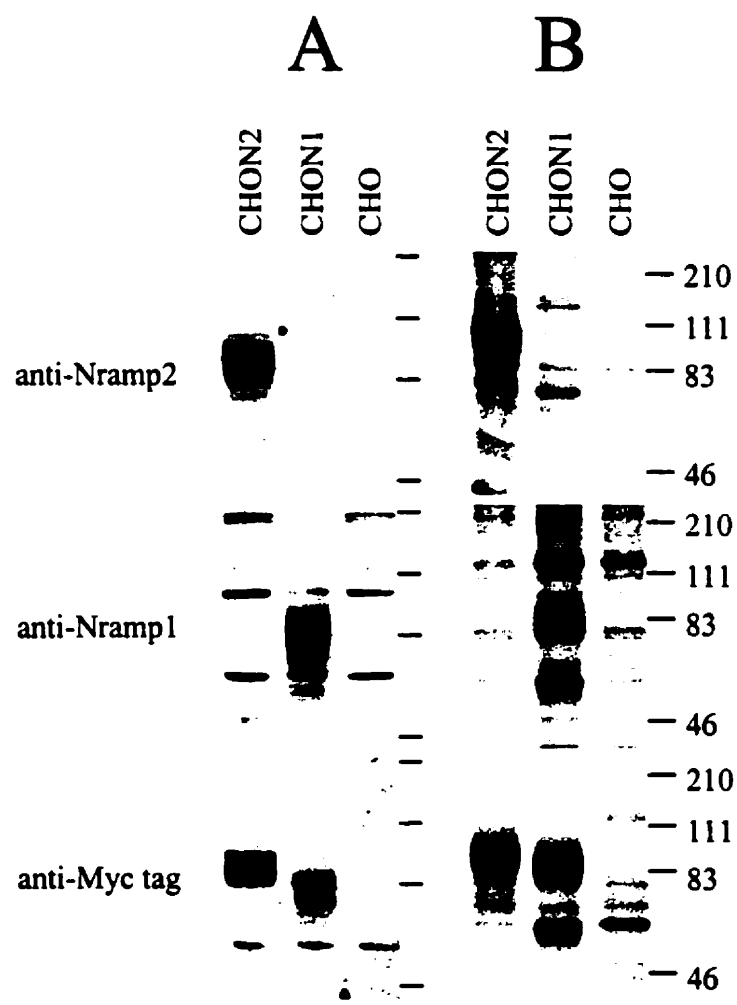
sucrose, 3 mM imidazole, pH 7.4) and homogenized by passage through a 22G needle until 90% of the cells were broken, as monitored by light microscopy. Nuclei and unbroken cells were pelleted and the supernatant loaded onto a sucrose step gradient as follows: the supernatant was brought up to 40% sucrose by addition of 62% sucrose, and loaded on top of a 1 ml 62% sucrose cushion. Layers of 2 ml of 35%, 25% and finally 10% sucrose (all sucrose solutions w/w in 3mM Imidazole, pH 7.4 + protease inhibitors) were sequentially added to the top of the tube, and the gradients were centrifuged at 100,000 g for 1 hour at 4°C (SW41; Beckman, Palo Alto, CA). Phagosomes were recovered from the 10 - 25% sucrose interface, washed with PBS containing protease inhibitors, and recovered by a final centrifugation at 40,000 g in an SW41 rotor at 4°C. The final pellets were resuspended in 2X Laemmli sample buffer. Phagosomes prepared by this protocol have been previously shown to be free of endoplasmic reticulum (endoplasmin, BiP and calnexin) and Golgi apparatus (galactosyl transferase) contaminants ⁶⁹.

Results

To generate an isoform-specific anti-Nramp2 antiserum, a protein segment derived from the amino terminus of Nramp2 was selected based on its predicted antigenicity and its sequence divergence from Nramp1 (28% identity). A GST-Nramp2 fusion protein containing the amino terminal Nramp2 segment was produced and used for immunization, and the anti-Nramp2 fraction was further isolated from the immune serum by affinity purification against a second immobilized Nramp2-DHFR fusion partner. The antiserum was tested for specificity by immunoblotting crude membrane fractions as well as by immunoprecipitation of ^{35}S -methionine-labeled cell lysates from transfected CHO cell clones expressing either cMyc-tagged Nramp1 or cMyc-tagged Nramp2 proteins (Fig. 1). The anti-cMyc monoclonal antibody (9E10 ²⁰⁵) specifically recognized a species of apparent molecular mass 90-100 kDa in the Nramp2-transfected CHO cells, and a protein of 85-95 kDa in the Nramp1 transfected cells that were absent from extracts of untransfected CHO controls (Fig 1A, 1B, bottom panels). These protein species migrated as broad bands in SDS-acrylamide gels. In membrane preparations from Nramp2-transfected CHO cells (CHON2), the affinity-purified anti-Nramp2 antiserum recognized a single protein species of apparent molecular weight 90-100 kDa (Fig. 1A, top panel). Immunoblotting analysis of the same set of membrane fractions with anti-Nramp1 antiserum, revealed a single protein species of 85-95 kDa in membranes from the Nramp1-transfected CHO cells (Fig. 1A, middle panel). These immunoreactive bands were absent from untransfected CHO cells and from transfected cells expressing the other Nramp isoform. The electrophoretic mobility characteristics of the Nramp1 and Nramp2 detected by the respective polyclonal antisera were very similar to those of the

Figure 1 *Specificity and immunoreactivity of affinity purified anti-Nramp2 and anti-Nramp1 antisera*

After affinity purification, anti-Nramp1 and anti-Nramp2 antisera were tested for specificity and reactivity by immunoblotting against crude membrane fractions (A) as well as by immunoprecipitation of [³⁵S]-methionine-labeled cell lysates (B) from CHO cells or from the same cells transfected with a cMyc-tagged (tag sequence, EQKLISEEDL) Nramp1 (CHON1) or a cMyc-tagged Nramp2 (CHON2). Protein extracts were separated by SDS-PAGE, and either transferred to membranes (A) or exposed to X-ray films after immunoprecipitation (B). Antisera directed against Nramp2 (top panels), Nramp1 (middle panels) or a commercially available mouse monoclonal anti-cMyc antibody (9E10, bottom panels) were used. The size of the molecular mass markers (in kDa) is indicated to the right of the gels.



species detected by the anti-cMyc antibody in the same cell extracts (Fig. 1A, bottom panel). The reactivity and isoform specificity of the antibodies were confirmed by immunoprecipitation studies of ^{35}S -methionine metabolically labeled cell extracts from CHO cells or from Nramp1 and Nramp2 CHO transfectants (Fig. 1B). These data indicate that the anti-Nramp1 and anti-Nramp2 antisera produced and purified according to our protocol are isoform-specific.

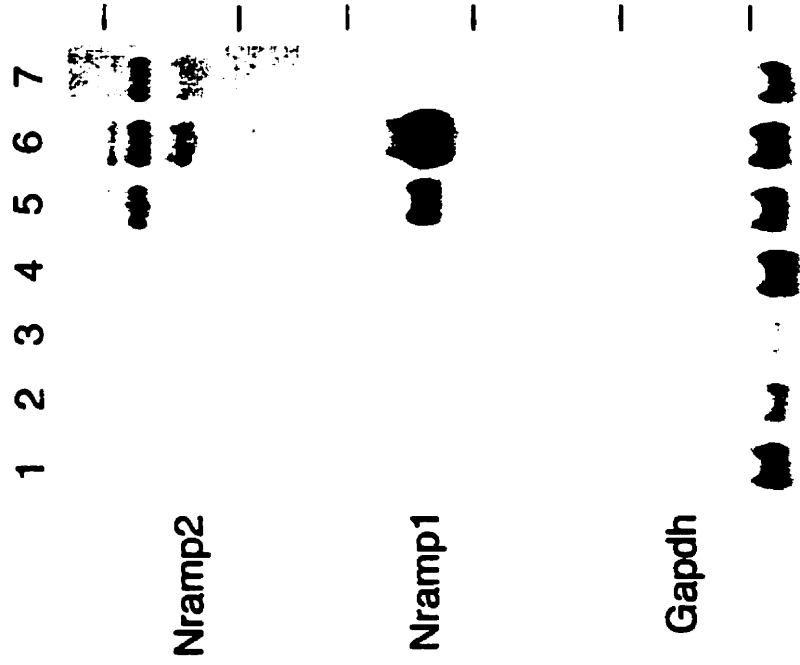
Northern blotting and *in situ* hybridization studies have shown that, as opposed to *Nramp1* which is expressed almost exclusively in mononuclear phagocytes, *Nramp2* mRNA is expressed in most tissues ^{141,193,263}. We questioned whether the two Nramp proteins would display an overlapping or mutually exclusive expression pattern. Northern blot analysis of total cellular RNA from a panel of murine hematological cell lines revealed a readily detectable level of *Nramp2* mRNA expression in the macrophage lines RAW 264.7 and J774a as well as in Friend virus-transformed erythroleukemia (MEL) cells (Fig 2A top panel; exposure time 1 week). A much lower level of expression of *Nramp2* was found in other cell lines: WEHI 231 (B lymphocyte), WEHI 3B (myelomonocyte), 70/Z (pre-B lymphocyte) and BI 141 (T lymphocyte). In comparison, *Nramp1* mRNA expression was restricted to the macrophage cell lines RAW264.7 and J774a and is expressed at levels approximately 50-fold higher than that of *Nramp2* (Fig 2A middle panel; exposure time 24 h). Thus, *Nramp1* and *Nramp2* mRNAs are co-expressed in macrophages.

To analyze Nramp2 protein expression in macrophages, membrane fractions were prepared from thioglycolate-induced primary mouse macrophages, from J774a and RAW 264.7 cultured macrophages. For comparison, membranes were also prepared from cell

Figure 2 *Nramp2* mRNA and protein expression in primary cells and cultured cell lines

(A). *Nramp2* mRNA expression in cultured cell lines. Northern blot analysis of total cellular RNA (20µg) from mouse cell lines: BI 141 (T lymphocyte; lane 1), 70/Z (pre-B lymphocyte; lane 2), WEHI 231 (B lymphocyte; lane 3), WEHI 3B (myelomonocyte; lane 4), RAW 264.7 (macrophage; lane 5), J774a (macrophage; lane 6), and MEL (erythroleukemia, lane 7). The RNA was electrophoresed in a denaturing agarose gel, followed by transfer to a nylon membrane and hybridization to gene-specific cDNA segments from either *Nramp2* (top panel), *Nramp1* (middle panel) or Glyceraldehyde phosphate dehydrogenase (*Gapdh*, bottom panel). Exposure time was 7 days for *Nramp2*, and 1 day for *Nramp1* and *Gapdh* (B). *Nramp2* protein expression in cultured cell lines. Crude membrane fractions were prepared from different cultured cell lines as well as from thioglycolate-induced primary mouse macrophages (Mø), and were separated by SDS-PAGE. Immunoblotting was performed using the anti-*Nramp2* antiserum. (C). *Glycosylation of Nramp2* protein. Membrane fractions from J774a cells (lanes 1-4) and *Nramp2*-transfected CHO cells (lanes 5-7) were treated with endoglycosidases followed by electrophoresis and immunoblotting with the anti-*Nramp2* antiserum. Membrane fractions were either mock-treated (lanes 1,3 and 5) or incubated with EndoH (lane 2) or PNGaseF (lanes 4, 6 and 7). A lighter exposure of lane 6 is shown in lane 7.

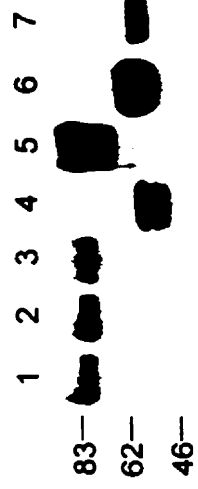
A



B



C



lines derived from tissues previously shown to express a high level of *Nramp2* mRNA: the Sertoli cell line TM4 and the kidney inner medullary collecting duct line mIMCD-3 [141]. Membranes were also prepared from control and *Nramp2*-transfected CHO cells, as well as from two cell lines expressing low levels of *Nramp2* mRNA (WEHI 231 and WEHI 3B, see Fig. 2A). The membranes were analyzed by immunoblotting with the anti-*Nramp2* antibody (Fig. 2B and 2C). The antibody detected a major heterogeneous immunoreactive protein species of broad electrophoretic mobility with an apparent molecular mass of 80-90 kDa. in all cells tested, with the exception of untransfected CHO, and WEHI 231 cells. The protein was most abundant in TM4, RAW 264.7, J774a and MEL cells. The protein was also detected in the membranes prepared from primary mouse macrophages and mIMCD-3 cells, although at a lower level. WEHI 3B membranes showed the lowest level of *Nramp2* expression, while WEHI 231 and untransfected CHO cells were negative for *Nramp2* expression. In the positive membrane samples, the electrophoretic mobility and heterogeneity of the immunoreactive species varied, possibly due to different post-translational modification of the protein in these cell types. Thus, *Nramp2* is expressed in a wide variety of tissues, including macrophages, and macrophages co-express *Nramp1* and *Nramp2*.

The apparent mass of endogenous *Nramp2* estimated by SDS-PAGE is considerably greater than the 62.3 kDa molecular mass predicted by the primary amino acid sequence of the cDNA. Together with the broadness of the immunoreactive band, this anomalous mobility suggests that *Nramp2* may be post-translationally modified by glycosylation. To test this hypothesis, membrane fractions from J774a cells and *Nramp2*-

transfected CHO cells were treated with endoglycosidases followed by electrophoresis and immunoblotting. Nramp2 was resistant to digestion with EndoH (Fig. 2C, lanes 1 and 2), which specifically cleaves high-mannose and some hybrid N-linked oligosaccharides from glycoproteins. In contrast, PNGaseF, which hydrolyzes high-mannose, hybrid and complex oligosaccharides, converted the 82 kDa Nramp2 species into smaller forms of approximate apparent molecular weights 50-55 kDa (Fig. 2C, lane 4). PNGase treatment of membranes from the Nramp2 CHO transfectants also resulted in a shift of the apparent molecular mass of the protein from 85 kDa to approximately 56 kDa (Fig. 2C, lanes 6 and 7). Therefore, Nramp2 is post-translationally modified extensively by complex N-linked glycosylation.

To gain insight into the subcellular localization of Nramp2, we first performed immunofluorescence studies on CHO and RAW 264.7 transfected cells, using an antibody directed against the cMyc epitope attached to the C-terminus of the transfected Nramp2 protein. The high levels of transfected protein in these cell lines facilitated non-ambiguous localization of Nramp2, without possible limitation associated with low levels of expression of the endogenous protein. We have previously observed that the cMyc-tagged Nramp2 protein is functional in both CHO and RAW macrophage backgrounds and carries out active Fe^{2+} transport in these cells²⁷⁰. We initially tested whether Nramp2 localizes to the late endosomal/ lysosomal compartment, as found earlier for Nramp1²⁶². To label the lysosomal compartment, cells were cultured in the presence of FITC-conjugated dextran, followed by a chase period of 30 min to remove the dextran from the early endosomal compartments, before fixation and immunostaining with the anti-cMyc antibody. In Nramp1 transfected CHO cells, there was clear colocalization of

the anti-cMyc staining (Fig. 3A) and the dextran-loaded late endosomal/lysosomal compartment (Fig. 3B). Nramp1-stained vesicles negative for FITC-dextran were also detected. In contrast, in Nramp2-transfected CHO cells, anti-cMyc staining revealed an intracellular network of finer punctate vesicles distributed throughout the cytoplasm (Fig. 3C). This staining does not appear to colocalize with the FITC-dextran (Fig. 3D). Similar results were obtained in parallel experiments using the cMyc-Nramp1 and cMyc-Nramp2 transfected RAW cells (data not shown), indicating that Nramp2 is not expressed in the lysosomal compartment. Thus, Nramp1 and Nramp2 clearly appear to have distinct, non-overlapping subcellular sites of expression.

Since Nramp2 is implicated in cellular iron uptake, it appears logical that Nramp2 be present at the plasma membrane and/or in recycling endosomes. To label these compartments, CHO (Fig. 4) and RAW transfected cells (Fig. 5) were cultured in the presence of FITC-conjugated transferrin before fixation and immunostaining with the anti-cMyc antibody. Analysis by confocal microscopy indicated that, as expected, transferrin (green) stained both the plasma membrane (ring-like staining at the edge of the cells) and the recycling endosomes (subcellular punctate staining) (Fig. 4B). A very similar and overlapping pattern was observed for Nramp2, as revealed by the anti-cMyc antibody (red) (Fig. 4A). Super-imposition of the two images (Fig. 4C) clearly identifies colocalization (yellow) of the two signals. Certain cells stained with FITC-transferrin but were negative for the cMyc staining, suggesting that although these cells are positive for the pSV2neo plasmid and are resistant to G418, they failed to express cMyc-tagged Nramp2. Such cells provide an internal control for the specificity of the anti-cMyc staining and for the overlapping staining with FITC-transferrin. Similarly, when untransfected CHO cells were identically processed and examined, the cells were not

Figure 3 *Subcellular Localization of Nramp1 and Nramp2 in transfected CHO cells*

Immunofluorescence was performed on CHO cell transfected with cMyc-tagged Nramp1 (A, B), or with cMyc-tagged Nramp2 (C, D) proteins. Immunofluorescence was with the anti-cMyc mouse monoclonal antibody 9E10 (A, C) which detects the transfected Nramp1 and Nramp2 proteins. Lysosomes were labeled by pre-incubation of the cells with FITC-conjugated dextran (B, D). Cells were then fixed, reacted with the anti-cMyc-tag antibody 9E10 and a Rhodamine-conjugated secondary antibody (A, C), followed by examination by fluorescence microscopy and photography.

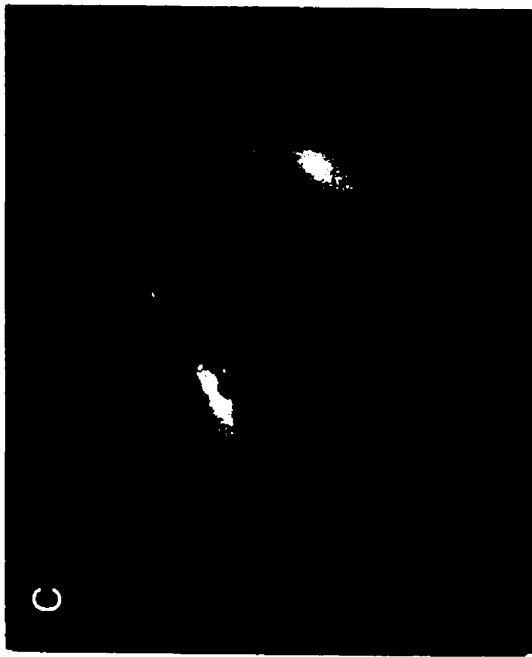
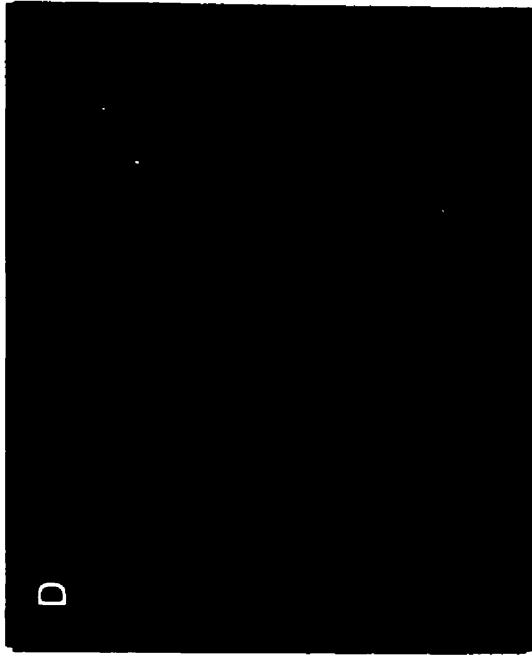
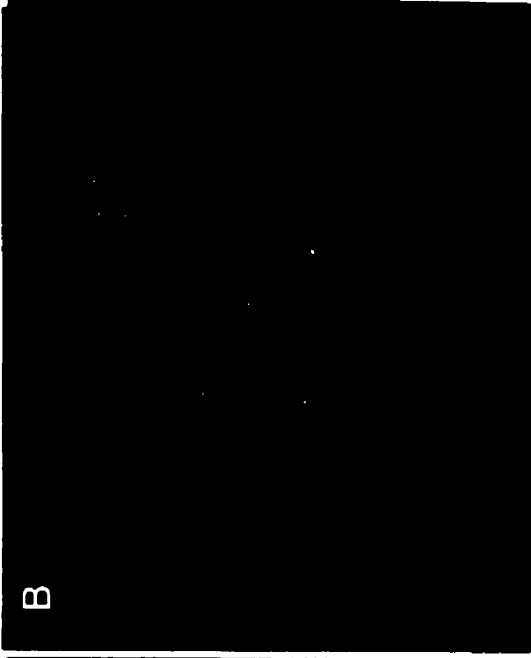


Figure 4 *Colocalization of Nramp2 with transferrin in transfected CHO cells*

Colocalization of Nramp2 and transferrin in early endosomes was determined by double immunofluorescence and confocal microscopy in either CHO control cells (D-F) or CHO cells transfected with a cMyc-tagged Nramp2 protein (A-C, G-I). Cells were cultured in the presence of FITC-conjugated transferrin (A-F) or FITC-conjugated dextran (G-I) before fixation and immunostaining with the anti-cMyc-tag antibody and a Rhodamine-conjugated secondary antibody (A, D, G). The slides were then examined by confocal microscopy, and the FITC (green; B, E, H) and Rhodamine (red; A, D, G) images were overlaid (yellow identify colocalization; C, F, I). In the Nramp2-transfected CHO cells, the Nramp2 staining (A, G) showed extensive overlap with the distribution of FITC-transferrin (A + B = C), but not with lysosomal FITC-dextran (G + H = I). FITC-transferrin staining was observed in the untransfected CHO cells (E), but the cells were negative for anti-cMyc staining (D).

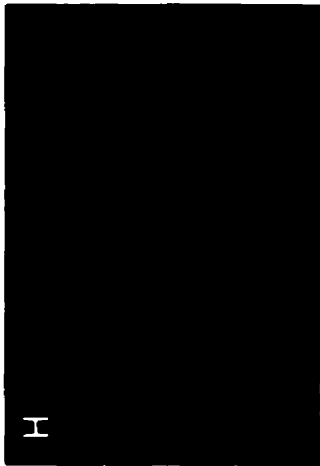
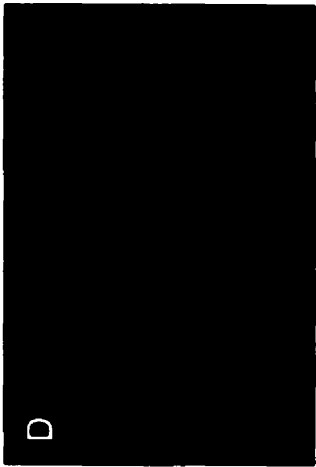
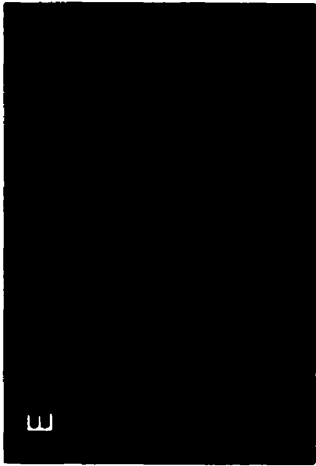
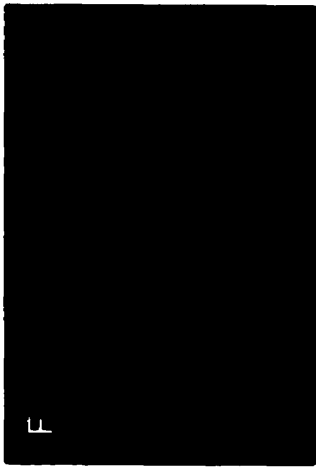
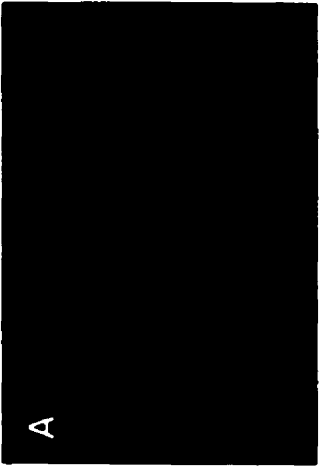
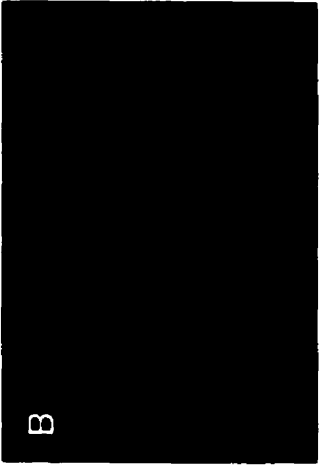
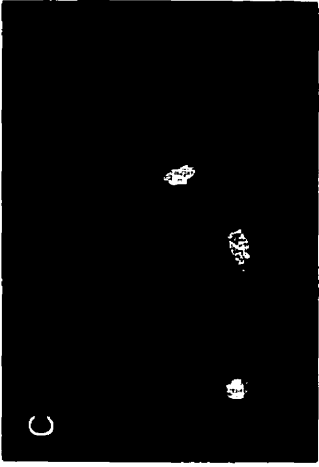
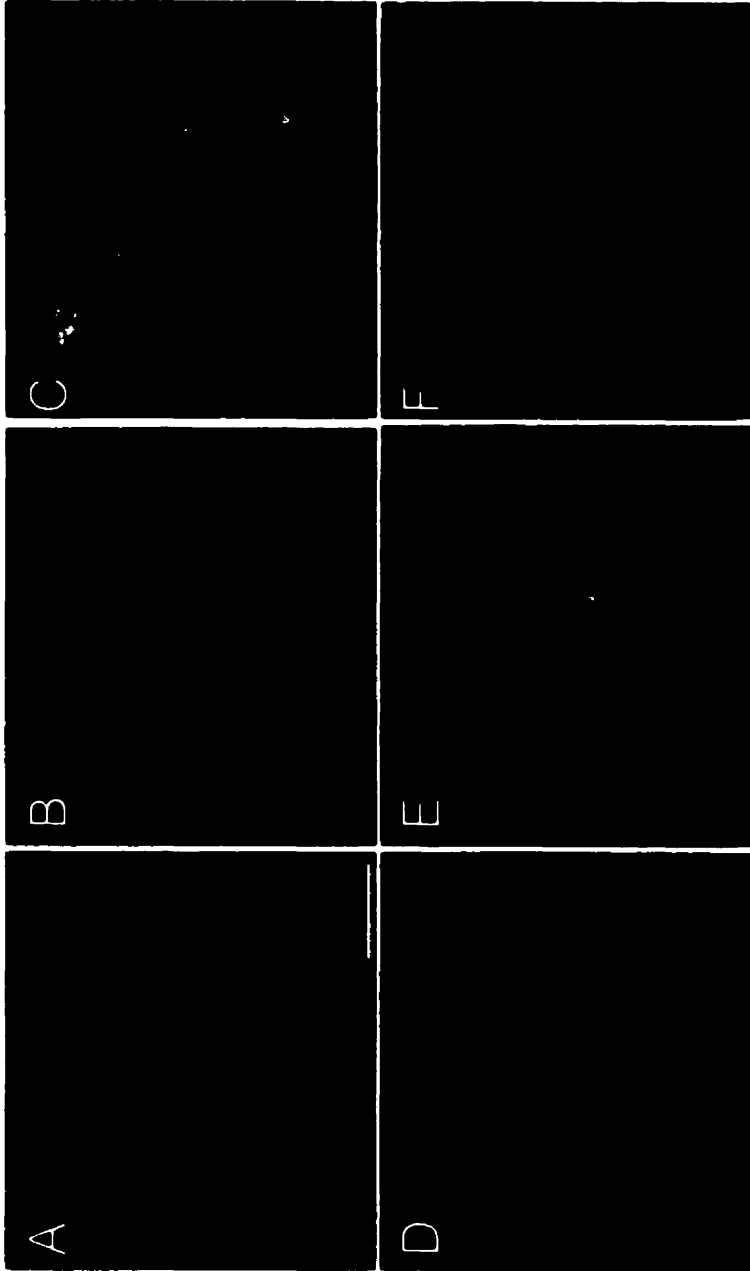


Figure 5 *Colocalization of Nramp2 with transferrin in transfected RAW macrophages.*

Colocalization of Nramp2 and transferrin in early endosomes was determined by double immunofluorescence and confocal microscopy in RAW macrophages transfected with a c-Myc tagged Nramp2 (A-C) and in control untransfected cells (D-F). Cells were cultured in the presence of FITC-conjugated transferrin before fixation and immunostaining with the primary anti-cMyc-tag antibody (9E10) and a secondary Rhodamine-conjugated anti-mouse antibody. The slides were then examined by confocal microscopy, and the FITC (green; B, E) and Rhodamine (red; A, D) images were overlaid to identify colocalization (C, F). The image in C shows colocalization of Nramp2 and FITC transferrin in several of the cells in the field.



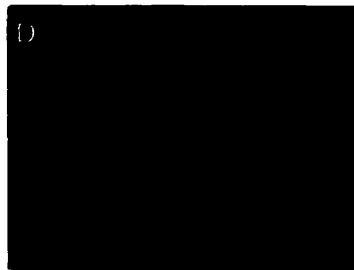
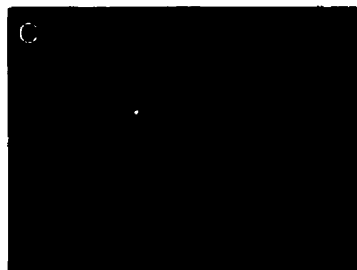
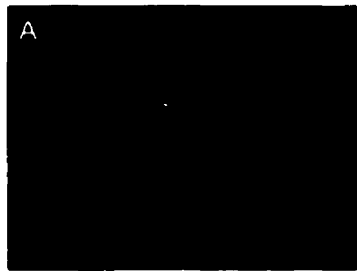
stained with the anti-cMyc antibody (Fig. 4D), but displayed a normal pattern of staining with FITC-transferrin (Fig. 4E). Finally, when the lysosomes of the Nramp2 transfected cells were stained with FITC-dextran (Fig. 4H) and for Nramp2 with the anti-cMyc antibody (Fig. 4G), no significant overlap between the two signals was detected (Fig. 4I). A similar colocalization of Nramp2 and FITC-transferrin was noted in parallel experiments with RAW macrophages expressing cMyc-Nramp2 (Figure 5). These results confirm that Nramp1 and Nramp2 have non-overlapping subcellular localization, and that Nramp2 colocalizes with transferrin in the early recycling endosomal compartment.

To confirm the endosomal localization of Nramp2 determined in transfected CHO and RAW cells, we performed immunofluorescence in non-transfected cell lines which tested positive (MEL, TM4) or negative (WEHI 231) for Nramp2 expression by immunoblotting (see Fig. 2). Immunofluorescence was performed with the anti-Nramp2 polyclonal antiserum and FITC-transferrin, and results are shown in Figure 6. In MEL (A,B) and TM4 (C,D) cells, the endogenous Nramp2 protein (B, D) showed very similar staining pattern to that generated by FITC-transferrin (A,C), similar to that seen in transfected cells (Figs. 4 and 5). Finally, in agreement with the absence of Nramp2 expression in WEHI 231 cells noted by immunoblotting (Fig. 2B), no Nramp2 staining was observed in WEHI 231 cells (F), although the endosomal compartment of these cells could readily be labeled by FITC-transferrin (E). Together, these results verify data obtained in transfected CHO and RAW cells.

The localization of Nramp2 to the plasma membrane and endosomal network raised the possibility that like Nramp1, Nramp2 may become associated with phagosomal membranes after phagocytosis. Phagosomes are initially derived from the plasma membrane, and are known to sequentially interact and acquire proteins from both early

Figure 6 *Subcellular localization of endogenous Nramp2*

Cell lines previously shown by immunoblotting to be either positive (MEL, TM4) or negative (WEHI 231) for Nramp2 expression were cultured in the presence of FITC-transferrin before fixation and immunostaining with the anti-Nramp2 antiserum and a Rhodamine conjugated secondary antibody. The slides were then examined by confocal microscopy, and FITC (A,C,E; transferrin) and Rhodamine (B,D,F; Nramp2) images were obtained from the samples. The same settings for the confocal microscope were used for all samples examined. The images show very similar subcellular localization of Nramp2 and FITC-transferrin in MEL and TM4 cells, while WEHI cells are negative for Nramp2.



and late endosomes, before their final fusion with lysosomes⁶⁹. We have shown that Nramp1 is acquired during the phagosomal maturation process, using the model system of latex bead-containing phagosomes²⁶². Latex bead-containing phagosomes are ideal for microscopic examination and can also be purified from cell homogenates by floatation on sucrose gradients. To determine if Nramp2 can associate with the phagosomal membrane, J774a cells were fed latex beads for 1 hour at 37°C, and the phagosomal fraction was isolated from cell homogenates by fractionation on sucrose gradient. Equal amounts of the purified phagosomal fraction and of a crude total membrane fraction were separated by SDS-PAGE, and the relative amount of endogenous Nramp2 in each sample was determined by immunoblotting. As shown in Fig. 7A (left panel), Nramp2 was significantly enriched in purified phagosomes, as compared to the crude membrane preparation. In these experiments, the Lamp1 protein (marker of the phagolysosome, middle panel) and the transferrin receptor (marker of the plasma membrane, right panel) were used as controls. As expected, significant enrichment of Lamp1 was seen in the phagosomal fraction while transferrin receptor was not enriched in phagosomes while it is readily detectable in crude membrane fractions. These results suggest that Nramp2 becomes associated with the phagosome during its maturation to phagolysosome. Possible association of Nramp2 with latex beads phagosomes was further analyzed in J774a cells by immunofluorescence and confocal microscopy. J774a cells were fed latex beads, then fixed and processed by double-immunofluorescence using anti-Nramp2 and anti-Lamp1 antibodies (Fig. 7B). In J774a cells, the Nramp2 signal obtained with our antibody was weak which limited the analysis. Nevertheless, in several of the sections analyzed a portion of the Nramp2 signal could

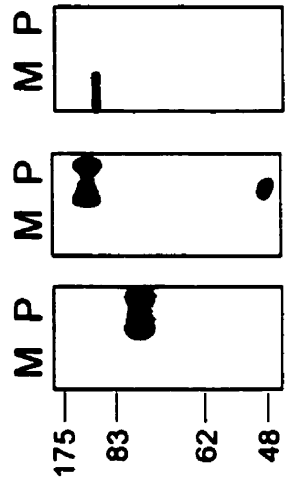
clearly be seen at the periphery of the bead, suggesting association with the phagosome. However, this signal was much weaker than that obtained using the anti-lamp1 antibody. Thus, results from immunoblotting and immunofluorescence suggest the possibility that a portion of the endosomal Nramp2 protein becomes associated with the phagosome during phagolysosome maturation.

Figure 7 *Nramp2 association with phagosomes*

(A) *Immunoblotting of latex bead-containing phagosomes isolated from J774a cells.*

Latex bead-containing phagosomes were purified from cell homogenates by subcellular fractionation on sucrose density gradients as described in Materials and Methods. Equal amounts of phagosomal proteins (P) and of a crude membrane protein extract prepared prior to phagocytosis (M) were separated by SDS-PAGE on a 7.5% gel. Proteins were transferred to nitrocellulose and the immunoblot was sequentially analyzed with anti-Nramp2 antiserum (left), anti-Lamp1 antibody (middle) and anti-transferrin receptor antibody (right). The position of molecular mass markers (in kDa) is indicated on the left side of the immunoblot. **(B)** *Localization of the Nramp2 and the Lamp1 proteins in J774a macrophages by immunofluorescence.* J774a macrophages were allowed to phagocytose latex beads, followed by fixation and staining with the anti-Nramp2 antiserum and a Rhodamine conjugated secondary antibody (a), and the anti-Lamp1 antibody and a secondary antibody coupled to FITC (b). A phase contrast image of the cells shown in (a) and (b) is also included (c).

A



B



Discussion

A large body of biochemical data supports the proposal that Nramp2 functions as a transporter for several divalent cations, including Fe^{2+} ^{141,145,148,182,185}. *Nramp2* is mutated in the *mk* mouse and in the *Belgrade (b)* rat^{145,148}, with both animals exhibiting a severe microcytic hypochromic anemia and a marked defect in iron absorption by intestinal cells^{152,153}. However, *in vitro* studies have shown that iron acquisition is also decreased in peripheral cells and tissues from these animals^{153,170,171,173,271,272} and that the anemia cannot be corrected by direct iron injections²⁷³, suggesting a second block of iron entry into peripheral tissues. Thus, physiological consequences of *Nramp2* mutations *in vivo* strongly suggest that Nramp2 is not only involved in iron uptake at the level of the intestinal enterocyte but also participates in iron acquisition in other cell types as well. In peripheral tissues, cellular iron uptake is through the transferrin cycle (reviewed by¹⁴⁷). Diferric transferrin binds to the transferrin receptor, is internalized and acidification of the internalized vesicles results in release of iron from transferrin, followed by recycling of the receptor to the cell surface¹⁷². Iron escapes the acidified endosomal compartment to reach the cytoplasm where it can be captured by mitochondria for heme biosynthesis and incorporation into heme-containing proteins, stored in the cytoplasm in the form of ferritin and/or used directly for synthesis of non-heme containing proteins (e.g. ribonucleotide reductase). The mechanism by which iron is extruded from the acidified endosome to enter the cytoplasm is unknown and has been a matter of considerable debate.

In the current study, we have raised isoform specific anti-Nramp2 antiserum and have used it to verify a number of structural and biochemical features of Nramp2

predicted from the primary amino acid sequence deduced from the cDNA. These analyses have shown that Nramp2 is an integral membrane protein that is extensively modified by N-linked glycosylation; As opposed to Nramp1 which is macrophage-specific, Nramp2 protein was found ubiquitously expressed in a majority of cell lines analyzed. The current study has also clearly established that Nramp2 and Nramp1 localize to distinct subcellular compartments. While Nramp1 co-localizes with the FITC-dextran in the lysosomal compartment, Nramp2 is not detectable in this compartment, but rather shows clear colocalization with FITC-transferrin both at the plasma membrane and also in recycling endosomes. The demonstration of Nramp2 expression in several peripheral tissues, the colocalization of Nramp2 and transferrin in plasma membrane and recycling endosomes, the iron transport properties of the Nramp2 protein, and the effect of Nramp2 mutations on iron metabolism in peripheral tissues are strong evidence that Nramp2 is responsible for transporting Fe^{2+} into the cytoplasm after acidification of the transferrin-positive endosome (Fig. 8). Interestingly, this acidification would simultaneously provide a gating mechanism for iron transport by Nramp2 and for release from transferrin (Fig. 8). Indeed, the pH dependence of iron transport by Nramp2 has been demonstrated in several systems, including *Xenopus* oocytes¹⁴¹, transfected HEK293T cells¹⁴⁵ and CHO cells²⁷⁰. Likewise, release of iron from transferrin and its subsequent release from endosomes is dependent on endosome acidification, which can be inhibited by bafilomycin²⁷⁴ and concanamycin⁷², specific inhibitors of the vacuolar H^+ /ATPase, but is insensitive to the Na^+ , K^+ /ATPase inhibitor ouabain^{274,275}. This suggests a critical role for the vacuolar H^+ /ATPase in this process. Indeed, the association of

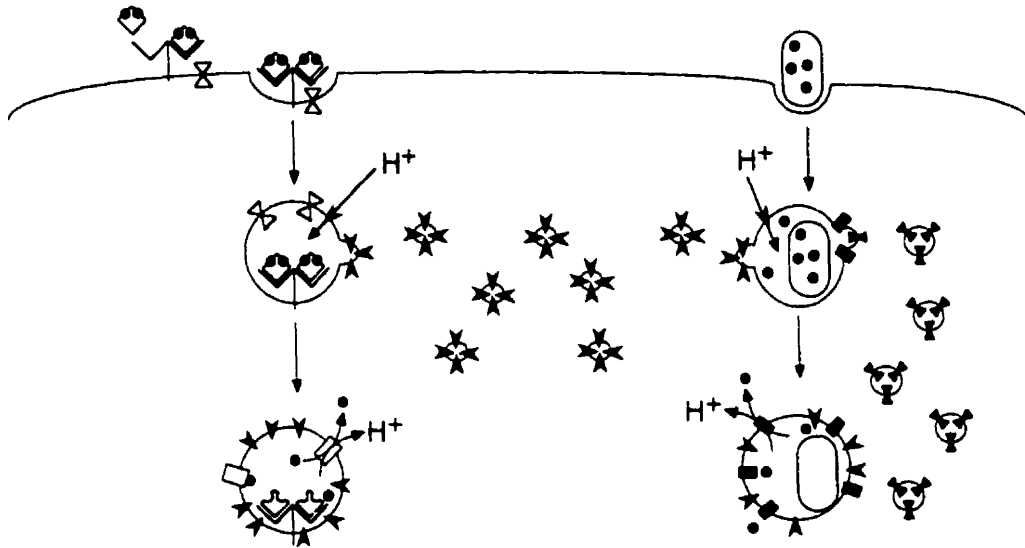
vacuolar H⁺/ATPase with transferrin-positive endosomal vesicles has been demonstrated by immunohistochemical means in LLC-PK1 cells ²⁷⁶.

The demonstration that Nramp1 and Nramp2 are co-expressed in the same cell type with distinct subcellular localizations suggests possible functional parallels between Nramp1 and Nramp2 (Fig. 8). Both the yeast Smf1 and the mammalian Nramp2 proteins can transport Mn²⁺, with the latter also transporting Fe²⁺ and other divalent cations. Nramp2 and Smf1 share approximately 40% sequence identity within the conserved hydrophobic core ¹⁷⁸. As the mammalian Nramp1 and Nramp2 proteins share almost 80% sequence identity within their hydrophobic core, it is thus likely that Nramp1 is involved in the transport of divalent cations as well. The removal of such metabolically essential ions from the phagosomal space would provide an attractive explanation for the observed pleiotropic effect of *Nramp1* mutations *in vivo* on the replicative potential of internalized microbes that inhabit that space in macrophages. Additionally, the observation that a portion of Nramp2 associates with latex bead phagosomes in J774a cells suggests that Nramp2 may also play a role in depleting the phagosomal space of divalent cations necessary for microbial survival.

Despite considerable efforts, transport studies in CHO and RAW cells transfected and overexpressing Nramp1 protein have so far failed to demonstrate an Nramp1-mediated transport of either ⁵⁴Mn or ⁵⁵Fe transport in these cells ²⁷⁰. The distinct, non-overlapping, distribution of Nramp1 and Nramp2 reported here provides an explanation for this apparent lack of transport activity associated with Nramp1. While the two proteins may have the same transport potential, the observed targeting of Nramp2 to the plasma membrane and recycling endosome compartment would result in net increase in

Figure 8. Proposed functional similarity between Nramp1 and Nramp2

Schematic representation of Nramp2 (left) and Nramp1 (right) function. Nramp2 is present at the plasma membrane and recycling endosomes, but is not functional at neutral pH (\otimes). When diferric transferrin (\blacklozenge) binds to the transferrin receptor (∇), the complex is internalized. Following recruitment of the V-ATPase (∇), the endosome acidifies, which causes dissociation of iron (\bullet) from transferrin as well as activation of Nramp2 function (\square). Iron can then be co-transported along with a proton across the endosomal membrane into the cytosol. In the case of Nramp1, bacteria that contain and require iron are taken up in phagosomes at the plasma membrane. These phagosomes acquire both Nramp1 (\otimes / \blacksquare) and the V-ATPase. Acidification of the phagosome provides the driving force for the co-transport of iron and protons out of the phagosome in order to sequester iron away from the bacteria.



- | | | | |
|---|--------------------------------------|---|----------------|
| ▼ | = V-ATPase | ⌘ | =Nramp2 pH 7.4 |
| ↘ | =transferrin receptor | □ | =Nramp2 pH 6 |
| ◊ | = diferric transferrin | ⌘ | =Nramp1 pH 7.4 |
| ◊ | =apotransferrin | ■ | =Nramp1 pH 6 |
| • | = Fe ²⁺ /Fe ³⁺ | | |

cellular accumulation of extracellularly added radiolabeled ligand under acidic pH transport assay conditions. On the other hand, the restricted expression of Nramp1 to the lysosomal compartment would not cause a similar increased cellular uptake of a ligand presented in the extracellular milieu, although it may act on such ligand if present in the phagolysosomal space. Therefore, it is tempting to speculate that both Nramp1 and Nramp2 have similar transport function but act at different, non-overlapping, intracellular sites (Fig. 8). If indeed Nramp1 and Nramp2 do transport the same substrates, it is also tempting to speculate that vesicular acidification via the vacuolar H⁺/ATPase may provide a key common gating mechanism for the activation of both transporters, through fusion with vacuolar H⁺/ATPase-positive vesicles (Figure 8). Possible similarities and differences in the mechanism of action and regulation of Nramp1 and Nramp2 in macrophages are currently being investigated.

Chapter 5
Summary and Perspectives

The work presented in this thesis contributes to our understanding of the Nramp family. Localization of Nramp1 to the membrane of the phagosome represents an advance in our knowledge of its mechanism of action during intracellular infection (Chapter 2). *Nramp2* was the first homolog of *Nramp1* that was identified and characterized. At the time, alignment of the two predicted protein sequences gave the first clues as to what residues might be important for structure or function (Chapter 3). At present, the power of these types of analyses is greatly increased, due to the identification of a large number of other *Nramp*-related sequences. The differential tissue-specific expression and subcellular localization of Nramp1 versus Nramp2 (Chapters 2,3,4) leads to the hypothesis that Nramp1 and 2 may transport the same substrate at different locations, a hypothesis which remains to be proven. Other groups' discoveries leading to the identification of Nramp2 as a metal transport protein allow further expansion of this hypothesis, including how metal transport at the phagosome by Nramp1 may affect resistance to infection (discussed below). Finally, the localization of Nramp2 to the transferrin cycle endosome clarifies its role in iron metabolism (Chapter 4).

5.1 Future perspectives: *Nramp1*

5.1.1 *Nramp1* and intracellular infections

The recruitment of Nramp1 to the membrane of phagosomes reported in Chapter 2 has recently been confirmed in parasite-containing phagosomes during infection with *Salmonella*, *Yersinia*, and *Mycobacterium* species^{60,277}. While Blackwell's group has

reported the localization of both the G169 (*Bcg^R*) and D169 (*Bcg^S*) Nramp1 proteins to endosomes, lysosomes, and *Leishmania* phagosomal membranes ²⁷⁸, it is unlikely that the antibodies used in their studies were specifically recognizing Nramp1 ^{279,280}. More recent studies from co-authors of this report, as well as previous work from our lab has established that the endogenous Nramp1 protein from macrophages is observed on SDS-PAGE gels as a broad species of 90-100 kDa, and is present in resistant macrophages only ^{49,280}. There were two types antibodies used in Blackwell's *Leishmania* studies: polyclonal antisera that recognized a thin species of 65 kDa in both resistant and susceptible macrophages, and a panel of monoclonal antibodies which was not characterized and was reported to not recognize any proteins specifically in Western blots ^{278,281}. These anomalies, as well as the co-authors later report that the Nramp1 protein is not present in susceptible macrophages ²⁸⁰, casts considerable doubt on the conclusions reached in this paper.

The targeting of Nramp1 to the phagosomal membrane brings forth the hypothesis that Nramp1 controls the replication of intracellular parasites by directly or indirectly altering the environment of the microbe-containing phagosome. Since Nramp2 shares divalent cation transport ability with its distant relatives yeast SMF and bacterial Nramp (see Chapter 1), it is almost certain, although not yet proven, that the more closely related Nramp1 is involved in the transport of divalent cations as well. The most compelling evidence to date is that the *malvolio* defect in *Drosophila* can be corrected either by supplementation with $\text{Fe}^{2+}/\text{Mn}^{2+}$, or by overexpression of human *NRAMP1* ^{187,189}. For several years, many groups have hypothesized that Nramp1 acts to deplete the phagosomal environment of iron and other heavy metals, although this has yet to be

definitively proven 148,179,182,262. The eventual proof or disproof of this hypothesis is most likely a top priority for many researchers working in this field, and when realized, it will represent a much-anticipated milestone.

Divalent metals are essential for survival of all organisms, including microbes. Iron, in particular, is essential for all living beings, with the exception of certain species of *Lactobacillus* that use cobalt and manganese in its place 282. Microbial depletion of iron generally leads to decreased DNA replication and decreased respiratory activity, due to iron requirements of ribonucleotide reductase and electron transport proteins respectively 283. In general, increased iron acquisition ability of a microbe can be correlated with increased virulence. Scientists and doctors have long been aware of the connection between iron and microbial pathogenicity: in 1872, a Parisian professor warned his class of medical students that it was dangerous to administer iron to patients with quiescent tuberculosis, as this often led to reactivation of the disease 284. In the 1930's and 40's research programs were aimed at developing iron-binding agents for antimicrobial therapy, however these programs fell by the wayside after the discovery and commercialization of penicillin 283. More recent studies have linked iron supplementation with gram negative sepsis, salmonellosis, and respiratory infections in human infants 285-287.

Why is increased iron availability associated with enhanced microbial proliferation? Divalent cations are essential co-factors for many enzymes including superoxide dismutase (SOD), and catalase, enzymes that neutralize some of the anti-microbial actions of the phagolysosome. Indeed, *Salmonella* and *Mycobacteria* encode their own SOD and catalase/peroxidase 288-292. *Leishmania* encodes two SOD

enzymes, and although the gene has not been cloned, catalase activity has been demonstrated in amastigotes ^{293,294}. This suggests that these enzymes play important roles in the intracellular survival strategies of these microbes. In support of this, it has been demonstrated that growth of another mycobacterial species, *M. smegmatis*, in low iron medium increases its susceptibility to killing by H₂O₂ ²⁹⁵. Additionally, transcriptional regulators such as the iron-dependant *iroA* and *fur* of *Salmonella*, and *fur* and *ideR* of *Mycobacteria*, lead to the downstream regulation of multiple pathways in response to divalent cation availability ^{282,296}.

Pathogens have evolved various strategies to obtain iron from the host, including expression of cell surface transferrin or lactoferrin receptors, siderophore systems, and heme catabolism following erythrocyte lysis ^{282,283}. Many pathogens have multiple iron transport systems: *E. coli* has at least eight, six of which are siderophore systems ²⁹⁷. A possible reason for this apparent redundancy is that differing biochemical environments in various host tissues might necessitate different iron acquisition schemes. For example, the TonB siderophore transporter of *Salmonella* is required for virulence in intragastric infections, but not required for infection via the intraperitoneal route ²⁹⁸. Similarly, the activity of mycobactin, a mycobacterial siderophore, was detectable in cultures of *M. avium* and *M. tuberculosis* grown *in vitro*, but its activity was absent during intracellular infections ²⁹⁹. These results suggest that while many of these iron acquisition systems seem well suited for scavenging iron from extracellular locations, their intracellular utility is not as clear. For example, bacterial transferrin receptors would be of no use at the acidic pH of the phagosome, where iron would not remain bound to transferrin. However, the discovery of bacterial *Nramp* homologs in *Salmonella*

and *Mycobacterium*, and the demonstration that bacterial Nramp transports Fe^{2+} at acidic pH¹⁸⁸, raises the possibility that these proteins transport iron and other divalent cations within the acidic environment of the phagosome. This would place the bacterial and mammalian Nramp proteins in direct competition to transport the available divalent ions into their respective cells. Expression of high levels of Nramp1 in the phagosome of resistant mice would favor sequestration of iron and other ions by the host, whereas a lack of Nramp1 expression in susceptible mice would favor their piracy by the pathogen. Interestingly, mycobacterial phagosomes have been shown to be accessible to exogenously administered transferrin, providing evidence that iron could be acquired in this way^{300,301}. Mycobacterial Nramp has the required transport activity to take up iron that would be expected to be released from transferrin upon encountering the acidic pH of the phagosome. Thus in mycobacterial infection, iron-loaded transferrin is directed to the parasite-containing phagosome, the iron is most likely released due to the acidic environment, and the mycobacterial Nramp has the required transport activity to direct its uptake. While a Nramp homolog has not yet been identified in *Leishmania* species, subverted transferrin trafficking to amastigote-containing phagosomes has been documented, suggesting that this hypothesis could be extended to *Leishmania* as well³⁰². *Salmonella* encode a Nramp homolog¹⁸⁸, but the accessibility of their phagosome to transferrin has not been studied. Therefore, I present this as an attractive but unproven model for iron acquisition inside the phagosome, and for Nramp1 function in resistance to infection. If experimental data provide support for this model, *Nramp1* joins the ranks of the host's iron withholding defense system³⁰³. This system involves other previously described mechanisms, such as the secretion of lactoferrin by activated neutrophils.

Lactoferrin serves as a sponge to chelate extracellular ionic iron until recruited macrophages clear up the complexes by phagocytosis²⁸⁴. Other responses in the iron-withholding system include cytokine-regulated decreased intestinal iron absorption and increased ferritin expression to promote storage of any intracellular iron that is present (reviewed in³⁰³.) However, despite the implications of Nramp1-mediated iron transport, it should not be overlooked that Nramp1 could transport other divalent cations such as Mn^{2+} and Zn^{2+} , and depletion of these ions would have an effect on microbial proliferation as well.

How can this model explain the disruption of the BCG-mediated block of phagosomal maturation observed in resistant mice? It is possible that divalent cations could be directly involved in the fusion and maturation process of phagosomes, and that Nramp1-mediated changes in divalent cation concentrations could be critical for phagosome maturation during the course of infection, when parasites are competing for available ions. Indeed, Zn^{2+} has been shown to be necessary in an *in vitro* endosome-endosome fusion assay³⁰⁴. Another possibility involves a more general effect of cations on bacterial metabolism and pathogenicity. Perhaps the mycobacterial genes involved in the mechanism by which BCG blocks phagosome maturation are directly regulated by transcriptional regulators such as *ideR* or *fur*, and the Nramp1-mediated depletion of ions results in a shutdown of their synthesis. Alternatively, the regulation could be more indirect. For example, in the absence of functional SOD and catalase to neutralize the harsh environment of the phagosome, the pathogen might be damaged or weakened to the point where it does not effectively express the genes necessary for attenuation of phagosomal maturation.

Some publications have attempted to demonstrate divalent cation transport activity of Nramp1, yet there is still a lack of definitive data. In the report of Nramp2-mediated electrogenic ion transport in *Xenopus* oocytes, it was mentioned that Nramp1 directed transport of divalent cations as well ¹⁴¹. However, no supportive data was presented at the time, and none has been published to date. Atkinson demonstrated lower cell-associated iron levels in *Nramp1* G169 transiently transfected COS-1 cells compared to vector-transfected control cells after 4h of uptake of Fe:NTA ³⁰⁵. The same group showed similar results in RAW 264.7 *Nramp1* G169 stable transfectants compared to antisense-transfected controls ²⁸⁰, and concluded that *Nramp1* was directing secretion of iron from the cells. However, an independent study of stable transfectants of RAW 264.7 cells reported absolutely no differences between clones transfected with the G169 or D169 allele of *Nramp1* in ⁵⁵Fe-citrate import and export time course experiments, at all times examined ³⁰⁶.

On a similar note, Zwilling's group published studies of iron uptake by latex bead and *Mycobacterium avium* containing phagosomes isolated from G169 and D169-transfected RAW 264.7 cells and resistant and susceptible macrophages ^{306,307}. Their results showed a 1.5-2.5X greater association of ⁵⁵Fe with Nramp1 G169-positive phagosomes. The authors suggested that Nramp1 transports iron into (rather than out of) phagosomes, catalyzing the production of toxic hydroxyl radicals via the Fenton reaction ($\text{Fe}^{2+} + \text{H}_2\text{O}_2 \rightarrow \text{Fe}^{3+} + \text{OH}^\bullet + \text{OH}^-$). On the other hand, Gomes and Appelberg obtained data that suggests Nramp1 transports iron out of phagosomes ³⁰⁸. Resistant and susceptible mice were pretreated for 20 days by injection of iron dextran or dextran alone and then infected with *Mycobacterium avium*. Iron administration increased *M. avium*

growth in a dose-dependent manner. The increase in *M. avium* growth was much more pronounced in resistant mice, leading to a significant reduction of the difference in microbes in resistant versus susceptible iron-treated mice. For example, in dextran-injected control mice, there was 10-fold more bacteria in the livers of susceptible compared to resistant mice, but in the mice injected with 1.2 mg iron + dextran, the difference was reduced to 1.6-fold. The authors hypothesized that overloading the phagocytic cells with iron would overwhelm the system responsible for pumping iron out of the phagosome (Nramp1), and therefore neutralize the advantage of resistant mice.

It is impossible to reconcile the results of all these studies, which emphasizes the need for further investigation. Many experiments could be proposed to clarify these results as well as to test the proposed models for the Nramp1 mechanism of action. Tools have recently been developed to analyze differential bacterial gene expression in different environments (reviewed in 309,310). This technology could be used to study bacterial genes expressed differentially in resistant versus susceptible macrophages, which in turn could give insight into the effects of Nramp1. In addition, manipulation of divalent cation availability could be used in parallel with many of the available assays - *in vitro* or *in vivo* infections, phagosome fusion or acidification -- to investigate a role for divalent cations in these processes in the presence and absence of Nramp1 expression. The most direct, and also the most difficult approach would be to target a divalent cation sensor to the phagosome in resistant and susceptible macrophages, in order to assess the concentration of these ions in the presence or absence of Nramp1. Through approaches such as these, more definitive answers regarding Nramp1 and its role in infection may soon be obtained.

5.1.2 *Nramp1* and iron recycling

Macrophages play a key role in iron metabolism, scavenging iron from senescent red blood cells and returning it back to circulation for incorporation into erythrocyte precursor cells. Whereas 0.5-2 mg of iron per day is exchanged through intestinal absorption and iron loss from the body, approximately 30 mg of iron per day is recycled by macrophages of the reticuloendothelial system ^{147,158,159}. The iron recycling pathway of macrophages is very poorly understood. Damaged red cells are thought to be recognized and phagocytosed by macrophages due to the exposure of inner leaflet lipids on their plasma membrane ³¹¹. After phagocytosis, iron is liberated from heme via heme oxygenase and is either stored in ferritin or released from the cell and returned back to plasma transferrin ^{158,312}. The high-level expression of *Nramp1* in macrophages, its localization at the phagosomal membrane, and its postulated iron transport activity have led to the hypothesis that *Nramp1* is involved in the recycling of iron from senescent red blood cells ¹⁴⁵. Although this hypothesis is rationally and intuitively sound based on the localization and activity of *Nramp1*, the phenotype of mice with a homozygous null allele at *Nramp1* suggests that if *Nramp1* does play a role in this process, its involvement is not obligatory. Since erythrocytes contain 70% of the body's iron, and 1% of erythrocytes are turned over each day ^{147,158,159}, mice with a block in erythrocyte iron recycling would be predicted to become progressively anemic. Yet despite the fact that they are sensitive to infection, *Nramp1*^{-/-} mice have no other phenotypic defects including any detectable abnormalities in iron metabolism. This suggests that if *Nramp1* is involved in the process of erythrophagocytosis and iron recycling there exists a redundancy either at

the level of the macrophage or at the level of the organism that is compensating for its absence in *Nramp1*^{-/-} mice. Future experiments may clarify the pathways of iron recycling in macrophages, and allow for evaluation of the putative role of *Nramp1* in this process.

5.2 Future perspectives: *Nramp2*

Despite its humble origin as the ubiquitous orphan homolog of *Nramp1*, it is now clear that *Nramp2* is interesting in its own right. The unexpected central role of *Nramp2* in the metabolism of iron and other metals has far-reaching implications in normal physiology and in disease states. The work discussed in previous chapters of this thesis represents substantial progress towards our understanding of these areas, yet our knowledge is still far from complete. There is still much to learn about *Nramp2* and the processes in which it is involved. At the electrophysiological level, detailed studies need to be done to determine the stoichiometry of transport including the possible involvement of counterions to balance the movement of at least three positive charges in the same direction¹⁴¹. Nothing is known about the structure/function relationships in the protein, including the molecular basis of substrate specificity, pH sensitivity, and subcellular targeting. The functional significance of the different C-terminal sequences in the two splice forms of *Nramp2*, which could theoretically direct differential targeting, substrate specificity, or regulation to their respective proteins, has not yet been explored. We also have very limited knowledge about the tissue distribution and relative abundance of the two splice forms (IRE and non-IRE: with or without an iron response element) at the mRNA and protein levels. Preliminary results suggest that the two splice form mRNAs

may be co-expressed in many tissues ^{144,145,313}, however the relative abundance of the two proteins appears to vary significantly from tissue to tissue ^{50,144}. The mechanisms behind this variance are not known. Regulation of *Nramp2* expression in response to various stimuli appears to occur in a very tissue-specific manner. For example, dietary iron depletion leads to a marked upregulation of the IRE splice form-encoded *Nramp2* protein only in the proximal duodenum, while other tissues show a modest upregulation at best ¹⁵⁵. Clearly, analysis of the regulation of *Nramp2* expression at the levels of transcription, splicing, and IRE-mediated mRNA half-life in various tissues could be very informative.

5.2.1 The recurring *Nramp2* mutation

One of the more mysterious issues regarding *Nramp2* is the observation that the same G185R mutation has arisen independently in two instances of *mk* mice as well as in the Belgrade rat ^{145,148}. The reasons for this are not obvious. It is possible that the mutant allele confers a selective advantage to animals possessing it, and therefore is under a certain positive selection pressure. However, this is somewhat unlikely, as animals are not exposed to many adverse conditions such as infection or dietary stresses in the types of animal facilities where these mutations arose, therefore the amount of natural selection that occurs in these facilities is debatable. The reasons for recurrence of the G185R allele may be complex. The nucleotide may be in a genomic context that is particularly susceptible to mutation. An analogous situation has been described for the human IFN- γ receptor, where 12 independent mutations at a single site were documented in 12 unrelated families ³¹⁴. Additionally, this mutation may be unique in its ability to

direct partial activity of the protein - enough for viability past birth, yet not enough to avoid a disease state. It could even be argued that the environment of animal facilities is what selects for this allele, through scientists' identification and propagation of anemic animals that would not be viable in the wild. Transfection experiments have shown that G185R has severely reduced transport activity compared to wildtype Nramp2¹⁵⁴. However, it is possible that expression of the mutated form of the protein in *mk* mice results in a reduced but still significant amount of iron absorption across the intestine. *b* rat intestine and other tissues have low but detectable uptake of iron and other metals¹⁵³, which may either be mediated by G185R protein or by other redundant transport processes. A more severe mutation than G185R in *Nramp2* may be lethal *in utero*, whereas a mutation less severe may be phenotypically normal, leaving the G185R to be the only one detected by scientists selecting viable but visibly anemic animals.

5.2.2 *NRAMP2* involvement in human disease

The involvement of *NRAMP2* in human diseases has not yet been extensively studied. However, there are several clinical cases documented in the literature that present with a microcytic, hypochromic anemia very similar to that found in *mk* mice and *b* rats³¹⁵⁻³¹⁷. If DNA or tissue is available from these patients, they could be examined for mutations in *NRAMP2*.

Some researchers have proposed that *NRAMP2* is upregulated in hereditary hemochromatosis, a disorder of iron overload that is essentially the clinical opposite of anemia^{141,261,318}. Hemochromatosis involves a defect whereby the intestine and other tissues steadily continue to absorb iron and other metals despite an iron-overloaded state.

A mutation in *NRAMP2* is not the basis of disease in a majority of patients, since the disease is known to be caused in over 80% of cases by a mutation in an unconventional class I MHC molecule known as HFE ³¹⁹. HFE has been definitively established as the cause of hemochromatosis, since mice with a homozygous null allele at *Hfe* have the disease as well ³²⁰. HFE interacts and traffics with the transferrin receptor, but its mechanism of action is not known ^{321,322}. It is possible that *NRAMP2* expression or activity is directly or indirectly affected by HFE and is therefore perturbed in hemochromatosis. Indeed, an increase in *NRAMP2/Nramp2* mRNA has been reported in hemochromatosis patients and *Hfe* knockout mice, although protein expression has yet to be monitored in these samples. Perhaps the development of specific pharmacological inhibitors of NRAMP2 may be of use for treatment of hemochromatosis disease, which is now treated by periodic bleeding.

5.2.3 Tissue-specific roles of *Nramp2*

While *Nramp2* is expressed ubiquitously (Chapter 3, 4, 141,263), it may be of special importance or interest in some specific tissues, due to their unique roles in the metabolism of iron or other metals. What follows below is a discussion of *Nramp2* expression and function with respect to its putative roles at some of these sites.

Intestine

In humans, the amount of iron in the body is controlled at the level of intestinal absorption. Loss of iron is mostly through sloughing off of cells, and this is balanced by iron absorption in the duodenum ^{158,159,323}. Intestinal iron uptake is normally exquisitely sensitive to the status of the body's iron stores, and adjusts itself accordingly

(reviewed in 174,324). This control appears to involve both upregulation of absorption under iron depleted conditions and down-regulation during iron overload. The molecular basis of the intestinal mechanism that senses the body's iron status has not been fully elucidated. There appears to be involvement of the transferrin cycle at the basal surface of enterocytes, iron response element/iron regulatory protein (IRE/IRP) interactions, and HFE. The exact role of any of these elements within this system is not well defined. As described above, HFE is an unconventional class I MHC molecule that is mutated in over 80% of patients with hereditary hemochromatosis³¹⁹ that associates with the transferrin receptor^{321,322}, but the mechanisms by which it causes disease are not well defined.

Some reports have directly implicated a role for IRE/IRP interactions in intestinal iron sensing. This is of interest since one of the splice forms of *Nramp2* has a putative IRE in its 3'UTR^{141,145}. In a study of IRE involvement in iron sensing, iron transport and IRP activity was measured in the duodenum of iron-starved rats following parenteral iron administration³²⁵. Initially, iron-deprived rats displayed increased IRP activity compared to rats on a control diet. Upon injection of radiolabelled iron into the bloodstream of iron-deprived rats, ⁵⁹Fe was taken up exclusively in crypt enterocytes and the IRP activity decreased at this site accordingly. At the villus tips, however, no change in iron uptake or IRP activity was observed until 48 hours after injection, when the IRP activity and iron uptake decreased. This corresponds to the estimated time it takes enterocytes to migrate from the crypts where they are formed, to the villi where they are functional³²⁶. This supports a previous hypothesis that the amount of iron that enterocytes are exposed to during their formation in the duodenal crypts sets a "program" for protein expression after their migration to the tips of the villi³²⁷, and this program is

what regulates iron uptake with respect to iron stores. The program referred to in this hypothesis appears to be actualized by IRPs. The IRP results and above hypothesis concur with a previous study on ferritin expression in the intestine of rats with varying iron stores, where upon iron loading, ferritin expression was increased at the mRNA level in the crypt cells, but at the protein level in the villus ³²⁸. The increase in ferritin expression upon iron loading is thought to be mediated by the IREs in the 5'UTR of the ferritin mRNA.

An analogous temporal/spatial effect appears to occur during iron deprivation as well. *Nramp2* expression is dramatically upregulated in the proximal duodenum in response to iron depletion ¹⁵⁵. High levels of *Nramp2* mRNA are observed in the crypts ¹⁴¹, but the protein is highly expressed in the villi ¹⁵⁵. Indirect evidence suggests that the upregulation of *Nramp2* in the duodenum is mediated by iron-regulatory proteins (IRP1/2) interacting with the iron regulatory element (IRE) in the 3'UTR of *Nramp2* mRNA: it is the protein encoded by the IRE-positive mRNA that is detected at this site after iron depletion ¹⁵⁵; the IRE in the 3'UTR of the *Nramp2* message has been shown to bind IRP1, suggesting that it is functional ³¹³; and IRP activity in the duodenum is higher in iron-deprived rats compared to control rats ³²⁵.

Despite these recent insights into the role and regulation of *Nramp2* in the intestine, several unanswered questions remain. It has yet to be directly demonstrated that IRP activity affects *Nramp2* expression. It is not clear as to whether the mechanism behind the crypt/villus differences in *Nramp2* mRNA and protein expression is simply due to the gradual accumulation of protein during enterocyte migration, or if there is another level of regulation involved in the delayed expression of the protein. In addition,

nothing is known about why the regulation described above is specific to the proximal duodenum, and not seen in other parts of the intestine ^{143,155,325}. Limited by the levels of detection, no one has explored the possibility of a decrease in Nramp2 levels upon iron loading. Also due to the sensitivity of detection, the subcellular localization of Nramp2 in the intestine has been limited to demonstration of high levels of the protein in the brush border under iron deprivation conditions ¹⁵⁵. However, the protein can be detected in the intestine under iron replete conditions by Western blotting ¹⁵⁵ and biochemically, as a pH-sensitive, divalent cation-competable iron transport activity ¹⁴³. Whether normal physiological expression of Nramp2 is limited to the villi or extends to the crypts as well is a question of particular interest, since crypt cells are thought to take up and sense iron from the blood via the transferrin cycle ^{329,330}, and Nramp2 is implicated in the transport of iron out of transferrin cycle endosomes (Chapter 4). Therefore, it is likely that the Nramp2 protein is present in the crypts, but at too low a level to be detected by current methods. If Nramp2 is not present at the crypts, this suggests that a novel endosomal iron transporter is acting at this location.

Red Blood Cells

As mentioned in section 5.1.2, red blood cells are the major iron reservoir in the body, containing 70% of total body iron. 1% of red blood cells are turned over on a daily basis: as old cells are phagocytosed by macrophages, reticulocytes are released from the bone marrow into circulation where they become mature erythrocytes within approximately 24 hours. Reticulocytes take up iron from transferrin for use in the synthesis of heme. In addition, under non-physiological conditions, reticulocyte uptake of non-transferrin bound iron (NTBI) can be demonstrated. Both transferrin-bound and

non-transferrin bound iron uptake in reticulocytes occurs via Nramp2^{272,331}. As reticulocytes mature into erythrocytes, they lose the capacities to transport iron and to synthesize heme. Accordingly, during maturation, red blood cells lose expression of the transferrin receptor and heme biosynthesis enzymes³³². Although there has not yet been any such studies published, it is anticipated that *Nramp2* expression will be regulated during erythrocyte maturation as well. Also of interest in reticulocytes is the proposal that in these cells, iron is delivered directly from the endosome to the mitochondria, via transient contacts between the two compartments¹⁴⁷. The possible contact between Nramp2-positive endosomes and mitochondria could be investigated in order to substantiate this hypothesis.

Brain

Nramp2 is expressed in the brain: in neurons and in epithelial cells of the choroid plexus, the major site of transport at the blood-cerebrospinal fluid barrier¹⁴¹. Expression of *Nramp2* in neurons is of interest since mutation of *malvolio*, the *Drosophila Nramp* homolog which is expressed in neurons results in a defect in the neurological pathway involved in taste discrimination behavior¹⁸⁶. Iron is involved in the function and synthesis of various neurotransmitters¹⁵⁹, and a defect in neuronal circuitry is thought to underlie the *malvolio* phenotype¹⁸⁶. However, the *malvolio* defect is specific to taste behaviour and does not involve a general defect in neuronal signalling¹⁸⁶, suggesting a unique role for divalent cations specifically in taste behaviour pathways. Parallels have been drawn between the human disease Pica and the behavior of *malvolio* mutant flies³³³. Like the defect in flies, Pica often involves the

ingestion of substances that are avoided by normal subjects, for example clay ³³⁴. Surprisingly, Pica is apparently cured in many patients following dietary iron supplementation ^{334,335}, suggesting that iron has a role in bizarre eating behavior in humans as well as flies. However, identification of *Nramp2* mRNA in neurons is far from demonstration of a causal role for the protein in Pica. To date no eating behavior abnormalities have been reported for *mk* mice or *b* rats, so this matter awaits further investigation.

In addition to the interest in neuronal expression of *Nramp2* because of Pica, many groups have noted a correlation between iron deposition in neurons and disorders such as Parkinson's and Alzheimer's diseases ^{159,336,337}. This suggests that deregulation of *Nramp2* expression may play a role in the pathogenesis of neurodegenerative diseases. However, to date there is no experimental data pertaining to *Nramp2* in the pathogenesis of these afflictions.

Another potentially interesting site of expression of *Nramp2* is at the blood-cerebrospinal fluid barrier and other related barriers, since a unique iron transport process is implicated at these sites. The choroid plexuses are small tufted structures, rich in capillaries that project into the ventricles of the brain. The surfaces of the plexuses are covered by a layer of epithelial cells through which fluid and molecules must pass before entering the cerebrospinal fluid (CSF) ^{338,339}. The choroid plexuses are thus referred to as the blood-CSF barrier. By *in situ* hybridization, a high level of *Nramp2* mRNA was detected in the epithelial cells of the choroid plexus, suggesting that *Nramp2* is involved in the passage of iron between the blood and the cerebrospinal fluid ¹⁴¹. Although the choroid plexuses technically comprise part of the blood-brain barrier ³³⁹, the term blood-

brain barrier often refers more specifically to the endothelial cells surrounding the capillaries passing through the solid tissues of the brain. Many studies on the passage of iron into the brain have concentrated on these endothelial cells³⁴⁰⁻³⁴², since they have been shown to express transferrin receptors³⁴³. There is currently no information on *Nramp2* expression at this site, but it would certainly be of interest to examine its possible localization here. On the other hand, the high expression of *Nramp2* in the choroid plexus calls for examination of the transport of iron and other metals at this location.

High levels of *Nramp2* mRNA were also detected in Sertoli cells of the testes¹⁴¹. Sertoli cells form the blood-testes barrier, controlling the composition of the fluid surrounding developing sperm cells in the same way the choroid plexus controls the composition of the CSF. Similarly, the trophoblast cells of the placenta protect the composition of body fluids in and around the developing fetus (reviewed in³²⁴). Although there has not yet been direct detection of *Nramp2* mRNA in the placenta, it has been previously shown that there is diminished transfer of iron from heterozygous mothers into homozygous *mk/mk* mice¹⁵³, suggesting a role for *Nramp2* at this site as well.

A unique iron transport process is implicated at these barriers, which has been most extensively studied in Sertoli cells (reviewed in³²⁴). The basal surface of Sertoli cells is in direct contact with the blood, and takes up iron via the transferrin cycle. However, once removed from the plasma-derived transferrin molecule, the iron is somehow transferred to a new transferrin molecule that is synthesized within the Sertoli cell. Iron-loaded testicular transferrin is then released into the luminal space, where it

can be taken up by spermatocytes. Similar processes are thought to occur at the placenta and blood-CSF barrier, although none of these processes have been characterized fully. The identification and characterization of *Nramp2* at these barriers may facilitate a better understanding of the mechanisms involved. *Mk* mice and *b* rats and their wildtype littermates provide a good model system to study the consequences of *Nramp2* deficiency in these processes.

5.3 Final Conclusions

The study of host resistance factors identified in mouse models of disease provides a means to identify novel mechanisms of defense against infection. The identification and continuing characterization of *Nramp1* is an exemplary illustration of the utility of this approach. Accumulating evidence suggests that *Nramp1* acts by sequestering iron and other divalent cations away from parasites during intracellular infections. *NRAMP1* may also be a determinant of disease resistance in humans. This information gives insights into new possibilities for therapeutic intervention in infectious disease. *Nramp2*, first identified through its homology to *Nramp1*, plays a pivotal role in iron metabolism. It is involved in the uptake of iron and other metals by many tissues, and regulation of its expression may be a central component of iron homeostasis. *NRAMP2* may be involved in human disorders of iron metabolism such as anemia and hemochromatosis. Though there has been substantial progress in our understanding of these genes and the processes in which they are involved in the last few years, there are still many exciting aspects to be examined in the future.

References

1. Young P: White house to expand response to infectious diseases. *ASM News* **62**:450-451, 1996.
2. Berkelman RL, Bryan RT, Osterholm MT, Leduc JW, Hughes JM: Infectious disease surveillance: A crumbling foundation. *Science* **264**:368-370, 1994.
3. Davies J: Inactivation of antibiotics and the dissemination of resistance genes. *Science* **264**:375-382, 1994.
4. Hill AV: The immunogenetics of human infectious diseases. *Annu Rev Immunol* **16**:593-617, 1998.
5. Skamene E: Genetic regulation of host resistance to bacterial infection. *Rev Infect Dis* **5** Suppl 4:S823-832, 1983.
6. Skamene E, Schurr E, Gros P: Infection genomics: Nramp1 as a major determinant of natural resistance to intracellular infections. *Annu Rev Med* **49**:275-287, 1998.
7. Lander ES, Schork NJ: Genetic dissection of complex traits. *Science* **265**:2037-2048, 1994.
8. Qureshi ST, Skamene E, Malo D: Comparative genomics and host resistance against infectious diseases. *Emerg Infect Dis* **5**:36-47, 1999.
9. Skamene E, Kongshavn PAL, Landy M: Genetic Control of Natural Resistance to Infection and Malignancy: Perspectives in Immunology. New York, NY, Academic Press, 1980, 598 pp.

10. Webster LT: Inherited and acquired factors in resistance to infection: development of resistant and susceptible lines of mice through selective breeding. *J Exp Med* **57**:793-817, 1933.
11. Plant J, Glynn AA: Natural resistance to Salmonella infection, delayed hypersensitivity and Ir genes in different strains of mice. *Nature* **248**:345-347, 1974.
12. Bradley DJ: Letter: Genetic control of natural resistance to Leishmania donovani. *Nature* **250**:353-354, 1974.
13. Bradley DJ: Regulation of Leishmania populations within the host. II. genetic control of acute susceptibility of mice to Leishmania donovani infection. *Clin Exp Immunol* **30**:130-140, 1977.
14. Plant J, Glynn AA: Genetics of resistance to infection with Salmonella typhimurium in mice. *J Infect Dis* **133**:72-78, 1976.
15. Plant J, Glynn AA: Locating salmonella resistance gene on mouse chromosome 1. *Clin Exp Immunol* **37**:1-6, 1979.
16. Bradley DJ, Taylor BA, Blackwell J, Evans EP, Freeman J: Regulation of Leishmania populations within the host. III. Mapping of the locus controlling susceptibility to visceral leishmaniasis in the mouse. *Clin Exp Immunol* **37**:7-14, 1979.
17. Forget A, Skamene E, Gros P, Mialhe AC, Turcotte R: Differences in response among inbred mouse strains to infection with small doses of Mycobacterium bovis BCG. *Infect Immun* **32**:42-47, 1981.
18. Brown IN, Glynn AA, Plant J: Inbred mouse strain resistance to Mycobacterium lepraemurium follows the Ity/Lsh pattern. *Immunology* **47**:149-156, 1982.

19. Gros P, Skamene E, Forget A: Genetic control of natural resistance to *Mycobacterium bovis* (BCG) in mice. *J Immunol* **127**:2417-2421, 1981.
20. Skamene E, Gros P, Forget A, Kongshavn PA, St Charles C, Taylor BA: Genetic regulation of resistance to intracellular pathogens. *Nature* **297**:506-509, 1982.
21. Hormaeche CE: The natural resistance of radiation chimeras to *S. typhimurium* C5. *Immunology* **37**:329-332, 1979.
22. O'Brien AD, Scher I, Formal SB: Effect of silica on the innate resistance of inbred mice to *Salmonella typhimurium* infection. *Infect Immun* **25**:513-520, 1979.
23. Gros P, Skamene E, Forget A: Cellular mechanisms of genetically controlled host resistance to *Mycobacterium bovis* (BCG). *J Immunol* **131**:1966-1972, 1983.
24. Crocker PR, Blackwell JM, Bradley DJ: Transfer of innate resistance and susceptibility to *Leishmania donovani* infection in mouse radiation bone marrow chimaeras. *Immunology* **52**:417-422, 1984.
25. Lissner CR, Swanson RN, O'Brien AD: Genetic control of the innate resistance of mice to *Salmonella typhimurium*: expression of the *Ity* gene in peritoneal and splenic macrophages isolated in vitro. *J Immunol* **131**:3006-3013, 1983.
26. Stach JL, Gros P, Forget A, Skamene E: Phenotypic expression of genetically-controlled natural resistance to *Mycobacterium bovis* (BCG). *J Immunol* **132**:888-892, 1984.
27. Denis M, Forget A, Pelletier M, Gervais F, Skamene E: Killing of *Mycobacterium smegmatis* by macrophages from genetically susceptible and resistant mice. *J Leukoc Biol* **47**:25-30, 1990.

28. Crocker PR, Blackwell JM, Bradley DJ: Expression of the natural resistance gene Lsh in resident liver macrophages. *Infect Immun* **43**:1033-1040, 1984.
29. Malo D, Vidal SM, Hu J, Skamene E, Gros P: High-resolution linkage map in the vicinity of the host resistance locus Bcg. *Genomics* **16**:655-663, 1993.
30. Malo D, Vidal S, Lieman JH, Ward DC, Gros P: Physical delineation of the minimal chromosomal segment encompassing the murine host resistance locus Bcg. *Genomics* **17**:667-675, 1993.
31. Vidal SM, Malo D, Vogan K, Skamene E, Gros P: Natural resistance to infection with intracellular parasites: isolation of a candidate for Bcg. *Cell* **73**:469-485, 1993.
32. Malo D, Vogan K, Vidal S, Hu J, Cellier M, Schurr E, Fuks A, Bumstead N, Morgan K, Gros P: Haplotype mapping and sequence analysis of the mouse Nramp gene predict susceptibility to infection with intracellular parasites. *Genomics* **23**:51-61, 1994.
33. Govoni G, Vidal S, Gauthier S, Skamene E, Malo D, Gros P: The Bcg/Ity/Lsh Locus - Genetic Transfer Of Resistance to Infections In C57bl/6j Mice Transgenic For the Nramp1(Gly169) Allele. *Infect Immun* **64**:2923-2929, 1996.
34. Vidal S, Tremblay ML, Govoni G, Gauthier S, Sebastiani G, Malo D, Skamene E, Olivier M, Jothy S, Gros P: The Ity/Lsh/Bcg locus: natural resistance to infection with intracellular parasites is abrogated by disruption of the Nramp1 gene. *J Exp Med* **182**:655-666, 1995.
35. Vidal S, Belouchi AM, Cellier M, Beatty B, Gros P: Cloning and characterization of a second human NRAMP gene on chromosome 12q13. *Mamm Genome* **6**:224-230, 1995.

36. Levee G, Liu J, Gicquel B, Chanteau S, Schurr E: Genetic control of susceptibility to leprosy in French Polynesia; no evidence for linkage with markers on telomeric human chromosome 2. *Int J Lepr Other Mycobact Dis* **62**:499-511, 1994.
37. Roger M, Levee G, Chanteau S, Gicquel B, Schurr E: No evidence for linkage between leprosy susceptibility and the human natural resistance-associated macrophage protein 1 (NRAMP1) gene in French Polynesia. *Int J Lepr Other Mycobact Dis* **65**:197-202, 1997.
38. Shaw MA, Atkinson S, Dockrell H, Hussain R, Lins-Lainson Z, Shaw J, Ramos F, Silveira F, Mehdi SQ, Kaukab F, et al.: An RFLP map for 2q33-q37 from multicausal mycobacterial and leishmanial disease families: no evidence for an Lsh/Ity/Bcg gene homologue influencing susceptibility to leprosy. *Ann Hum Genet* **57**:251-271, 1993.
39. Abel L, Sanchez FO, Oberti J, Thuc NV, Hoa LV, Lap VD, Skamene E, Lagrange PH, Schurr E: Susceptibility to leprosy is linked to the human NRAMP1 gene. *J Infect Dis* **177**:133-145, 1998.
40. Bellamy R, Ruwende C, Corrah T, McAdam KP, Whittle HC, Hill AV: Variations in the NRAMP1 gene and susceptibility to tuberculosis in West Africans. *N Engl J Med* **338**:640-644, 1998.
41. Searle S, Blackwell JM: Evidence for a functional repeat polymorphism in the promoter of the human NRAMP1 gene that correlates with autoimmune versus infectious disease susceptibility. *J Med Genet* **36**:295-299, 1999.
42. John S, Myerscough A, Marlow A, Hajeer A, Silman A, Ollier W, Worthington J: Linkage of cytokine genes to rheumatoid arthritis. Evidence of genetic heterogeneity. *Ann Rheum Dis* **57**:361-365, 1998.

43. John S, Marlow A, Hajeer A, Ollier W, Silman A, Worthington J: Linkage and association studies of the natural resistance associated macrophage protein 1 (NRAMP1) locus in rheumatoid arthritis. *J Rheumatol* **24**:452-457, 1997.
44. Hofmeister A, Neibergs HL, Pokorny RM, Galandiuk S: The natural resistance-associated macrophage protein gene is associated with Crohn's disease. *Surgery* **122**:173-178, 1997.
45. Stokkers PC, de Heer K, Leegwater AC, Reitsma PH, Tytgat GN, van Deventer SJ: Inflammatory bowel disease and the genes for the natural resistance-associated macrophage protein-1 and the interferon-gamma receptor 1. *Int J Colorectal Dis* **14**:13-17, 1999.
46. White JK, Shaw MA, Barton CH, Cerretti DP, Williams H, Mock BA, Carter NP, Peacock CS, Blackwell JM: Genetic and physical mapping of 2q35 in the region of the NRAMP and IL8R genes: identification of a polymorphic repeat in exon 2 of NRAMP. *Genomics* **24**:295-302, 1994.
47. Govoni G, Gauthier S, Billia F, Iscove NN, Gros P: Cell-specific and inducible Nramp1 gene expression in mouse macrophages in vitro and in vivo. *J Leukoc Biol* **62**:277-286, 1997.
48. Cellier M, Shustik C, Dalton W, Rich E, Hu J, Malo D, Schurr E, Gros P: Expression of the human NRAMP1 gene in professional primary phagocytes: studies in blood cells and in HL-60 promyelocytic leukemia. *J Leukoc Biol* **61**:96-105, 1997.
49. Vidal SM, Pinner E, Lepage P, Gauthier S, Gros P: Natural resistance to intracellular infections: Nramp1 encodes a membrane phosphoglycoprotein absent in macrophages from susceptible (Nramp1 D169) mouse strains. *J Immunol* **157**:3559-3568, 1996.

50. Canonne-Hergaux F, Gros P: unpublished data.
51. Cheng SH, Gregory RJ, Marshall J, Paul S, Souza DW, White GA, O'Riordan CR, Smith AE: Defective intracellular transport and processing of CFTR is the molecular basis of most cystic fibrosis. *Cell* **63**:827-834, 1990.
52. Jensen TJ, Loo MA, Pind S, Williams DB, Goldberg AL, Riordan JR: Multiple proteolytic systems, including the proteasome, contribute to CFTR processing. *Cell* **83**:129-135, 1995.
53. Loo TW, Clarke DM: Functional consequences of glycine mutations in the predicted cytoplasmic loops of P-glycoprotein. *J Biol Chem* **269**:7243-7248, 1994.
54. Radzioch D, Hudson T, Boule M, Barrera L, Urbance JW, Varesio L, Skamene E: Genetic resistance/susceptibility to mycobacteria: phenotypic expression in bone marrow derived macrophage lines. *J Leukoc Biol* **50**:263-272, 1991.
55. Potter M, O'Brien AD, Skamene E, Gros P, Forget A, Kongshavn PA, Wax JS: A BALB/c congenic strain of mice that carries a genetic locus (*Ityr*) controlling resistance to intracellular parasites. *Infect Immun* **40**:1234-1235, 1983.
56. Mouse Genome Database (MGD), Mouse Genome Informatics, The Jackson Laboratory, Bar Harbor, Maine.
57. Denis M, Forget A, Pelletier M, Skamene E: Pleiotropic effects of the *Bcg* gene. I. Antigen presentation in genetically susceptible and resistant congenic mouse strains. *J Immunol* **140**:2395-2400, 1988.
58. Pirami L, Stockinger B, Corradin SB, Sironi M, Sassano M, Valsasini P, Righi M, Ricciardi-Castagnoli P: Mouse macrophage clones immortalized by retroviruses are functionally heterogeneous. *Proc Natl Acad Sci U S A* **88**:7543-7547, 1991.

59. Witsell AL, Schook LB: Macrophage heterogeneity occurs through a developmental mechanism. *Proc Natl Acad Sci U S A* **88**:1963-1967, 1991.
60. Govoni G, Canonne-Hergaux F, Pfeifer CG, Marcus SL, Mills SD, Hackam DJ, Grinstein S, Malo D, Finlay BB, Gros P: Functional expression of Nramp1 in vitro in the murine macrophage line RAW264.7. *Infect Immun* **67**:2225-2232, 1999.
61. Barton CH, Whitehead SH, Blackwell JM: Nramp transfection transfers Ity/Lsh/Bcg-related pleiotropic effects on macrophage activation: influence on oxidative burst and nitric oxide pathways. *Mol Med* **1**:267-279, 1995.
62. Lang T, Prina E, Sibthorpe D, Blackwell JM: Nramp1 transfection transfers Ity/Lsh/Bcg-related pleiotropic effects on macrophage activation: influence on antigen processing and presentation. *Infect Immun* **65**:380-386, 1997.
63. Geuze HJ: The role of endosomes and lysosomes in MHC class II functioning. *Immunol Today* **19**:282-287, 1998.
64. Govoni G, Gros P: Macrophage NRAMP1 and its role in resistance to microbial infections. *Inflamm Res* **47**:277-284, 1998.
65. Brown DH, Miles BA, Zwilling BS: Growth of *Mycobacterium tuberculosis* in BCG-resistant and -susceptible mice: establishment of latency and reactivation. *Infect Immun* **63**:2243-2247, 1995.
66. Rojas M, Olivier M, Gros P, Barrera LF, Garcia LF: TNF-alpha and IL-10 modulate the induction of apoptosis by virulent *Mycobacterium tuberculosis* in murine macrophages. *J Immunol* **162**:6122-6131, 1999.

67. North RJ, LaCourse R, Ryan L, Gros P: Consequence of Nramp1 deletion on resistance of mice to Mycobacterium tuberculosis infection. submitted , 1999.
68. Medina E, North RJ: Resistance ranking of some common inbred mouse strains to Mycobacterium tuberculosis and relationship to major histocompatibility complex haplotype and Nramp1 genotype. Immunology 93:270-274, 1998.
69. Desjardins M, Huber LA, Parton RG, Griffiths G: Biogenesis of phagolysosomes proceeds through a sequential series of interactions with the endocytic apparatus. J Cell Biol 124:677-688, 1994.
70. Desjardins M, Celis JE, van Meer G, Dieplinger H, Jahraus A, Griffiths G, Huber LA: Molecular characterization of phagosomes. J Biol Chem 269:32194-32200, 1994.
71. Hackam DJ, Rotstein OD, Zhang WJ, Demaurex N, Woodside M, Tsai O, Grinstein S: Regulation of phagosomal acidification. Differential targeting of Na⁺/H⁺ exchangers, Na⁺/K⁺-ATPases, and vacuolar-type H⁺-atpases. J Biol Chem 272:29810-29820, 1997.
72. Hackam DJ, Rotstein OD, Zhang W, Gruenheid S, Gros P, Grinstein S: Host resistance to intracellular infection: mutation of natural resistance-associated macrophage protein 1 (Nramp1) impairs phagosomal acidification. J Exp Med 188:351-364, 1998.
73. Lukacs GL, Rotstein OD, Grinstein S: Phagosomal acidification is mediated by a vacuolar-type H(+)-ATPase in murine macrophages. J Biol Chem 265:21099-21107, 1990.
74. Armstrong JA, D'Arcy Hart P: Response of cultured macrophages to mycobacterium tuberculosis, with observations on fusion of lysosomes with phagosomes. J Exp Med 134:713-740, 1971.

75. Hart PD, Armstrong JA, Brown CA, Draper P: Ultrastructural study of the behavior of macrophages toward parasitic mycobacteria. *Infect Immun* **5**:803-807, 1972.
76. Lowrie DB, Aber VR, Jackett PS: Phagosome-lysosome fusion and cyclic adenosine 3':5'-monophosphate in macrophages infected with *Mycobacterium microti*, *Mycobacterium bovis* BCG or *Mycobacterium lepraemurium*. *J Gen Microbiol* **110**:431-441, 1979.
77. Frehel C, de Chastellier C, Lang T, Rastogi N: Evidence for inhibition of fusion of lysosomal and prelysosomal compartments with phagosomes in macrophages infected with pathogenic *Mycobacterium avium*. *Infect Immun* **52**:252-262, 1986.
78. Xu S, Cooper A, Sturgill-Koszycki S, van Heyningen T, Chatterjee D, Orme I, Allen P, Russell DG: Intracellular trafficking in *Mycobacterium tuberculosis* and *Mycobacterium avium*-infected macrophages. *J Immunol* **153**:2568-2578, 1994.
79. Oh YK, Straubinger RM: Intracellular fate of *Mycobacterium avium*: use of dual-label spectrofluorometry to investigate the influence of bacterial viability and opsonization on phagosomal pH and phagosome-lysosome interaction. *Infect Immun* **64**:319-325, 1996.
80. Sturgill-Koszycki S, Schlesinger PH, Chakraborty P, Haddix PL, Collins HL, Fok AK, Allen RD, Gluck SL, Heuser J, Russell DG: Lack of acidification in *Mycobacterium* phagosomes produced by exclusion of the vesicular proton-ATPase. *Science* **263**:678-681, 1994.
81. Deretic V, Fratti RA: *Mycobacterium tuberculosis* phagosome. *Mol Microbiol* **31**:1603-1609, 1999.
82. Ferrari G, Langen H, Naito M, Pieters J: A coat protein on phagosomes involved in the intracellular survival of mycobacteria. *Cell* **97**:435-447, 1999.

83. Schaible UE, Sturgill-Koszycki S, Schlesinger PH, Russell DG: Cytokine activation leads to acidification and increases maturation of *Mycobacterium avium*-containing phagosomes in murine macrophages. *J Immunol* **160**:1290-1296, 1998.
84. Goren MB, D'Arcy Hart P, Young MR, Armstrong JA: Prevention of phagosome-lysosome fusion in cultured macrophages by sulfatides of *Mycobacterium tuberculosis*. *Proc Natl Acad Sci U S A* **73**:2510-2514, 1976.
85. Spargo BJ, Crowe LM, Ionedo T, Beaman BL, Crowe JH: Cord factor (α,α -trehalose 6,6'-dimycolate) inhibits fusion between phospholipid vesicles. *Proc Natl Acad Sci U S A* **88**:737-740, 1991.
86. Russell DG: personal communication.
87. de Chastellier C, Frehel C, Offredo C, Skamene E: Implication of phagosome-lysosome fusion in restriction of *Mycobacterium avium* growth in bone marrow macrophages from genetically resistant mice. *Infect Immun* **61**:3775-3784, 1993.
88. DeChastellier C, Gros P: unpublished data.
89. Chang KP, Dwyer DM: Multiplication of a human parasite (*Leishmania donovani*) in phagolysosomes of hamster macrophages in vitro. *Science* **193**:678-680, 1976.
90. Winn RE, Prechter GC: Pulmonary Tuberculosis, in Hoeprich PD, Jordan MC, Ronald AR (eds): *Infectious Diseases* (ed 5th Edition). Philadelphia, J.B. Lippincott Company, 1994, p 447-454.
91. Calmette A, Guerin C: *Ann. Inst. Pasteur* **34**:553, 1920.

92. Grange JM: Complications of bacille Calmette-Guerin (BCG) vaccination and immunotherapy and their management. *Commun Dis Public Health* 1:84-88, 1998.
93. Jouanguy E, Altare F, Lamhamedi S, Revy P, Emile JF, Newport M, Levin M, Blanche S, Seboun E, Fischer A, Casanova JL: Interferon-gamma-receptor deficiency in an infant with fatal bacille Calmette-Guerin infection. *N Engl J Med* 335:1956-1961, 1996.
94. Altare F, Durandy A, Lammas D, Emile JF, Lamhamedi S, Le Deist F, Drysdale P, Jouanguy E, Doffinger R, Bernaudin F, Jeppsson O, Gollob JA, Meinel E, Segal AW, Fischer A, Kumararatne D, Casanova JL: Impairment of mycobacterial immunity in human interleukin-12 receptor deficiency. *Science* 280:1432-1435, 1998.
95. de Jong R, Altare F, Haagen IA, Elferink DG, Boer T, van Breda Vriesman PJ, Kabel PJ, Draaisma JM, van Dissel JT, Kroon FP, Casanova JL, Ottenhoff TH: Severe mycobacterial and Salmonella infections in interleukin-12 receptor-deficient patients. *Science* 280:1435-1438, 1998.
96. Kobayashi Y, Komazawa Y, Kobayashi M, Matsumoto T, Sakura N, Ishikawa K, Usui T: Presumed BCG infection in a boy with chronic granulomatous disease. A report of a case and a review of the literature. *Clin Pediatr (Phila)* 23:586-589, 1984.
97. Gros P, Skamene E, Forget A, Taylor B: Host response to infection with mycobacterium bovis (BCG) in mice: genetic study of natural resistance. *Adv Exp Med Biol* 162:183-188, 1983.
98. Pelletier M, Forget A, Bourassa D, Gros P, Skamene E: Immunopathology of BCG infection in genetically resistant and susceptible mouse strains. *J Immunol* 129:2179-2185, 1982.

99. Rook GA: The role of activated macrophages in protection and immunopathology in tuberculosis. *Res Microbiol* **141**:253-256, 1990.
100. Rastogi N, David HL: Mechanisms of pathogenicity in mycobacteria. *Biochimie* **70**:1101-1120, 1988.
101. Stead WW, Senner JW, Reddick WT, Lofgren JP: Racial differences in susceptibility to infection by *Mycobacterium tuberculosis*. *N Engl J Med* **322**:422-427, 1990.
102. Stead WW: Genetics and resistance to tuberculosis. Could resistance be enhanced by genetic engineering? *Ann Intern Med* **116**:937-941, 1992.
103. Comstock GW: Tuberculosis in twins: a re-analysis of the Proffit survey. *Am Rev Respir Dis* **117**:621-624, 1978.
104. Ji B, Grosset J: Leprosy, in Hoeprich PD, Jordan MC, Ronald AR (eds): *Infectious Diseases*. Philadelphia, J.B. Lippincott Company, 1994, p 1008-1014.
105. Ottenhoff TH, de Vries RR: HLA class II immune response and suppression genes in leprosy. *Int J Lepr Other Mycobact Dis* **55**:521-534, 1987.
106. Fine PE: Immunogenetics of susceptibility to leprosy, tuberculosis, and leishmaniasis. An epidemiological perspective. *Int J Lepr Other Mycobact Dis* **49**:437-454, 1981.
107. Abel L, Vu DL, Oberti J, Nguyen VT, Van VC, Guilloud-Bataille M, Schurr E, Lagrange PH: Complex segregation analysis of leprosy in southern Vietnam. *Genet Epidemiol* **12**:63-82, 1995.

108. Skamene E, Gros P, Forget A, Patel PJ, Nesbitt MN: Regulation of resistance to leprosy by chromosome 1 locus in the mouse. *Immunogenetics* **19**:117-124, 1984.
109. Manson-Bahr PEC: Leishmaniasis, in Hoeprich PD, Jordan MC, Ronald AR (eds): *Infectious Diseases* (ed 5th Edition). Philadelphia, J.B. Lippincott Company, 1994, p 1348-1357.
110. Desjardins M, Descoteaux A: Inhibition of phagolysosomal biogenesis by the *Leishmania* lipophosphoglycan. *J Exp Med* **185**:2061-2068, 1997.
111. Blackwell J, Freeman J, Bradley D: Influence of H-2 complex on acquired resistance to *Leishmania donovani* infection in mice. *Nature* **283**:72-74, 1980.
112. Hornick RB: Typhoid Fever, in Hoeprich PD, Jordan MC, Ronald AR (eds): *Infectious Diseases* (ed 5th Edition). Philadelphia, J.B. Lippincott Company, 1994, p 747-753.
113. Jones BD, Falkow S: Salmonellosis: host immune responses and bacterial virulence determinants. *Annu Rev Immunol* **14**:533-561, 1996.
114. Alpuche-Aranda CM, Racoosin EL, Swanson JA, Miller SI: Salmonella stimulate macrophage macropinocytosis and persist within spacious phagosomes. *J Exp Med* **179**:601-608, 1994.
115. Rathman M, Barker LP, Falkow S: The unique trafficking pattern of *Salmonella typhimurium*-containing phagosomes in murine macrophages is independent of the mechanism of bacterial entry. *Infect Immun* **65**:1475-1485, 1997.
116. Garcia-del Portillo F, Finlay BB: Targeting of *Salmonella typhimurium* to vesicles containing lysosomal membrane glycoproteins bypasses compartments with mannose 6-phosphate receptors. *J Cell Biol* **129**:81-97, 1995.

117. Garcia-del Portillo F, Zwick MB, Leung KY, Finlay BB: Salmonella induces the formation of filamentous structures containing lysosomal membrane glycoproteins in epithelial cells. *Proc Natl Acad Sci U S A* **90**:10544-10548, 1993.
118. Rathman M, Sjaastad MD, Falkow S: Acidification of phagosomes containing *Salmonella typhimurium* in murine macrophages. *Infect Immun* **64**:2765-2773, 1996.
119. Oh YK, Alpuche-Aranda C, Berthiaume E, Jinks T, Miller SI, Swanson JA: Rapid and complete fusion of macrophage lysosomes with phagosomes containing *Salmonella typhimurium*. *Infect Immun* **64**:3877-3883, 1996.
120. Ishibashi Y, Arai T: Specific inhibition of phagosome-lysosome fusion in murine macrophages mediated by *Salmonella typhimurium* infection. *FEMS Microbiol Immunol* **2**:35-43, 1990.
121. Buchmeier NA, Heffron F: Inhibition of macrophage phagosome-lysosome fusion by *Salmonella typhimurium*. *Infect Immun* **59**:2232-2238, 1991.
122. Uchiya K, Barbieri MA, Funato K, Shah AH, Stahl PD, Groisman EA: A *Salmonella* virulence protein that inhibits cellular trafficking. *EMBO J* **18**:3924-3933, 1999.
123. Ochman H, Soncini FC, Solomon F, Groisman EA: Identification of a pathogenicity island required for *Salmonella* survival in host cells. *Proc Natl Acad Sci U S A* **93**:7800-7804, 1996.
124. Shea JE, Beuzon CR, Gleeson C, Mundy R, Holden DW: Influence of the *Salmonella typhimurium* pathogenicity island 2 type III secretion system on bacterial growth in the mouse. *Infect Immun* **67**:213-219, 1999.

125. Robson HG, Vas SI: Resistance of inbred mice to *Salmonella typhimurium*. *J Infect Dis* **126**:378-386, 1972.
126. Poltorak A, He X, Smirnova I, Liu MY, Huffel CV, Du X, Birdwell D, Alejos E, Silva M, Galanos C, Freudenberg M, Ricciardi-Castagnoli P, Layton B, Beutler B: Defective LPS signaling in C3H/HeJ and C57BL/10ScCr mice: mutations in *Tlr4* gene. *Science* **282**:2085-2088, 1998.
127. Qureshi ST, Lariviere L, Leveque G, Clermont S, Moore KJ, Gros P, Malo D: Endotoxin-tolerant mice have mutations in Toll-like receptor 4 (*Tlr4*). *J Exp Med* **189**:615-625, 1999.
128. O'Brien AD, Scher I, Campbell GH, MacDermott RP, Formal SB: Susceptibility of CBA/N mice to infection with *Salmonella typhimurium*: influence of the X-linked gene controlling B lymphocyte function. *J Immunol* **123**:720-724, 1979.
129. Rawlings DJ, Saffran DC, Tsukada S, Largaespada DA, Grimaldi JC, Cohen L, Mohr RN, Bazan JF, Howard M, Copeland NG, et al.: Mutation of unique region of Bruton's tyrosine kinase in immunodeficient *XID* mice. *Science* **261**:358-361, 1993.
130. Thomas JD, Sideras P, Smith CI, Vorechovsky I, Chapman V, Paul WE: Colocalization of X-linked agammaglobulinemia and X-linked immunodeficiency genes. *Science* **261**:355-358, 1993.
131. Vetrie D, Vorechovsky I, Sideras P, Holland J, Davies A, Flinter F, Hammarstrom L, Kinnon C, Levinsky R, Bobrow M, et al.: The gene involved in X-linked agammaglobulinaemia is a member of the *src* family of protein-tyrosine kinases. *Nature* **361**:226-233, 1993.

132. Tsukada S, Saffran DC, Rawlings DJ, Parolini O, Allen RC, Klisak I, Sparkes RS, Kubagawa H, Mohandas T, Quan S, et al.: Deficient expression of a B cell cytoplasmic tyrosine kinase in human X-linked agammaglobulinemia. *Cell* **72**:279-290, 1993.
133. Kirkpatrick CE, Farrell JP: Leishmaniasis in beige mice. *Infect Immun* **38**:1208-1216, 1982.
134. Osterrieder N, Wolf E: Lessons from gene knockouts. *Rev Sci Tech* **17**:351-364, 1998.
135. Murray HW, Nathan CF: Macrophage microbicidal mechanisms in vivo: reactive nitrogen versus oxygen intermediates in the killing of intracellular visceral *Leishmania donovani*. *J Exp Med* **189**:741-746, 1999.
136. MacMicking JD, North RJ, LaCourse R, Mudgett JS, Shah SK, Nathan CF: Identification of nitric oxide synthase as a protective locus against tuberculosis. *Proc Natl Acad Sci U S A* **94**:5243-5248, 1997.
137. Kamijo R, Le J, Shapiro D, Havell EA, Huang S, Aguet M, Bosland M, Vilcek J: Mice that lack the interferon-gamma receptor have profoundly altered responses to infection with *Bacillus Calmette-Guerin* and subsequent challenge with lipopolysaccharide. *J Exp Med* **178**:1435-1440, 1993.
138. Swihart K, Fruth U, Messmer N, Hug K, Behin R, Huang S, Del Giudice G, Aguet M, Louis JA: Mice from a genetically resistant background lacking the interferon gamma receptor are susceptible to infection with *Leishmania major* but mount a polarized T helper cell 1-type CD4⁺ T cell response. *J Exp Med* **181**:961-971, 1995.
139. Thompson-Snipes L, Skamene E, Radzioch D: Acquired resistance but not innate resistance to *Mycobacterium bovis* bacillus Calmette-Guerin is compromised by interleukin-12 ablation. *Infect Immun* **66**:5268-5274, 1998.

140. Mattner F, Magram J, Ferrante J, Launois P, Di Padova K, Behin R, Gately MK, Louis JA, Alber G: Genetically resistant mice lacking interleukin-12 are susceptible to infection with *Leishmania major* and mount a polarized Th2 cell response. *Eur J Immunol* **26**:1553-1559, 1996.
141. Gunshin H, Mackenzie B, Berger UV, Gunshin Y, Romero MF, Boron WF, Nussberger S, Gollan JL, Hediger MA: Cloning and characterization of a mammalian proton-coupled metal-ion transporter. *Nature* **388**:482-488, 1997.
142. Muir WA, Hopfer U, King M: Iron transport across brush-border membranes from normal and iron-deficient mouse upper small intestine. *J Biol Chem* **259**:4896-4903, 1984.
143. Muir A, Hopfer U: Regional specificity of iron uptake by small intestinal brush-border membranes from normal and iron-deficient mice. *Am J Physiol* **248**:G376-379, 1985.
144. Lee PL, Gelbart T, West C, Halloran C, Beutler E: The Human Nramp2 Gene: Characterization of the Gene Structure, Alternative Splicing, Promoter Region and Polymorphisms. *Blood Cells Mol Dis* **24**:199-215, 1998.
145. Fleming MD, Romano MA, Su MA, Garrick LM, Garrick MD, Andrews NC: Nramp2 is mutated in the anemic Belgrade (b) rat: evidence of a role for Nramp2 in endosomal iron transport. *Proc Natl Acad Sci U S A* **95**:1148-1153, 1998.
146. Klausner RD, Rouault TA, Harford JB: Regulating the fate of mRNA: the control of cellular iron metabolism. *Cell* **72**:19-28, 1993.
147. Ponka P, Beaumont C, Richardson DR: Function and regulation of transferrin and ferritin. *Semin Hematol* **35**:35-54, 1998.

148. Fleming MD, Trenor CC, 3rd, Su MA, Foernzler D, Beier DR, Dietrich WF, Andrews NC: Microcytic anaemia mice have a mutation in Nramp2, a candidate iron transporter gene. *Nat Genet* **16**:383-386, 1997.
149. Russell ES, Nash DJ, Bernstein SE, Kent EL, McFarland EC, Matthews SM, Norwood MS: Characterization and genetic studies of microcytic anemia in house mouse. *Blood* **35**:838-850, 1970.
150. Russell ES, McFarland EC, Kent EL: Low viability, skin lesions, and reduced fertility associated with microcytic anemia in the mouse. *Transplant Proc* **2**:144-151, 1970.
151. Bannerman RM, Edwards JA, Kreimer-Birnbaum M, McFarland E, Russell ES: Hereditary microcytic anaemia in the mouse; studies in iron distribution and metabolism. *Br J Haematol* **23**:235-245, 1972.
152. Edwards JA, Hoke JE: Defect of intestinal mucosal iron uptake in mice with hereditary microcytic anemia. *Proc Soc Exp Biol Med* **141**:81-84, 1972.
153. Farcich EA, Morgan EH: Diminished iron acquisition by cells and tissues of Belgrade laboratory rats. *Am J Physiol* **262**:R220-224, 1992.
154. Su MA, Trenor CC, Fleming JC, Fleming MD, Andrews NC: The G185R mutation disrupts function of the iron transporter Nramp2. *Blood* **92**:2157-2163, 1998.
155. Canonne-Hergaux F, Gruenheid S, Ponka P, Gros P: Cellular and subcellular localization of the Nramp2 iron transporter in the intestinal brush border and regulation by dietary iron. *Blood* **93**:4406-4417, 1999.

156. O'Riordan DK, Sharp P, Sykes RM, Srai SK, Epstein O, Debnam ES: Cellular mechanisms underlying the increased duodenal iron absorption in rats in response to phenylhydrazine-induced haemolytic anaemia . *Eur J Clin Invest* **25**:722-727, 1995.
157. O'Riordan DK, Debnam ES, Sharp PA, Simpson RJ, Taylor EM, Srai SK: Mechanisms involved in increased iron uptake across rat duodenal brush- border membrane during hypoxia. *J Physiol* **500**:379-384, 1997.
158. Bezkorovainy A: *Biochemistry of Nonheme Iron*. New York, Plenum Press, 1980.
159. Crichton RR, Ward RJ: Iron Homeostasis, in Sigel A, Sigel H (eds): *Iron transport and storage in microorganisms, plants and animals*, vol. 35, *Metal Ions in Biological Systems*. New York, Marcel Dekker, Inc., 1998, p 775.
160. Andrews NC, Levy JE: Iron is hot: an update on the pathophysiology of hemochromatosis. *Blood* **92**:1845-1851, 1998.
161. Fleet JC: Identification of Nramp2 as an iron transport protein: another piece of the intestinal iron absorption puzzle. *Nutr Rev* **56**:88-89, 1998.
162. Wood RJ, Han O: Recently identified molecular aspects of intestinal iron absorption. *J Nutr* **128**:1841-1844, 1998.
163. Riedel HD, Remus AJ, Fitscher BA, Stremmel W: Characterization and partial purification of a ferrireductase from human duodenal microvillus membranes. *Biochem J* **309**:745-748, 1995.
164. Han O, Failla ML, Hill AD, Morris ER, Smith JC, Jr.: Reduction of Fe(III) is required for uptake of nonheme iron by Caco-2 cells. *J Nutr* **125**:1291-1299, 1995.

165. Jordan I, Kaplan J: The mammalian transferrin-independent iron transport system may involve a surface ferrireductase activity. *Biochem J* **302**:875-879, 1994.
166. Flanagan PR, Haist J, MacKenzie I, Valberg LS: Intestinal absorption of zinc: competitive interactions with iron, cobalt, and copper in mice with sex-linked anemia (sla). *Can J Physiol Pharmacol* **62**:1124-1128, 1984.
167. Schade SG, Felsher BF, Glader BE, Conrad ME: Effect of cobalt upon iron absorption. *Proc Soc Exp Biol Med* **134**:741-743, 1970.
168. Thomson AB, Valberg LS, Sinclair DG: Competitive nature of the intestinal transport mechanism for cobalt and iron in the rat. *J Clin Invest* **50**:2384-2394, 1971.
169. Thomson AB, Valberg LS: Intestinal uptake of iron, cobalt, and manganese in the iron-deficient rat. *Am J Physiol* **223**:1327-1329, 1972.
170. Edwards JA, Hoke JE: Red cell iron uptake in hereditary microcytic anemia. *Blood* **46**:381-388, 1975.
171. Edwards JA, Sullivan AL, Hoke JE: Defective delivery of iron to the developing red cell of the Belgrade laboratory rat. *Blood* **55**:645-648, 1980.
172. Dautry-Varsat A, Ciechanover A, Lodish HF: pH and the recycling of transferrin during receptor-mediated endocytosis. *Proc Natl Acad Sci U S A* **80**:2258-2262, 1983.
173. Farcich EA, Morgan EH: Uptake of transferrin-bound and nontransferrin-bound iron by reticulocytes from the Belgrade laboratory rat: comparison with Wistar rat transferrin and reticulocytes. *Am J Hematol* **39**:9-14, 1992.
174. De Silva DM, Askwith CC, Kaplan J: Molecular mechanisms of iron uptake in eukaryotes. *Physiol Rev* **76**:31-47, 1996.

175. Sturrock A, Alexander J, Lamb J, Craven CM, Kaplan J: Characterization of a transferrin-independent uptake system for iron in HeLa cells. *J Biol Chem* **265**:3139-3145, 1990.
176. Garrick LM, Dolan KG, Romano MA, Garrick MD: Non-transferrin-bound iron uptake in belgrade and normal rat erythroid cells. *J Cell Physiol* **178**:349-358, 1999.
177. Chua A, Morgan EH: Manganese metabolism is impaired in the Belgrade rat. *J Comp Physiol* **167**:361-369, 1997.
178. Cellier M, Prive G, Belouchi A, Kwan T, Rodrigues V, Chia W, Gros P: Nramp defines a family of membrane proteins. *Proc Natl Acad Sci U S A* **92**:10089-10093, 1995.
179. Cellier M, Belouchi A, Gros P: Resistance to Intracellular Infections - Comparative Genomic Analysis Of Nramp. *Trends Genet* **12**:201-204, 1996.
180. Donovan A, Brownlie A, Pratt SJ, Shepard J, Paw BH, Dorschner MO, Fleming MD, ,, Thisse B, Andrews NC, Zon LI: Positional cloning of two zebrafish mutant genes involved in hypochromic anemia: the iron transporter *dmt1*(Nramp2) and a novel integral membrane protein (Abstract). Bioiron conference. Italy, 1999.
181. West AH, Clark DJ, Martin J, Neupert W, Hartl FU, Horwich AL: Two related genes encoding extremely hydrophobic proteins suppress a lethal mutation in the yeast mitochondrial processing enhancing protein. *J Biol Chem* **267**:24625-24633, 1992.
182. Supek F, Supekova L, Nelson H, Nelson N: A yeast manganese transporter related to the macrophage protein involved in conferring resistance to mycobacteria. *Proc Natl Acad Sci U S A* **93**:5105-5110, 1996.

183. Liu XF, Supek F, Nelson N, Culotta VC: Negative control of heavy metal uptake by the *Saccharomyces cerevisiae* BSD2 gene. *J Biol Chem* **272**:11763-11769, 1997.
184. Liu XF, Culotta VC: Post-translation control of Nramp metal transport in yeast. Role of metal ions and the BSD2 gene. *J Biol Chem* **274**:4863-4868, 1999.
185. Pinner E, Gruenheid S, Raymond M, Gros P: Functional complementation of the yeast divalent cation transporter family SMF by NRAMP2, a member of the mammalian natural resistance-associated macrophage protein family. *J Biol Chem* **272**:28933-28938, 1997.
186. Rodrigues V, Cheah PC, Ray K, Chia W: *malvolio*, the *Drosophila* homologue of mouse Nramp1 (*Bcg*) is expressed in macrophages and in the nervous system and is required for normal taste behaviour. *EMBO J* **14**:3007-3020, 1995.
187. Orgad S, Nelson H, Segal D, Nelson N: Metal ions suppress the abnormal taste behavior of the *Drosophila* mutant *malvolio*. *J Exp Biol* **201**:115-120, 1998.
188. Cellier M, Roig E, Makui S, Cole S, Gros P, Beaubien J: The bacterial gene YfeP is a functional homolog of mammalian Nramp and functions as a divalent cation transporter in *E. coli* (submitted). , 1999.
189. D'Souza J, Cheah PY, Gros P, Chia W, Rodrigues V: Functional complementation of the *malvolio* mutation in the taste pathway of *Drosophila melanogaster* by the human natural resistance-associated macrophage protein 1 (Nramp-1). *J Exp Biol* **202**:1909-1915, 1999.
190. Alonso JM, Hirayama T, Roman G, Nourizadeh S, Ecker JR: EIN2, a bifunctional transducer of ethylene and stress responses in *Arabidopsis*. *Science* **284**:2148-2152, 1999.

191. Appelberg R, Sarmiento AM: The role of macrophage activation and of Bcg-encoded macrophage function(s) in the control of *Mycobacterium avium* infection in mice. *Clin Exp Immunol* **80**:324-331, 1990.
192. Goto Y, Buschman E, Skamene E: Regulation of host resistance to *Mycobacterium intracellulare* in vivo and in vitro by the Bcg gene. *Immunogenetics* **30**:218-221, 1989.
193. Gruenheid S, Cellier M, Vidal S, Gros P: Identification and characterization of a second mouse Nramp gene. *Genomics* **25**:514-525, 1995.
194. Wood MW, VanDongen HM, VanDongen AM: Structural conservation of ion conduction pathways in K channels and glutamate receptors. *Proc Natl Acad Sci U S A* **92**:4882-4886, 1995.
195. Garcia-del Portillo F, Finlay BB: The varied lifestyles of intracellular pathogens within eukaryotic vacuolar compartments. *Trends Microbiol* **3**:373-380, 1995.
196. Gros P: unpublished data.
197. Coligan JE, Kruisbeek AM, Margulies DH, Shevach EM, Strober W: , in Coico R (ed): *Current Protocols in Immunology*. New York, John Wiley and Sons, Inc., 1995, p 2.4.1-2.7.11.
198. Chen JW, Murphy TL, Willingham MC, Pastan I, August JT: Identification of two lysosomal membrane glycoproteins. *J Cell Biol* **101**:85-95, 1985.
199. Wada I, Rindress D, Cameron PH, Ou WJ, Doherty JJD, Louvard D, Bell AW, Dignard D, Thomas DY, Bergeron JJ: SSR alpha and associated calnexin are major calcium binding proteins of the endoplasmic reticulum membrane. *J Biol Chem* **266**:19599-19610, 1991.

200. Croul S, Mezitis SG, Stieber A, Chen YJ, Gonatas JO, Goud B, Gonatas NK: Immunocytochemical visualization of the Golgi apparatus in several species, including human, and tissues with an antiserum against MG-160, a sialoglycoprotein of rat Golgi apparatus. *J Histochem Cytochem* **38**:957-963, 1990.
201. Gonatas JO, Mezitis SG, Stieber A, Fleischer B, Gonatas NK: MG-160. A novel sialoglycoprotein of the medial cisternae of the Golgi apparatus. *J Biol Chem* **264**:646-653, 1989.
202. Mort JS, Poole AR, Decker RS: Immunofluorescent localization of cathepsins B and D in human fibroblasts. *J Histochem Cytochem* **29**:649-657, 1981.
203. Chavrier P, Parton RG, Hauri HP, Simons K, Zerial M: Localization of low molecular weight GTP binding proteins to exocytic and endocytic compartments. *Cell* **62**:317-329, 1990.
204. Meresse S, Gorvel JP, Chavrier P: The rab7 GTPase resides on a vesicular compartment connected to lysosomes. *J Cell Sci* **108**:3349-3358, 1995.
205. Evan GI, Lewis GK, Ramsay G, Bishop JM: Isolation of monoclonal antibodies specific for human c-myc proto- oncogene product. *Mol Cell Biol* **5**:3610-3616, 1985.
206. Canfield VA, Levenson R: Transmembrane organization of the Na,K-ATPase determined by epitope addition. *Biochemistry* **32**:13782-13786, 1993.
207. Laemmli UK: Cleavage of structural proteins during the assembly of the head of bacteriophage T4. *Nature* **227**:680-685, 1970.

208. Towbin H, Staehelin T, Gordon J: Electrophoretic transfer of proteins from polyacrylamide gels to nitrocellulose sheets: procedure and some applications. *Proc Natl Acad Sci U S A* **76**:4350-4354, 1979.
209. Rutherford MS, Witsell A, Schook LB: Mechanisms generating functionally heterogeneous macrophages: chaos revisited. *J Leukoc Biol* **53**:602-618, 1993.
210. Rabinowitz S, Horstmann H, Gordon S, Griffiths G: Immunocytochemical characterization of the endocytic and phagolysosomal compartments in peritoneal macrophages. *J Cell Biol* **116**:95-112, 1992.
211. Laurent M, Johannin G, Gilbert N, Lucas L, Cassio D, Petit PX, Fleury A: Power and limits of laser scanning confocal microscopy. *Biol Cell* **80**:229-240, 1994.
212. Blackwell JM: Structure and function of the natural-resistance-associated macrophage protein (Nramp1), a candidate protein for infectious and autoimmune disease susceptibility. *Mol Med Today* **2**:205-211, 1996.
213. Barton CH, White JK, Roach TI, Blackwell JM: NH₂-terminal sequence of macrophage-expressed natural resistance-associated macrophage protein (Nramp) encodes a proline/serine-rich putative Src homology 3-binding domain. *J Exp Med* **179**:1683-1687, 1994.
214. Kishi F, Nobumoto M: Identification of natural resistance-associated macrophage protein in peripheral blood lymphocytes. *Immunol Lett* **47**:93-96, 1995.
215. Muller WA, Steinman RM, Cohn ZA: Membrane proteins of the vacuolar system. III. Further studies on the composition and recycling of endocytic vacuolar membrane in cultured macrophages. *J Cell Biol* **96**:29-36, 1983.

216. Jahraus A, Storrie B, Griffiths G, Desjardins M: Evidence for retrograde traffic between terminal lysosomes and the prelysosomal/late endosome compartment. *J Cell Sci* **107**:145-157, 1994.
217. Pitt A, Mayorga LS, Schwartz AL, Stahl PD: Transport of phagosomal components to an endosomal compartment. *J Biol Chem* **267**:126-132, 1992.
218. Rothman JE, Warren G: Implications of the SNARE hypothesis for intracellular membrane topology and dynamics. *Curr Biol* **4**:220-233, 1994.
219. Beutler E, Lichtman MA, Coller BS, Kipps TJ: , in Williams (ed): *Hematology*. New York, McGraw Hill Inc., 1995, p 869-875.
220. Titus RG, Theodos CM, Shankar AH, Hall LR: Interactions between *Leishmania major* and macrophages. *Immunol Ser* **60**:437-459, 1994.
221. Clemens DL, Horwitz MA: Characterization of the *Mycobacterium tuberculosis* phagosome and evidence that phagosomal maturation is inhibited. *J Exp Med* **181**:257-270, 1995.
222. Tilney LG, Portnoy DA: Actin filaments and the growth, movement, and spread of the intracellular bacterial parasite, *Listeria monocytogenes*. *J Cell Biol* **109**:1597-1608, 1989.
223. Schurr E, Skamene E, Forget A, Gros P: Linkage analysis of the *Bcg* gene on mouse chromosome 1. Identification of a tightly linked marker. *J Immunol* **142**:4507-4513, 1989.
224. Malo D, Schurr E, Epstein DJ, Vekemans M, Skamene E, Gros P: The host resistance locus *Bcg* is tightly linked to a group of cytoskeleton-associated protein genes that include villin and desmin. *Genomics* **10**:356-364, 1991.

225. Buckler AJ, Chang DD, Graw SL, Brook JD, Haber DA, Sharp PA, Housman DE: Exon amplification: a strategy to isolate mammalian genes based on RNA splicing. *Proc Natl Acad Sci U S A* **88**:4005-4009, 1991.
226. Dassa E, Hofnung M: Sequence of gene *malG* in *E. coli* K12: homologies between integral membrane components from binding protein-dependent transport systems. *EMBO J* **4**:2287-2293, 1985.
227. Kerppola RE, Ames GF: Topology of the hydrophobic membrane-bound components of the histidine periplasmic permease. Comparison with other members of the family. *J Biol Chem* **267**:2329-2336, 1992.
228. Unkles SE, Hawker KL, Grieve C, Campbell EI, Montague P, Kinghorn JR: *crnA* encodes a nitrate transporter in *Aspergillus nidulans*. *Proc Natl Acad Sci U S A* **88**:204-208, 1991.
229. Stuehr DJ, Nathan CF: Nitric oxide. A macrophage product responsible for cytostasis and respiratory inhibition in tumor target cells. *J Exp Med* **169**:1543-1555, 1989.
230. Nathan C: Nitric oxide as a secretory product of mammalian cells. *FASEB J* **6**:3051-3064, 1992.
231. Cellier M, Govoni G, Vidal S, Kwan T, Groulx N, Liu J, Sanchez F, Skamene E, Schurr E, Gros P: Human natural resistance-associated macrophage protein: cDNA cloning, chromosomal mapping, genomic organization, and tissue-specific expression. *J Exp Med* **180**:1741-1752, 1994.

232. Feinberg AP, Vogelstein B: "A technique for radiolabeling DNA restriction endonuclease fragments to high specific activity". *Anal Biochem* **137**:266-267, 1984.
233. Sanger F, Nicklen S, Coulson AR: DNA sequencing with chain-terminating inhibitors. *Proc Natl Acad Sci U S A* **74**:5463-5467, 1977.
234. Devereux J: The GCG sequence analysis software package (ed 7.0). Madison, WI, USA, Genetics Computer Group, Inc., 1991.
235. Mangalan H: Striding the turf of the gang of four. *Trends Genet* **18**:187-188, 1993.
236. Auffray C, Rougeon F: Purification of mouse immunoglobulin heavy-chain messenger RNAs from total myeloma tumor RNA. *Eur J Biochem* **107**:303-314, 1980.
237. Chirgwin JM, Przybyla AE, MacDonald RJ, Rutter WJ: Isolation of biologically active ribonucleic acid from sources enriched in ribonuclease. *Biochemistry* **18**:5294-5299, 1979.
238. Dietrich W, Katz H, Lincoln SE, Shin HS, Friedman J, Dracopoli NC, Lander ES: A genetic map of the mouse suitable for typing intraspecific crosses. *Genetics* **131**:423-447, 1992.
239. Green MC: Gene Mapping, in Foster HL, Small JD, Fox JG (eds): *The mouse in biomedical research*, vol. 1. New York, Academic Press, 1981, p 105-117.
240. Kozak M: Point mutations define a sequence flanking the AUG initiator codon that modulates translation by eukaryotic ribosomes. *Cell* **44**:283-292, 1986.
241. Kyte J, Doolittle RF: A simple method for displaying the hydropathic character of a protein. *J Mol Biol* **157**:105-132, 1982.

242. Eisenberg D, Schwarz E, Komaromy M, Wall R: Analysis of membrane and surface protein sequences with the hydrophobic moment plot. *J Mol Biol* **179**:125-142, 1984.
243. Devault A, Gros P: Two members of the mouse *mdr* gene family confer multidrug resistance with overlapping but distinct drug specificities. *Mol Cell Biol* **10**:1652-1663, 1990.
244. Marshall RD: Glycoproteins. *Ann Rev Biochem* **41**:673-702, 1972.
245. Kishimoto A, Nishiyama K, Nakanishi H, Uratsuji Y, Nomura H, Takeyama Y, Nishizuka Y: Studies on the phosphorylation of myelin basic protein by protein kinase C and adenosine 3':5'-monophosphate-dependent protein kinase. *J Biol Chem* **260**:12492-12499, 1985.
246. Woodgett JR, Gould KL, Hunter T: Substrate specificity of protein kinase C. Use of synthetic peptides corresponding to physiological sites as probes for substrate recognition requirements. *Eur J Biochem* **161**:177-184, 1986.
247. Pinna LA: Casein kinase 2: an 'eminence grise' in cellular regulation? *Biochim Biophys Acta* **1054**:267-284, 1990.
248. Bairoch A: PROSITE: a dictionary of sites and patterns in proteins. *Nucleic Acids Res* **19 Suppl**:2241-2245, 1991.
249. Bairoch A: The PROSITE dictionary of sites and patterns in proteins, its current status. *Nucleic Acids Res* **21**:3097-3103, 1993.

250. Chen MS, Obar RA, Schroeder CC, Austin TW, Poodry CA, Wadsworth SC, Vallee RB: Multiple forms of dynamin are encoded by shibire, a *Drosophila* gene involved in endocytosis. *Nature* **351**:583-586, 1991.
251. Webb DC, Rosenberg H, Cox GB: Mutational analysis of the *Escherichia coli* phosphate-specific transport system, a member of the traffic ATPase (or ABC) family of membrane transporters. A role for proline residues in transmembrane helices. *J Biol Chem* **267**:24661-24668, 1992.
252. Sahin-Toth M, Dunten RL, Gonzalez A, Kaback HR: Functional interactions between putative intramembrane charged residues in the lactose permease of *Escherichia coli*. *Proc Natl Acad Sci U S A* **89**:10547-10551, 1992.
253. Sheppard DN, Rich DP, Ostedgaard LS, Gregory RJ, Smith AE, Welsh MJ: Mutations in CFTR associated with mild-disease-form Cl⁻ channels with altered pore properties. *Nature* **362**:160-164, 1993.
254. Anderson MP, Gregory RJ, Thompson S, Souza DW, Paul S, Mulligan RC, Smith AE, Welsh MJ: Demonstration that CFTR is a chloride channel by alteration of its anion selectivity. *Science* **253**:202-205, 1991.
255. Yorifuji T, Lemna WK, Ballard CF, Rosenbloom CL, Rozmahel R, Plavsic N, Tsui LC, Beaudet AL: Molecular cloning and sequence analysis of the murine cDNA for the cystic fibrosis transmembrane conductance regulator. *Genomics* **10**:547-550, 1991.
256. Nathan CF, Hibbs JB, Jr.: Role of nitric oxide synthesis in macrophage antimicrobial activity. *Curr Opin Immunol* **3**:65-70, 1991.
257. Gould GW, Holman GD: The glucose transporter family: structure, function and tissue-specific expression. *Biochem J* **295**:329-341, 1993.

258. Ruetz S, Gros P: Functional expression of P-glycoproteins in secretory vesicles. *J Biol Chem* **269**:12277-12284, 1994.
259. Higgins CF: ABC transporters: from microorganisms to man. *Annu Rev Cell Biol* **8**:67-113, 1992.
260. Saurin W, Koster W, Dassa E: Bacterial binding protein-dependent permeases: characterization of distinctive signatures for functionally related integral cytoplasmic membrane proteins. *Mol Microbiol* **12**:993-1004, 1994.
261. Fleming RE, Migas MC, Zhou X, Jiang J, Britton RS, Brunt EM, Tomatsu S, Waheed A, Bacon BR, Sly WS: Mechanism of increased iron absorption in murine model of hereditary hemochromatosis: increased duodenal expression of the iron transporter DMT1. *Proc Natl Acad Sci U S A* **96**:3143-3148, 1999.
262. Gruenheid S, Pinner E, Desjardins M, Gros P: Natural resistance to infection with intracellular pathogens: the Nramp1 protein is recruited to the membrane of the phagosome. *J Exp Med* **185**:717-730, 1997.
263. Moffett P, Dayo M, Reece M, McCormick MK, Pelletier J: Characterization of msim, a murine homologue of the *Drosophila* sim transcription factor. *Genomics* **35**:144-155, 1996.
264. Ausubel F, Brent R, Kingston RE, Moore DD, Seidman JG, Smith JA, Struhl K: , in Janssen K (ed): *Current Protocols in Molecular Biology*, vol. 2, John Wiley and sons, Inc., 1996.
265. Smith DE, Fisher PA: Identification, developmental regulation, and response to heat shock of two antigenically related forms of a major nuclear envelope protein in *Drosophila* embryos: application of an improved method for affinity purification of

antibodies using polypeptides immobilized on nitrocellulose blots. *J Cell Biol* **99**:20-28, 1984.

266. Chow LM, Davidson D, Fournel M, Gosselin P, Lemieux S, Lyu MS, Kozak CA, Matis LA, Veillette A: Two distinct protein isoforms are encoded by *ntk*, a *csk*-related tyrosine protein kinase gene. *Oncogene* **9**:3437-3448, 1994.

267. Pollard JW, Stanners CP: Characterization of cell lines showing growth control isolated from both the wild type and a leucyl-tRNA synthetase mutant of Chinese hamster ovary cells. *J Cell Physiol* **98**:571-585, 1979.

268. Kaufman RJ, Davies MV, Pathak VK, Hershey JWB: The phosphorylation site of eucaryotic initiation factor 2 alters translational efficiency of specific mRNAs. *Molecular and Cellular Biology* **9**:946, 1989.

269. Kast C, Canfield V, Levenson R, Gros P: Membrane topology of P-Glycoprotein as determined by epitope insertion: transmembrane organization of the N-terminal domain of *mdr3*. *Biochemistry* **34**:4402-4411, 1995.

270. Govoni G, Gros P: unpublished data.

271. Edwards JA, Garrick LM, Hoke JE: Defective iron uptake and globin synthesis by erythroid cells in the anemia of the Belgrade laboratory rat. *Blood* **51**:347-357, 1978.

272. Garrick MD, Gniecko K, Liu Y, Cohan DS, Garrick LM: Transferrin and the transferrin cycle in Belgrade rat reticulocytes. *J Biol Chem* **268**:14867-14874, 1993.

273. Bannerman RM: Genetic defects of iron transport. *Fed Proc* **35**:2281-2285, 1976.

274. Teter K, Chandy G, Quinones B, Pereyra K, Machen T, Moore HPH: Cellubrevin-targeted fluorescence uncovers heterogeneity in the recycling endosomes. *J Biol Chem* **273**:19625-19633, 1998.
275. Sipe DM, Jesurum A, Murphy RF: Absence of Na⁺,K⁽⁺⁾-ATPase regulation of endosomal acidification in K562 erythroleukemia cells. Analysis via inhibition of transferrin recycling by low temperatures. *J Biol Chem* **266**:3469-3474, 1991.
276. Yurko MA, Gluck S: Production and characterization of a monoclonal antibody to vacuolar H⁺ATPase of renal epithelia. *J Biol Chem* **262**:15770-15779, 1987.
277. Russell DG, Gros P: unpublished data.
278. Searle S, Bright NA, Roach TI, Atkinson PG, Barton CH, Melen RH, Blackwell JM: Localisation of Nramp1 in macrophages: modulation with activation and infection. *J Cell Sci* **111**:2855-2866, 1998.
279. Barton CH: personal communication.
280. Atkinson PG, Barton CH: High level expression of Nramp1G169 in RAW264.7 cell transfectants: analysis of intracellular iron transport. *Immunology* **96**:656-662, 1999.
281. Atkinson PG, Blackwell JM, Barton CH: Nramp1 locus encodes a 65 kDa interferon-gamma-inducible protein in murine macrophages. *Biochem J* **325**:779-786, 1997.
282. Byers BR, Arceneaux JEL: Microbial Iron Transport: iron acquisition by pathogenic microorganisms, in Sigel A, Sigel H (eds): *Iron Transport and Storage in microorganisms, plants, and animals.*, vol. 35, *Metal Ions in Biological Systems*. New York, Marcel Dekker, Inc., 1998, p 37-66.

283. Weinberg ED: Acquisition of Iron and other nutrients in vivo, in Roth JA (ed): Virulence Mechanisms of Bacterial Pathogens (ed 2). Washington, D.C., American Society for Microbiology, 1995
284. Weinberg ED: The development of awareness of iron-withholding defense. *Perspect Biol Med* 36:215-221, 1993.
285. Barry DM, Reeve AW: Increased incidence of gram-negative neonatal sepsis with intramuscular iron administration. *Pediatrics* 60:908-912, 1977.
286. Oppenheimer SJ: Iron and infection: the clinical evidence. *Acta Paediatr Scand Suppl* 361:53-62, 1989.
287. Lepper AW, Embury DH, Anderson DA, Lewis VM: Effects of altered dietary iron intake in *Mycobacterium paratuberculosis*-infected dairy cattle: sequential observations on growth, iron and copper metabolism and development of paratuberculosis. *Res Vet Sci* 46:289-296, 1989.
288. Tsolis RM, Baumler AJ, Heffron F: Role of *Salmonella typhimurium* Mn-superoxide dismutase (SodA) in protection against early killing by J774 macrophages. *Infect Immun* 63:1739-1744, 1995.
289. Canvin J, Langford PR, Wilks KE, Kroll JS: Identification of sodC encoding periplasmic [Cu,Zn]-superoxide dismutase in *Salmonella*. *FEMS Microbiol Lett* 136:215-220, 1996.
290. Zhang Y, Lathigra R, Garbe T, Catty D, Young D: Genetic analysis of superoxide dismutase, the 23 kilodalton antigen of *Mycobacterium tuberculosis*. *Mol Microbiol* 5:381-391, 1991.

291. Loewen PC, Stauffer GV: Nucleotide sequence of katG of *Salmonella typhimurium* LT2 and characterization of its product, hydroperoxidase I. *Mol Gen Genet* **224**:147-151, 1990.
292. Heym B, Zhang Y, Poulet S, Young D, Cole ST: Characterization of the katG gene encoding a catalase-peroxidase required for the isoniazid susceptibility of *Mycobacterium tuberculosis*. *J Bacteriol* **175**:4255-4259, 1993.
293. Channon JY, Blackwell JM: A study of the sensitivity of *Leishmania donovani* promastigotes and amastigotes to hydrogen peroxide. II. Possible mechanisms involved in protective H₂O₂ scavenging. *Parasitology* **91**:207-217, 1985.
294. Paramchuk WJ, Ismail SO, Bhatia A, Gedamu L: Cloning, characterization and overexpression of two iron superoxide dismutase cDNAs from *Leishmania chagasi*: role in pathogenesis. *Mol Biochem Parasitol* **90**:203-221, 1997.
295. Lundrigan MD, Arceneaux JE, Zhu W, Byers BR: Enhanced hydrogen peroxide sensitivity and altered stress protein expression in iron-starved *Mycobacterium smegmatis*. *Biometals* **10**:215-225, 1997.
296. Wong DK, Lee BY, Horwitz MA, Gibson BW: Identification of fur, aconitase, and other proteins expressed by *Mycobacterium tuberculosis* under conditions of low and high concentrations of iron by combined two-dimensional gel electrophoresis and mass spectrometry. *Infect Immun* **67**:327-336, 1999.
297. Braun V, Hantke K, Koster W: Bacterial iron Transport: Mechanisms, Genetics, and Regulation, in Sigel. A., Sigel H (eds): *Iron Transport and storage in microorganisms, plants, and animals*, vol. 35, *Metal Ions in Biological Systems*. New York, Marcel Dekker, Inc., 1998, p 67-146.

298. Tsolis RM, Baumler AJ, Heffron F, Stojiljkovic I: Contribution of TonB- and Feo-mediated iron uptake to growth of *Salmonella typhimurium* in the mouse. *Infect Immun* **64**:4549-4556, 1996.
299. Lambrecht RS, Collins MT: Inability to detect mycobactin in mycobacteria-infected tissues suggests an alternative iron acquisition mechanism by mycobacteria in vivo. *Microb Pathog* **14**:229-238, 1993.
300. Sturgill-Koszycki S, Schaible UE, Russell DG: Mycobacterium-containing phagosomes are accessible to early endosomes and reflect a transitional state in normal phagosome biogenesis. *EMBO J* **15**:6960-6968, 1996.
301. Clemens DL, Horwitz MA: The Mycobacterium tuberculosis phagosome interacts with early endosomes and is accessible to exogenously administered transferrin. *J Exp Med* **184**:1349-1355, 1996.
302. Borges VM, Vannier-Santos MA, de Souza W: Subverted transferrin trafficking in Leishmania-infected macrophages. *Parasitol Res* **84**:811-822, 1998.
303. Kontoghiorghes GJ, Weinberg ED: Iron: mammalian defense systems, mechanisms of disease, and chelation therapy approaches. *Blood Rev* **9**:33-45, 1995.
304. Aballay A, Sarrouf MN, Colombo MI, Stahl PD, Mayorga LS: Zn²⁺ depletion blocks endosome fusion. *Biochem J* **312**:919-923, 1995.
305. Atkinson PG, Barton CH: Ectopic expression of natural resistance-associated macrophage protein- 1 in COS-1 cells modulates iron accumulation. *Biochem Soc Trans* **26**:S199, 1998.

306. Kuhn DE, Baker BD, Lafuse WP, Zwilling BS: Differential iron transport into phagosomes isolated from the RAW264.7 macrophage cell lines transfected with Nramp1Gly169 or Nramp1Asp169 . *J Leukoc Biol* **66**:113-119, 1999.
307. Zwilling BS, Kuhn DE, Wikoff L, Brown D, Lafuse W: Role of iron in Nramp1-mediated inhibition of mycobacterial growth. *Infect Immun* **67**:1386-1392, 1999.
308. Gomes MS, Appelberg R: Evidence for a link between iron metabolism and Nramp1 gene function in innate resistance against *Mycobacterium avium*. *Immunology* **95**:165-168, 1998.
309. Valdivia RH, Falkow S: Flow cytometry and bacterial pathogenesis. *Curr Opin Microbiol* **1**:359-363, 1998.
310. Valdivia RH, Falkow S: Probing bacterial gene expression within host cells. *Trends Microbiol* **5**:360-363, 1997.
311. Schroit AJ, Madsen JW, Tanaka Y: In vivo recognition and clearance of red blood cells containing phosphatidylserine in their plasma membranes. *J Biol Chem* **260**:5131-5138, 1985.
312. Bothwell TH: *Iron Metabolism in man*. St. Louis, Blackwell Scientific Publications, 1979.
313. Wardrop SL, Richardson DR: The effect of intracellular iron concentration and nitrogen monoxide on nramp2 expression and non-transferrin-bound iron uptake . *Eur J Biochem* **263**:41-50, 1999.
314. Jouanguy E, Lamhamedi-Cherradi S, Lammas D, Dorman SE, Fondaneche MC, Dupuis S, Doffinger R, Altare F, Girdlestone J, Emile JF, Ducoulombier H, Edgar D, Clarke J, Oxelius VA, Brai M, Novelli V, Heyne K, Fischer A, Holland SM,

Kumararatne DS, Schreiber RD, Casanova JL: A human IFNGR1 small deletion hotspot associated with dominant susceptibility to mycobacterial infection . *Nat Genet* **21**:370-378, 1999.

315. Gross SJ, Stuart MJ, Swender PT, Oski FA: Malabsorption of iron in children with iron deficiency. *J Pediatr* **88**:795-799, 1976.

316. Buchanan GR, Sheehan RG: Malabsorption and defective utilization of iron in three siblings. *J Pediatr* **98**:723-728, 1981.

317. Hartman KR, Barker JA: Microcytic anemia with iron malabsorption: an inherited disorder of iron metabolism . *Am J Hematol* **51**:269-275, 1996.

318. Zoller H, Pietrangelo A, Vogel W, Weiss G: Duodenal metal-transporter (DMT-1, NRAMP-2) expression in patients with hereditary haemochromatosis . *Lancet* **353**:2120-2123, 1999.

319. Feder JN, Gnirke A, Thomas W, Tsuchihashi Z, Ruddy DA, Basava A, Dormishian F, Domingo R, Jr., Ellis MC, Fullan A, Hinton LM, Jones NL, Kimmel BE, Kronmal GS, Lauer P, Lee VK, Loeb DB, Mapa FA, McClelland E, Meyer NC, Mintier GA, Moeller N, Moore T, Morikang E, Wolff RK, et al.: A novel MHC class I-like gene is mutated in patients with hereditary haemochromatosis . *Nat Genet* **13**:399-408, 1996.

320. Zhou XY, Tomatsu S, Fleming RE, Parkkila S, Waheed A, Jiang J, Fei Y, Brunt EM, Ruddy DA, Prass CE, Schatzman RC, O'Neill R, Britton RS, Bacon BR, Sly WS: HFE gene knockout produces mouse model of hereditary hemochromatosis . *Proc Natl Acad Sci U S A* **95**:2492-2497, 1998.

321. Waheed A, Parkkila S, Saarnio J, Fleming RE, Zhou XY, Tomatsu S, Britton RS, Bacon BR, Sly WS: Association of HFE protein with transferrin receptor in crypt enterocytes of human duodenum. *Proc Natl Acad Sci U S A* **96**:1579-1584, 1999.

322. Gross CN, Irrinki A, Feder JN, Enns CA: Co-trafficking of HFE, a nonclassical major histocompatibility complex class I protein, with the transferrin receptor implies a role in intracellular iron regulation. *J Biol Chem* **273**:22068-22074, 1998.
323. McCance RA, Widdowson EM: Absorption and Excretion of Iron. *The Lancet* **233**:680-684, 1937.
324. Richardson DR, Ponka P: The molecular mechanisms of the metabolism and transport of iron in normal and neoplastic cells. *Biochim Biophys Acta* **1331**:1-40, 1997.
325. Schumann K, Moret R, Kunzle H, Kuhn LC: Iron regulatory protein as an endogenous sensor of iron in rat intestinal mucosa. Possible implications for the regulation of iron absorption. *Eur J Biochem* **260**:362-372, 1999.
326. King IS, Paterson JY, Peacock MA, Smith MW, Syme G: Effect of diet upon enterocyte differentiation in the rat jejunum. *J Physiol* **344**:465-481, 1983.
327. Conrad ME, Crosby WH: Intestinal Mucosal Mechanisms controlling iron absorption. *Blood* **22**:406-415, 1963.
328. Oates PS, Morgan EH: Ferritin gene expression and transferrin receptor activity in intestine of rats with varying iron stores. *Am J Physiol* **273**:G636-646, 1997.
329. Nunez MT, Tapia V, Arredondo M: Intestinal epithelia (Caco-2) cells acquire iron through the basolateral endocytosis of transferrin. *J Nutr* **126**:2151-2158, 1996.
330. Anderson GJ: Control of iron absorption. *J Gastroenterol Hepatol* **11**:1030-1032, 1996.

331. Garrick LM, Dolan KG, Romano MA, Garrick MD: Non-transferrin-bound iron uptake in Belgrade and normal rat erythroid cells. *J Cell Physiol* **178**:349-358, 1999.
332. Ponka P: Tissue-specific regulation of iron metabolism and heme synthesis: distinct control mechanisms in erythroid cells. *Blood* **89**:1-25, 1997.
333. Nelson N: Metal ion transporters and homeostasis. *EMBO J* **18**:4361-4371, 1999.
334. Moore DF, Jr., Sears DA: Pica, iron deficiency, and the medical history. *Am J Med* **97**:390-393, 1994.
335. Marinella MA: "Tomatophagia" and iron-deficiency anemia. *N Engl J Med* **341**:60-61, 1999.
336. Jenner P: Oxidative damage in neurodegenerative disease. *Lancet* **344**:796-798, 1994.
337. Wang X, Manganaro F, Schipper HM: A cellular stress model for the sequestration of redox-active glial iron in the aging and degenerating nervous system. *J Neurochem* **64**:1868-1877, 1995.
338. Guyton AC: *Textbook of Medical Physiology* (ed 3). Philadelphia, W.B. Saunders Company, 1966.
339. Ham AW: *Histology* (ed 6). Philadelphia, J.B. Lippincott Company, 1969.
340. Connor JR, Benkovic SA: Iron regulation in the brain: histochemical, biochemical, and molecular considerations. *Ann Neurol* **32**:S51-61, 1992.
341. Roberts R, Sandra A, Siek GC, Lucas JJ, Fine RE: Studies of the mechanism of iron transport across the blood-brain barrier. *Ann Neurol* **32**:S43-50, 1992.

342. Bradbury MW: Transport of iron in the blood-brain-cerebrospinal fluid system. *J Neurochem* **69**:443-454, 1997.
343. Jefferies WA, Brandon MR, Hunt SV, Williams AF, Gatter KC, Mason DY: Transferrin receptor on endothelium of brain capillaries. *Nature* **312**:162-163, 1984.
344. Sebastiani G, Olien L, Gauthier S, Skamene E, Morgan K, Gros P, Malo D: Mapping of genetic modulators of natural resistance to infection with *Salmonella typhimurium* in wild-derived mice. *Genomics* **47**:180-186, 1998.

Original contributions to knowledge

- 1. Subcellular localization of endogenous Nramp1 to the late endosomal and lysosomal compartments of macrophages and demonstration of its association with the phagosomal membrane.**
- 2. Identification of a second *Nramp* gene co-expressed with *Nramp1* in mammals.**
- 3. Characterization of *Nramp2* including chromosomal localization and analysis of tissue-specific expression.**
- 4. Generation and affinity-purification of specific antiserum directed against Nramp2. This reagent is the only anti-Nramp2 antiserum available worldwide at this time, and has been used by other members of our lab and distributed widely for use by other groups.**
- 5. Characterization of endogenous Nramp2 protein including range of tissue expression, glycosylation analysis and subcellular localization to the plasma membrane and recycling endosomes.**